

NASA
TP
1240
c.1

NASA Technical Paper 1240

TECH LIBRARY KAFB, NM
0134526

LOAN COPY: RETURN TO
AFWL TECHNICAL LIBRARY
KIRTLAND AFB, N. M.

Ground-Based and In-Flight Simulator Studies of Low-Speed Handling Characteristics of Two Supersonic Cruise Transport Concepts

William D. Grantham, Luat T. Nguyen,
Perry L. Deal, M. J. Neubauer, Jr.,
Paul M. Smith, and Frederick D. Gregory

JULY 1978





NASA Technical Paper 1240

Ground-Based and In-Flight Simulator Studies of Low-Speed Handling Characteristics of Two Supersonic Cruise Transport Concepts

William D. Grantham, Luat T. Nguyen,
Perry L. Deal, M. J. Neubauer, Jr.,
and Frederick D. Gregory

*Langley Research Center
Hampton, Virginia*

Paul M. Smith
*Vought Corporation Hampton Technical Center
Hampton, Virginia*

NASA

National Aeronautics
and Space Administration

**Scientific and Technical
Information Office**

1978

SUMMARY

Fixed ground-based and in-flight simulator studies have been conducted to determine the low-speed flight characteristics of two advanced supersonic cruise transport concepts, each having an arrow wing, a horizontal tail, and four dry (nonafterburning) turbojets with variable geometry turbines. The major differences between the two simulated transport concepts were that the first, or baseline, concept incorporated four under-the-wing engines, whereas the second concept utilized powered lift and was configured to incorporate two under-the-wing engines on the outboard portion of the wing with the two inboard engines located on the wing upper surface to induce additional circulation lift. The primary piloting task was the approach and landing.

The results of the studies indicated that the statically (longitudinal) unstable transport concepts had unacceptable longitudinal low-speed handling qualities with no augmentation. In order to achieve "satisfactory" handling qualities, considerable augmentation was required. Although the SCAS developed in this study to achieve satisfactory handling qualities was complex, it is within current technology. A hardened stability augmentation system (HSAS) was required to achieve "acceptable" handling qualities should the normal operational stability and control augmentation system (SCAS) fail.

The available roll-control power was found to be inadequate to meet existing crosswind-landing requirements for the baseline concept; but roll control was acceptable for the powered-lift concept. Other advantages of the powered-lift concept over the baseline concept were the ability to perform segmented-decelerating approaches for community noise abatement, and the ability to perform landing approaches at considerably reduced angles of attack; thereby, the possibility of eliminating the "drooped-nose" requirement for acceptable pilot field of view was increased.

The results of this study indicate that the maximum allowable peak values of lateral acceleration (a_y) at passenger and pilot stations during coordinated turns may be unsatisfactory based on proposed requirements for large supersonic transport airplanes. It was further concluded that additional research is required to obtain satisfactory ride qualities while maintaining satisfactory handling qualities for either of the supersonic cruise transport concepts at low speeds.

INTRODUCTION

During the National Supersonic Transport (SST) Program of the early 1960's, various aerodynamic research studies conducted at the NASA Langley Research Center to develop an efficient supersonic cruise transport airplane resulted in a highly swept arrow-wing configuration designated the SCAT-15F. The arrow-wing concept offered considerable promise for superior supersonic cruise performance; unfortunately, such configurations usually do not possess good low-speed handling characteristics. Early wind-tunnel and piloted simulation studies (for

example, see refs. 1 and 2) identified some of the low-speed handling problems of the SCAT-15F. Later, in 1968, the Boeing Company made an in-depth study (ref. 3) of a supersonic cruise transport concept which was based on the NASA arrow-wing configuration, but which had a lifting canard and a small horizontal tail (fig. 1). That particular configuration promised good take-off and landing performance. Although the canard improved the trimmed lift-drag ratio, it reduced longitudinal stability.

Since the early 1970's, the Langley Research Center has been conducting extensive wind-tunnel studies to improve the low-speed handling characteristics of the arrow-wing configuration without a canard. (See fig. 2.) Some improvements were achieved by careful attention to wing planform, wing leading-edge design, and high-lift devices. Performance calculations have shown that with such modifications and with 2- to 3-percent negative static margin, the resulting configuration should produce lift-drag ratios as good as those of a stable concept with a forebody canard. However, the landing attitude was such that nose droop probably would be required for an acceptable pilot field of view. In addition, stability and control analyses indicated that the concept might have some deficiencies in the high-lift landing-approach configuration. Preliminary conceptual studies have indicated that these problems could be minimized by application of powered-lift principles. Whereas the baseline concept had four under-the-wing turbojets with variable geometry turbines (fig. 2), the simulated powered-lift concept incorporated two under-the-wing engines on the outboard portion of the wing with the other two engines located inboard and on the wing upper surface to induce significant circulation lift. (See fig. 3.) The major advantage of this powered-lift concept is that it can provide the capability to approach at lower angles of attack; thereby, the possibility of eliminating the "drooped-nose" requirement for acceptable pilot field of view is increased, and more roll-control power at the approach lift coefficient is achieved.

Results obtained from the aforementioned configuration refinements were sufficiently promising to justify conducting piloted simulator investigations of the approach and landing characteristics of two of the most recent supersonic cruise transport concepts - conventional and powered lift.

The primary objectives of these studies were to evaluate the low-speed handling characteristics of the two SCAR concepts and to obtain sufficient information to provide guidance for future low-speed research requirements. Other major objectives of these studies were

- (1) Evaluate the general handling qualities of the unaugmented airplanes in the approach configuration.

- (2) Develop the stability augmentation and flight control systems required to achieve satisfactory handling qualities.

- (3) Determine the control power required to meet established handling qualities criteria.

- (4) Evaluate the effects of various atmospheric conditions, including heavy turbulence, steady winds, and wind shear on the ability of the pilot to make a satisfactory approach and landing.

(5) Determine the advantages and/or disadvantages of the powered-lift, arrow-wing concept as compared with the conventional (baseline) arrow-wing concept.

SYMBOLS AND DEFINITIONS

Values are given in both the International System of Units (SI) and U.S. Customary Units. The measurements and calculations were made in U.S. Customary Units. Dots over symbols denote differentiation with respect to time. All calculations are based on the aircraft body axes.

a_n	normal acceleration, g units
a_y	lateral acceleration, g units
C_L	lift coefficient
$C_{L\alpha}$	lift-curve slope per unit angle of attack per rad
C_l	rolling-moment coefficient
$C_{l\beta}$	rolling-moment coefficient due to sideslip per deg
C_m	pitching-moment coefficient
C_n	yawing-moment coefficient
C_T	thrust coefficient
C_x	longitudinal-force coefficient
C_y	side-force coefficient
C_z	vertical-force coefficient
\bar{c}	mean aerodynamic chord, m (ft)
f_n	longitudinal short-period undamped natural frequency, Hz
g	acceleration due to gravity, m/sec ² (ft/sec ²)
h	altitude, m (ft)
I_x, I_y, I_z	moment of inertia about X, Y, and Z body axes, respectively, kg-m ² (slug-ft ²)
I_{xz}	product of inertia, kg-m ² (slug-ft ²)
K_1	rudder aerodynamic effectiveness gain
K_2	rudder flexibility gain

K_{δ_a}	flexibility gain for δ_a
$K_{\delta_{af}}$	flexibility gain for δ_{af}
$K_{\delta_{afi}}$	flexibility gain for δ_{afi}
$K_{\delta_{afo}}$	flexibility gain for δ_{afo}
K_{δ_s}	flexibility gain for δ_s
L/D	lift-drag ratio
L_{α}	lift per unit angle of attack per unit momentum $(\bar{q}S/mV)C_{L\alpha}$ per sec
m	airplane mass, kg (slugs)
n/α	steady-state normal acceleration change per unit change in angle of attack for an incremental horizontal-tail deflection at constant airspeed, gravity units/rad
P_d	period of Dutch roll oscillation, sec
P_{ph}	period of longitudinal phugoid oscillation, sec
P_{sp}	period of longitudinal short-period oscillation, sec
p, q, r	rolling, pitching, and yawing angular velocities, respectively, deg/sec or rad/sec
P_1, P_2	roll rates at first and second peaks, respectively, deg/sec or rad/sec
\bar{q}	dynamic pressure, Pa (lbf/ft ²)
S	reference wing area, m ² (ft ²)
s	Laplace operator
T	thrust, N (lbf)
$t_{1/2}$	time to damp to one-half amplitude, sec
t_2	time to double amplitude, sec
$t_{\phi=30^\circ}$	time to achieve 30° bank angle, sec
V	airspeed, knots (ft/sec)
W	airplane weight, N (lbf)
\bar{x}	longitudinal distance from aircraft center of gravity to pilot station, m (ft)

y lateral displacement from localizer center line, m (ft)
 \bar{z} vertical distance from aircraft center of gravity to pilot station,
 positive when pilot located below center of gravity, m (ft)
 α angle of attack, deg
 β angle of sideslip, deg
 γ flight-path angle, deg
 Δ increment
 δ_a aileron deflections, positive for right roll command, deg
 $\delta_{a,c}$ commanded aileron deflection, deg
 δ_{af} flaperon deflection, deg
 δ_{afi} inboard flaperon deflection, deg
 δ_{afo} outboard flaperon deflection, deg
 δ_c column deflection, deg
 δ_f trailing-edge flap deflection, deg
 δ_{lat} lateral control surface deflections (combination of all roll-control
 surfaces used), deg
 δ_p pedal deflection, cm (in.)
 δ_r rudder deflection, deg
 δ_s deflection of spoiler-slot and inverted spoiler-slot deflectors, deg
 δ_t horizontal tail with geared elevator deflection, deg
 δ_w wheel deflection, deg
 ϵ_{zh} glide-slope error, m (ft)
 ζ_d Dutch roll mode damping ratio
 ζ_{ph} longitudinal phugoid mode damping ratio
 ζ_{sp} longitudinal short-period mode damping ratio
 ζ_ϕ damping ratio of numerator quadratic ϕ/δ_{lat} transfer function
 Θ pitch attitude, deg

τ_R	roll mode time constant, sec
ϕ	angle of roll, deg
ψ	heading angle, deg
ψ_β	phase angle expressed as a lag for a cosine representation of Dutch roll oscillation in sideslip, deg
ω_d	undamped natural frequency of Dutch roll mode, rad/sec
ω_{ph}	undamped natural frequency of phugoid mode, rad/sec
ω_{sp}	longitudinal short-period undamped natural frequency, rad/sec
ω_ϕ	undamped natural frequency appearing in numerator quadratic of ϕ/δ_{lat} transfer function, rad/sec

Subscripts:

av	average
c	commanded
cg	center of gravity
ge	ground effect
lg	landing gear
lat	lateral
o	all surfaces zero degrees
osc	oscillatory
rms	root mean square
ps	pilot station
ss	steady state
max	maximum

Abbreviations:

ADI	attitude director indicator
ARI	aileron-rudder interconnect
HSAS	hardened stability augmentation system
IFR	instrument flight rules

ILS	instrument landing system
PR	pilot rating
RAH	roll attitude hold mode on
<u>RAH</u>	roll attitude hold mode off
SAS	stability augmentation system
SCAR	supersonic cruise aircraft research
SCAS	stability and control augmentation system
SJT	subsonic jet transport
SST	supersonic transport
STOL	short take-off and landing
TIFS	total in-flight simulator
VFR	visual flight rules
WL	wings leveler mode on
<u>WL</u>	wings leveler mode off

DESCRIPTION OF SIMULATED AIRPLANES*

Both of the simulated airplanes (conventional and powered lift) were, in general, resized versions of the configuration described in reference 4. Three-view sketches of the two concepts are presented in figures 2 and 3; mass and dimensional characteristics, and the control-surface deflection and deflection rate limits for these concepts are presented in table I; and the aerodynamic data used in the study are presented in tables II and III. The "conventional" supersonic cruise transport concept will hereafter be referred to as the baseline concept.

Baseline Concept

The static aerodynamic data used for the baseline configuration were estimated on the basis of the various low-speed wind-tunnel test results (e.g., refs. 5 and 6) and corrected for configuration differences. The control surfaces used for low-speed lateral control consisted of outboard ailerons, outboard spoiler-slot and inverted spoiler-slot deflectors, and inboard flaperons. The lateral control system was designed in such a manner that all lateral con-

*The work-up and analyses of the aerodynamic and geometric data packages utilized for this SCAR simulation program were performed under contract number NAS1-13500 by Paul M. Smith of Vought Corporation.

control surfaces were driven by the commanded aileron deflection, and each surface was deflected so that each reached its limit simultaneously. The rigid aileron control data were estimated on the basis of unpublished wind-tunnel tests, and the flaperon, spoiler-slot, and inverted spoiler-slot deflector data were taken from reference 3 and modified to account for the size and location of the subject airplane's control surfaces. A 40-percent-chord, full-span rudder was used for low-speed directional control. The rigid rudder effectiveness data were estimated by using the method presented in reference 4. The reduction of lateral control effectiveness due to wing flexibility was estimated from the data presented in reference 3; and the reduction of directional control effectiveness due to fuselage side bending was based on unpublished data. (See fig. 4 for an indication of flexibility effects.) The methods presented in reference 7 were used to estimate the aerodynamic effects of ground proximity, and the data are shown in figure 5.

The dynamic aerodynamic derivatives were estimated by using a combination of the forced oscillation test data of reference 1 and the estimation techniques of reference 8.

An example of the engine response characteristics used for both the baseline and powered-lift concepts is shown in figure 6.

Powered-Lift Concept

The powered-lift airplane simulated had the same overall dimensions as the baseline airplane, except that the horizontal- and vertical-tail sizes were increased. The static longitudinal and lateral-directional aerodynamic characteristics for the powered-lift airplane were developed by using the wind-tunnel test data of references 6 and 9, respectively, with the appropriate corrections applied to include the effects of the differences in horizontal- and vertical-tail volume coefficients. To obtain the same horizontal-tail trim download as for the baseline concept required that the center of gravity of the powered-lift concept be located at $0.72\bar{c}$. Configuration rebalance and main landing gear location analyses determined that the most aft center-of-gravity position was at $0.66\bar{c}$.

For the powered-lift airplane, the control surfaces used for low-speed lateral control consisted of outboard ailerons, outboard flaperons, and inboard flaperons. The lateral control system was designed in the same manner as the baseline concept; all surfaces were driven by the commanded aileron deflection. Since no lateral control surface effectiveness data were measured with the power on for the powered-lift wind-tunnel model (ref. 6), the measured unpowered data of reference 9 were modified to approximate the effects of upper-surface blowing. This was achieved by conservatively assuming that the measured values of rolling- and yawing-moment coefficients as functions of thrust coefficient and outboard engine nozzle deflections (thrust vectoring) would represent the increments in lateral control due to upper-surface blowing effects. For convenience and ease of implementation, these measured increments were added to the unpowered aerodynamic effectiveness of the outboard flaperon data. (Experience with

powered-lift STOL wind-tunnel models has indicated that substantially more roll-control power can be achieved by utilizing deflection of trailing-edge surfaces of wings incorporating upper-surface blowing than that from use of thrust vectoring alone.) An all-movable vertical tail was used for low-speed directional control. (The aerodynamic effectiveness data were developed from the data of ref. 9.) The flexibility effects on lateral control were estimated from the data in reference 3; whereas, the flexibility effects on directional control were based on unpublished data. (See fig. 4.)

The aerodynamic effects of ground proximity (fig. 5) used for the baseline airplane were also used for the powered-lift airplane.

The dynamic stability derivatives used for the powered-lift airplane were estimated by using the data for the baseline airplane and corrections were made to include the effects of (1) the increase in horizontal- and vertical-tail size, and (2) the blowing of the two upper-surface engines.

DESCRIPTION OF SIMULATION EQUIPMENT

Evaluations of the low-speed landing-approach handling characteristics were made at Langley Research Center by using a fixed-base ground simulator with a visual landing scene. After the ground-based study, a brief in-flight simulation program was conducted by using Calspan's Total In-Flight Simulator (TIFS) airplane in order to provide (1) points of reference for interpretation of the ground simulator results, (2) data for control system design trade-offs, and (3) data on the effects of motion cues not available in the fixed-base simulation.

Fixed-Base Simulator

The fixed-base simulator had a transport-type cockpit which was equipped with conventional flight and engine-thrust controls and with a flight-instrument display representative of those found in current transport airplanes. (See fig. 7.) Instruments indicating angle of attack, sideslip, and flap angle were also provided. A conventional cross-pointer-type flight director instrument was used, and the command bars (cross pointers) were driven by the main computer program.

Real-time digital simulation techniques were used wherein a digital computer was programmed with equations of motion for six degrees of freedom.

A visual display of an airport scene (fig. 8) was used in order to provide visual cues for the flare and landing. The display consisted of a closed-circuit television presentation, viewed through a collimating lens in the pilot's windshield, of the simulated approach to a 3505-m (11 500-ft) runway. (See fig. 9.) Each flight was terminated at touchdown; the roll-out was not simulated.

In-Flight Simulator

The TIFS is a fly-by-wire C-131 airplane with controllers for all six degrees of freedom and a separate evaluation cockpit forward and below the normal C-131 cockpit. (See fig. 10.) When flown from the evaluation cockpit, the pilot control commands are the inputs to a model computer which determine the aircraft motion commands to be reproduced. These are combined with the TIFS motion sensor signals in another portion of the onboard computer to provide TIFS controller commands. The simulated airplane motions are produced with maximum time lags of 50 to 150 msec in the frequency range of interest.

The evaluation cockpit instruments were mostly conventional and were positioned as shown in figure 11. In addition to the conventional instruments displays of sideslip angle and angle of attack were provided. Airspeed error was displayed as a tape motion on the left side of the ADI. Aircraft position relative to the ILS glide slope was displayed (in ft) as a vertical bug motion on the left side of the ADI. A flight director computer producing the same functions as the computer used in the ground-based simulator was mechanized in the TIFS computer. This instrument was used in lieu of the conventional flight director on board the TIFS airplane in order to insure that the flight director was compatible with the simulated supersonic cruise transport dynamics.

Cardboard masking was used on the TIFS evaluation cockpit windshield to simulate the view expected from the cockpit of the supersonic cruise transport.

TESTS AND PROCEDURES

Two research pilots participated in the simulation program and each used standard flight-test procedures in the evaluation of the handling qualities. The primary piloting task was the approach and landing.

The tests consisted of IFR and simulated VFR landing approaches with crosswinds, turbulence, localizer offsets, glide slope offsets, and engine failure as added complicating factors. The ILS approach was initiated with the airplane in the power-approach condition (power for level flight), at an altitude below the glide slope, and on a 45° intercept course to the localizer. (See fig. 12.) The pilot's task was to capture the localizer and glide slope and to maintain them as closely as possible while under simulated IFR conditions. At an altitude of approximately 91 m (300 ft), the pilot converted to VFR conditions and attempted to land the airplane visually (with limited reference to the flight instruments).

The results of these studies using the aforementioned evaluation procedures are in the form of time-history records of airplane motions and pilot comments regarding the low-speed handling qualities of the two supersonic cruise transport concepts and the effects of various stability and control augmentation systems on these characteristics. The more significant results are reviewed in the following sections.

RESULTS AND DISCUSSION

The results of these studies are discussed in terms of the previously stated objectives, and the pilot ratings listed for the various conditions evaluated are an average of the ratings from all pilots who flew that particular condition. (See table IV for the pilot rating system.) Also, the results discussed pertain to the data obtained on the baseline supersonic cruise transport concept utilizing the fixed-base ground simulator unless specifically noted.

No Stability Augmentation

The baseline concept had a negative static margin of approximately 4 percent to improve the approach L/D, and the unaugmented handling qualities were rated as unacceptable (PR = 7) by the evaluation pilots. As can be seen from table V, the time to double amplitude (t_2) of the longitudinal aperiodic mode is 4.8 sec, which might be expected to be unacceptable since the landing-approach minimum-safe (PR = 6.5) criterion of reference 10 stated that a $t_2 < 6$ sec would be unacceptable. (See fig. 13.) A comparison of the pitch rate response of the unaugmented airplane to the desired response is presented in figure 14 and shows that the response to a column step input appears as an acceleration command instead of the desired rate command. The pitch control power of this baseline concept was rated as acceptable insofar as the longitudinal control power requirements for the approach and landing tasks are concerned, in agreement with the control power requirements criterion of reference 11 as shown in figure 15. Recent unpublished studies have indicated that an acceptable pitch acceleration criterion at the minimum demonstrated air-

speed is said to be acceptable if $\ddot{\Theta} \leq -0.05 \text{ rad/sec}^2$ and satisfactory if $\ddot{\Theta} \leq -0.08 \text{ rad/sec}^2$. By using this criterion the pitch control power was determined to be acceptable, but not satisfactory. (See table VI.)

A pilot rating of 7 was assigned to the unaugmented lateral-directional handling qualities of the baseline configuration. The major objections were (1) unacceptable large adverse sideslip excursions in turns; (2) easily excited, lightly damped Dutch roll mode; (3) poor roll and heading control; and (4) sluggish roll response with low roll damping. The primary factor that contributed to the poor pilot rating for the lateral-directional characteristics was the large adverse sideslip excursions experienced during rolling maneuvers. This characteristic is indicated in figure 16, and compared with the desired response for a lateral control step input. For a step input it is desirable to have (1) a rapid roll-rate response that reaches a reasonably steady-state value with a minimum of oscillation; (2) essentially zero sideslip produced by the roll-control input; and (3) an immediate response in heading. However, it is evident from figure 16 that for a lateral control step input for this unaugmented configuration, a large amount of adverse sideslip is experienced that washes out

the roll rate ($\dot{\phi}$) in a short period of time and also causes an undesirable lag in the initiation of turn rate ($\dot{\psi}$). This large adverse sideslip characteristic,

in combination with the low roll damping, required constant attention and considerable effort on the part of the pilot and still resulted in very poor lateral-directional control.

It must be noted that although the longitudinal and lateral-directional handling qualities of this unaugmented supersonic cruise transport airplane were assigned a pilot rating of 7 when evaluated individually, the combination of poor characteristics resulted in an overall pilot rating of 10 for the airplane. Therefore, it was apparent that considerable stability and control augmentation will be required to achieve satisfactory handling qualities for the landing-approach piloting task.

Normal Operational Stability and Control Augmentation System (SCAS)

Based on the results obtained for the unaugmented configuration, the objective for the design of the SCAS was that the system should provide satisfactory handling qualities ($PR \leq 3.5$) at all flight conditions evaluated during the study. A block diagram of the SCAS design obtained is shown in figure 17.

Longitudinally, a high-gain pitch rate command/attitude hold system was chosen because (1) stabilization of the unstable mode could be achieved with the pitch attitude feedback, (2) the system provided good short-period characteristics and rapid response to pilot inputs, and (3) the attitude-hold feature minimized disturbances due to turbulence or variations in thrust.

Laterally, a roll rate command/attitude hold system was employed to provide a rapid roll mode and quick uniform response to pilot inputs; the attitude-hold feature resulted in a desirable neutrally stable spiral mode while counteracting disturbances due to turbulence. In addition, a wings-leveler feature was provided to the pilot (to be used at his option) which automatically leveled the wings ($\phi = 0^\circ$) whenever the bank angle was less than 2° and the wheel was centered. This feature relieved the pilot of the task of hunting for zero bank angle and was particularly useful when rolling out of a turn to a desired heading.

Directionally, roll-rate and roll-attitude feedbacks were used to provide turn coordination and improved Dutch roll characteristics. A roll control to rudder interconnect was also included to reduce adverse sideslip during turn entry and therefore minimize Dutch roll excitation during roll maneuvers.

An autothrottle that maintained the selected airspeed throughout the approach and landing was also used as part of the normal operational augmentation. Since the simulated engine dynamics (for example, see fig. 6) produced very rapid thrust response, the autothrottle generally maintained the desired airspeed within ± 3 knots and considerably reduced the pilot workload on the landing approach. Although this airplane is flown well up the "backside" of the thrust required curve at the approach speed of 153 knots ($\partial T/W/\partial V \approx -0.0023/\text{knot}$) where normally the pilot would primarily use pitch attitude for airspeed control and thrust for glide-path control, the simulated quick engine-thrust response allowed the use of thrust (manually or automati-

cally) for airspeed control and thus enabled the pilot to use pitch attitude for glide-path control - which is a very natural, simple technique.

The longitudinal SCAS (fig. 17) provided pitch rate proportional to column deflection, and produced the desired characteristics of rapid, well-damped responses to pilot inputs as well as inherent attitude stability. Figure 18 shows the improvement in pitch rate response provided by the SCAS, and it can be seen from table V that the time to double amplitude (t_2) of the longitudinal aperiodic mode increased from 4.8 sec with no augmentation to infinity with the SCAS configuration. With this augmentation system operative, the average pilot rating for the longitudinal handling qualities on the ILS approach was improved from PR = 7 to PR = 2.

Also shown in figure 17 is a block diagram of the lateral-directional SCAS. Laterally, a rate command system provided roll rate proportional to wheel position, and the directional system consisted of several turn coordination features. Table V shows that the Dutch roll characteristics were improved considerably; (ω_ϕ/ω_d) was increased from 0.565 to 1.004 (which indicates that the Dutch roll oscillation should be much less easily excited for roll-control inputs), and the damping parameter ($\zeta_d\omega_d$) was increased from 0.064 rad/sec to 0.197 rad/sec. The improvement in the roll response and damping are indicated by the reduction of τ_R from 1.689 to 0.27 sec. (See table V.)

Figure 19 shows the improvement in the roll-rate response provided by the SCAS. By elimination of the large adverse sideslip, the roll-rate reversal was eliminated, and the heading response was immediate (no lag). The lateral SCAS also provided a desirable roll-attitude-hold feature which proved to be very beneficial, particularly during landing approaches made in simulated heavy turbulence. With this augmentation system operative, the average pilot rating for the lateral-directional handling qualities on the ILS approach was improved from PR = 7 to PR = 2.

With the SCAS operative, the overall pilot rating of the simulated baseline SCAR concept for the landing-approach task was 2.

Hardened Stability Augmentation System (HSAS)

As discussed previously, the baseline SCAR concept had unacceptable low-speed handling qualities with no augmentation. A hardened stability augmentation system (HSAS) was therefore required to achieve acceptable handling qualities should the normal operational augmentation (SCAS) fail. (The term "hardened" SAS implies sufficient redundancy to negate loss of the system.)

The HSAS design objective was to provide improved handling qualities so that acceptable pilot ratings ($PR \leq 6.5$) could be obtained for the approach and landing task and so that the system could be kept as simple as possible to maximize reliability and ease of implementation. A block diagram of the HSAS design is shown in figure 20. Longitudinally, a filtered pitch rate feedback signal acting through a relatively high gain was used to reduce the instability of the unstable mode and to enhance the short-period characteristics. Laterally, a simple roll damper provided a smaller roll mode time constant and increased

Dutch roll damping. Directionally, roll-rate feedback was used to provide: (1) improved turn-entry coordination; (2) reduced Dutch roll coupling during roll maneuvers (increased ω_{ϕ}/ω_d); and (3) further enhancement of the Dutch roll damping. Note that only two angular rate signals (pitch rate and roll rate) were required for the HSAS implementation so that sensor reliability problems and mechanization complexity would be minimized. The autothrottle was also considered to be part of the HSAS.

The average pilot rating assigned to the longitudinal handling qualities when the HSAS was operative was 4. The primary objection was the less-than-desired pitch damping. Table V shows that the short-period damping ratio (ζ_{sp}) for this configuration is 0.693, which would normally indicate adequate damping; however, the slowly divergent aperiodic mode ($t_2 = 44$ sec) superimposed on the short-period response caused the motions to appear to the pilot as being inadequately damped. It should be noted that reference 10 also indicated acceptable pilot ratings ($PR \leq 6.5$) when t_2 was greater than 6 sec. (See fig. 13.) Figure 21 compares the pitch response to a column step for the unaugmented airplane with SCAS operative and with HSAS operative. The reason a higher gain was not implemented for the pitch rate damper, in order to satisfy the pilot's objection of low pitch damping, was that more damping would make the pitch axis unacceptably sluggish. It is evident from figure 21 that the HSAS configuration is already very sluggish in pitch, compared with the SCAS configuration.

The average pilot rating assigned to the lateral-directional handling qualities with the HSAS operative was 4. The primary objections were sluggish roll response, Dutch roll excitation during turns, less than desired roll damping, and a lack of steady-state turn coordination. Figure 22 shows a comparison of the roll response to a lateral control step input for the HSAS, SCAS, and unaugmented configurations.

Effects of Center-of-Gravity Location

As previously stated, the airplane was configured to be slightly statically unstable at a center-of-gravity position of $0.56\bar{c}$ to minimize the required trim download of the tail. The resulting negative static margin was approximately 4 percent. Handling qualities evaluations for the landing-approach task at this "basic" center-of-gravity position ($0.56\bar{c}$) resulted in a pilot rating of 2 with the SCAS operative and a pilot rating of 4 with the HSAS operative. To evaluate the effects of center-of-gravity location on the low-speed handling qualities, the airplane was flown with increasing levels of negative static margin. The technique used to determine the most tolerable aft center-of-gravity location was to determine the center-of-gravity position at which the pilots evaluated the low-speed handling qualities as being "satisfactory" with the SCAS operative, $PR \leq 3.5$, and also as being "acceptable" with the HSAS operative ($PR \leq 6.5$). It was determined that for a center-of-gravity location of $0.66\bar{c}$, the pilots rated the landing-approach task as being marginally satisfactory ($PR = 3.5$) with the SCAS operative and marginally acceptable ($PR = 6.5$) with the HSAS operative. Therefore, from handling qualities considerations, the aft center-of-gravity limit was said to be $0.66\bar{c}$ (approximately 14-percent negative static margin).

To illustrate the effect of center-of-gravity position on the low-speed airplane performance, the data in figure 23 are presented. Note that as the center-of-gravity location is moved rearward, the approach lift-drag ratio increases only slightly; however, the trim angle of attack decreases significantly. Although it is not presented in figure 23, it should be mentioned that for flap settings less than the landing-approach flap setting ($\delta_f = 40^\circ$), the increase in airplane performance (lift drag) as the center of gravity is moved rearward is much more pronounced.

Crosswind Landings

Both steady crosswinds (up to 20 knots) and crosswinds with horizontal shear (8 knots per 30 m) were simulated. The piloting technique used for making the approach and landing consisted of an initial crabbed approach, and at a nominal altitude (usually about 15 m (50 ft)), transitioning to a wing-down sideslip.

The requirements of reference 12 state that transport airplanes without crosswind-landing gear should be capable of landing in 90° crosswinds up to 30 knots, and that the lateral control used shall not exceed 75 percent of the control power available. Figure 24 indicates the amount of steady-state sideslip, bank angle, rudder deflection, and lateral control deflection required for sideslipping crosswind approaches at an airspeed of 153 knots (the nominal approach speed). It can be seen that 75 percent of the available lateral control was required for a crosswind component of approximately 20 knots. It is, therefore, obvious that this baseline supersonic cruise transport airplane could not be landed with an adequate lateral control margin in 90° crosswinds higher than approximately 20 knots. Also, from a piloting standpoint, the lateral-directional control coordination required for the transition from a crabbed-approach condition to a sideslipping, wing-down condition becomes increasingly difficult as the 90° crosswind increases above approximately 15 knots. It is, therefore, concluded from these ground-based, fixed-cockpit simulator results that the subject supersonic cruise transport airplane concept should be equipped with crosswind gear and/or provided with additional roll-control power.

It should be mentioned that although the accuracy of the control coordination was the prime factor that affected the pilot's ability to make "precise" landings in high crosswinds, deficiencies of the visual presentation (lack of peripheral vision and adequate height cues) and possibly the lack of cockpit motion also affected the pilot's ability to make satisfactory landings in large crosswinds.

Effects of Turbulence on Landing Approach

Flight in rough air was evaluated by using a turbulence model based on the Dryden spectral form. The root-mean-square value of the longitudinal, lateral, and vertical gust-velocity components was varied from 0.61 m/sec (2 ft/sec) to 2.7 m/sec (9 ft/sec). These values were described by the pilots as being repre-

sentative of light and heavy turbulence, respectively. The pilots commented that the pilot rating for the approach task on the baseline supersonic cruise transport concept was degraded by one rating when the landing approach was made in the simulated heavy turbulence because of the increased workload required to maintain ILS tracking.

Figure 25 presents plots of the root-mean-square values of the vertical and lateral accelerations at the airplane center of gravity experienced during ILS approaches made in various levels of simulated turbulence for both the baseline supersonic cruise transport simulated and a typical subsonic jet transport. The root-mean-square values are compared with the ride quality criterion of reference 13. As can be seen, the normal and lateral acceleration root-mean-square values are lower for the supersonic cruise transport than for the subsonic jet transport. Therefore, the response of the simulated supersonic cruise airplane to atmospheric turbulence would not be expected to be any worse than the response of present-day subsonic transport airplanes, effects of airframe flexibility being neglected.

Comparison of Baseline Concept With Powered-Lift Concept

Powered-lift concepts, such as those utilizing upper-surface engine blowing, offer several aerodynamic improvements over the baseline concept. Practically all these improvements are achieved from the increased circulation lift that can be obtained by blowing the jet efflux over larger trailing-edge flaps. (The trailing-edge flap size, and hence lift generation, is limited on the baseline concept because of the location of the aft-wing-mounted turbojet engines.)

Aerodynamics.- Figure 26 indicates the increase in lift coefficient that was achieved with the simulated powered-lift concept. Note that a C_L of 0.66, which corresponds to a trimmed approach speed of 153 knots, is achieved at $\alpha \approx 0^\circ$ on the powered-lift concept compared with $\alpha \approx 8^\circ$ on the baseline concept. This allows the pilot to fly the landing approach with the powered-lift concept at a significantly reduced pitch attitude which minimizes the length of the main landing-gear struts, and it also offers the potential of eliminating the drooped-nose requirement for an acceptable pilot field of view. Figure 27 presents a view of the runway as seen by the pilot prior to touchdown for both the baseline and powered-lift concepts with the nose of the aircraft drooped for maximum pilot visibility, as well as with the nose in the "up" position. Note that with the nose drooped, the pilot field of view indicated for both concepts appears to be sufficient to make a simulated approach and landing, somewhat better visibility being indicated for the powered-lift concept because of the difference in the approach attitude. The nose-up scenes are presented to further indicate the advantage of the lower approach attitude. Note that the pilot cannot see the runway with the nose in the up position while flying the baseline concept.

The reduction in approach angle of attack also reduces the dihedral effect (fig. 28) which, in turn, improves the inherent lateral-directional handling qualities. The more effective wing trailing-edge flaps on the powered-lift concept also offer a means of increasing the available roll-control power (fig. 29). As shown in figure 30, the combination of reduced dihedral effect

and increased roll-control power result in acceptable crosswind-landing capability, which was not the case for the baseline concept.

A segmented landing approach (for community noise abatement considerations) could also be readily flown on the powered-lift concept and still maintain a relatively low pitch attitude. As indicated in figure 31, the powered-lift concept could be flown on an approach angle of -5° at an airspeed of 170 knots for one segment; then, at some designated altitude (nominally 152 m (500 ft)) transition to an approach angle of -2.7° and an airspeed of 153 knots could be made. In addition, if the drooped-nose consideration is ignored, the transition could be made to an approach angle of -2.7° and an airspeed of 136 knots - which is the nominal approach speed of present-day subsonic jet transports.

It should be mentioned that although the aforementioned advantages of the powered-lift concept are considerable for terminal area operations, this concept does have some disadvantages during cruise. Potentially, the disadvantages of the powered-lift concept during cruise are (1) upper-surface wing-nacelle interference drag, (2) increased wave drag due to the increase in slope of the forward cross-sectional area distribution curve, (3) airframe strength degradation due to thermal and acoustic effects, and (4) more complex engine inlet flow field.

Handling qualities.- The handling qualities of the unaugmented powered-lift concept were, in general, the same (unacceptable) as those previously discussed for the baseline concept. However, both satisfactory and acceptable handling qualities were achieved by utilizing the same augmentation systems as discussed for the baseline concept. See tables V and VI for a comparison of the dynamic stability and control response characteristics of the two concepts.

Engine failure.- Lateral-directional control with a critical engine (outboard) failed has always been a prime consideration in the rudder design for multiengine airplanes. Control of asymmetries due to engine failure can be easily analyzed from static conditions by calculating the steady-state sideslip angle, bank angle, and control deflections for a straight flight path over the ground. The transient responses immediately following an engine failure, however, present problems involving pilot reaction time, the manner in which controls are applied, and, of course, the altitude and configuration of the airplane at the time of the failure. During the subject program, attempts were made to simulate the wave-off capabilities as well as continued approaches and landings after an outboard engine failure on both supersonic cruise transport concepts (baseline concept and powered-lift concept).

The manner in which an engine was failed during this simulation study was that which would be considered the most severe; that is, the engine failed instantaneously (a step form of thrust loss). Also, the configuration flown for both concepts incorporated what was considered to be the best stability and control augmentation system (SCAS) and autothrottle. The requirement used for evaluating the wave-off capability of the baseline concept after engine failure was determined based on the proposed airworthiness standards for supersonic transports (ref. 14) - "With the approach flap setting, the aircraft shall be capable of a 2.7 percent gradient (1.5°) climb, in rectilinear flight, with one

engine inoperative at an airspeed no greater than the determined operational and performance speed." (The baseline concept has an operational approach speed of 153 knots which is equivalent to 1.22 times the minimum demonstrated speed.) The requirements used when documenting the wave-off capability of the powered-lift concept were based on NASA powered-lift flight experience (for example, ref. 15) - "In the event of failure of one engine on approach, it should be possible to arrest the descent and maintain level flight without change in flap setting or airspeed. It should also be possible after arresting the descent to establish a sustained climb angle of 2° (3.5% gradient) by retraction of the flaps and without change in airspeed."

With the relatively high thrust-weight ratio available on both of these concepts (four-engine approach $T/W \approx 0.5$), the wave-off capability of both simulated concepts, from performance considerations, was no problem and met the aforementioned requirements with ease. However, typical of most multiengine aircraft, the increase in pilot workload caused by the necessity to retrim after an engine failure degraded the pilot ratings for the wave-off task to 3 for the baseline concept and 4 for the powered-lift concept. (A pilot rating of 2 was assigned to both concepts with no engine failure.) It should be mentioned that the amount of rudder required to trim the baseline and powered-lift concepts after an outboard engine failure was approximately 4° and 15° , respectively.

Attempts were made to simulate a continued approach and landing following the loss of an outboard engine on both the baseline and powered-lift concepts. Typical approaches, for which the number four engine was failed during the approach, are presented in figure 32. The most interesting points indicated are the excursions from the localizer and glide slope immediately following the engine failure. As can be seen from figure 32(a), the maximum lateral displacement from the localizer beam was approximately 10 m (33 ft), and the maximum vertical displacement from the glide-slope beam was approximately 5 m (16 ft) for the baseline concept compared with 17 m (56 ft) and more than 12 m (39 ft), respectively, for the powered-lift concept. (See figure 32(b).)

The pilots commented that the loss of a critical engine during an ILS approach on either concept posed no problems (insofar as tracking localizer and glide slope) but that the requirement of using rudder for trimming sideslip was bothersome, particularly for the powered-lift concept. For the continued approach task after an engine failure, the pilots assigned ratings of 2.5 and 4 to the baseline concept and powered-lift concept, respectively. In addition, the pilots commented that they would probably choose to perform a wave-off on the powered-lift concept if the engine failure occurred below an altitude of approximately 91 m (300 ft), whereas they would probably continue the approach and landing on the baseline concept regardless of the altitude at which the engine failed.

Comparison of Fixed-Base and In-Flight Results

As stated previously, upon completion of the fixed-base ground simulator tests, a brief in-flight simulation program was conducted in order to provide (1) points of reference for interpretation of the ground simulator results; (2) data for control system design trade-offs; and (3) data of effects of

motion cues not available in the fixed-base simulation. Only the baseline supersonic cruise transport concept was flown during the in-flight simulation program - the powered-lift concept was not simulated.

In general, the handling qualities assessments determined on the fixed-base simulator were substantiated during the in-flight simulator tests. Although the in-flight tests were more realistic (for example, the motions were realistic and the scene out of the window was the real world), these factors did not change the pilots' opinions of the handling characteristics of the simulated airplane. However, it was determined during the in-flight tests that the SCAS produced unacceptable ride qualities (lateral accelerations) at the pilot station (cockpit). As indicated in figure 33, the SCAS developed for the lateral-directional axes during the fixed-base tests provides a quick, uniform roll-rate (\dot{p}) response to a lateral control input and at the same time provides good turn coordination (small β produced). In addition, the lateral acceleration indicated for the center of gravity of the airplane ($(a_y)_{CG}$) is acceptable from ride qualities considerations. However, the lateral acceleration indicated for the pilot's station ($(a_y)_{PS}$) and particularly the rate of buildup of ($(a_y)_{PS}$) following a lateral control input was said to be unacceptable (uncomfortable) by the evaluation pilots during the in-flight tests. This unacceptable lateral acceleration at the pilot's station was produced primarily by the unusually long distance between the center-of-gravity location and the pilot's station on this supersonic cruise transport airplane. Figure 34 indicates a comparison of pilot location, relative to the center of gravity, between the subject supersonic cruise transport airplane and the Boeing 747 subsonic jet transport airplane.

The relationship between the lateral acceleration at the pilot station and that at the center of gravity may be approximated as follows:

$$(a_y)_{PS} \approx (a_y)_{CG} + \frac{\dot{r}(\bar{x}) - \dot{p}(\bar{z})}{32.17}$$

As can be seen from figure 33, the $\dot{r}(\bar{x})$ term is the predominant factor. (The distance from the simulated center-of-gravity location to the simulated pilot station \bar{x} was 44.2 m (145.1 ft).) It may be erroneously concluded that any airplane that has a very long distance between the center of gravity and the cockpit will have unacceptable ride qualities, whereas compromises can be made between handling qualities and ride qualities and achieve satisfactory (or at least acceptable) characteristics for both. For example, the hardened stability augmentation system (HSAS) developed during the fixed-base tests produced acceptable (but not satisfactory) handling qualities during both fixed-base and in-flight tests and also had acceptable ride qualities ($(a_y)_{PS}$) during the in-flight tests. As shown in figure 35, the initial roll-rate response for a lateral control input is good for the HSAS configuration but the adverse sideslip continues to build up and "washes out" some of the roll rate. As stated previously, the lateral-directional handling qualities of this airplane with the HSAS operative were assigned a pilot rating of 4 (acceptable). Since the HSAS did not produce good turn coordination ($\beta \approx 0^\circ$), the yaw acceleration produced by a lateral control input was not appreciable (when compared with the SCAS response) and therefore the lateral acceleration at the cockpit was not as large as that produced with the SCAS operative.

Modified SCAS

The results from the in-flight simulation tests implied that "acceptable" lateral acceleration characteristics could be achieved if the lateral-directional handling qualities were compromised. Therefore, an attempt was made to modify the lateral-directional part of the SCAS in such a manner as to maintain "satisfactory" handling qualities ($PR \leq 3.5$) and at the same time attain "acceptable" $(a_y)_{ps}$ characteristics. (The dynamic stability and response characteristics of the simulated airplanes with the modified SCAS operative are presented in tables V and VI.) These goals were accomplished by slowing the initial roll-rate response by applying a first-order lag to the roll-rate command signal, by reducing the wheel roll-rate command sensitivity, and by substantially reducing the ARI (aileron-to-rudder interconnect) gain. The modifications to the initial lateral-directional SCAS are indicated in the block diagram presented in figure 36. Time histories of the motions obtained for a roll-control step input with the modified SCAS are presented in figure 37 and compared with the motions obtained with the initial SCAS. It can be seen that the roll-rate response for the modified SCAS is not as fast as that for the initial SCAS, but that good turn coordination is maintained (small β) and an appreciable improvement in the lateral acceleration characteristics is achieved. The pilots assigned a rating of 3 to the lateral-directional handling qualities when the modified lateral-directional SCAS was used (compared with a PR of 2 for the initial SCAS) and said the lateral accelerations experienced for roll-control inputs were "acceptable," but not satisfactory.

Dynamic Stability Requirements and Criteria

For several years the aircraft industry has been aware that many of the existing stability requirements of aircraft are outdated because of the expansion of flight envelopes and the increases in airplane size. Although research is presently being conducted in an effort to remedy this situation, to date essentially no clearly defined stability requirements and criteria have been established for aircraft similar to those for the supersonic cruise transport. Therefore, in an effort to aid in the future establishment of new stability requirements, the low-speed handling qualities parameters of the supersonic cruise transport concepts are compared with some existing handling qualities criteria.

Two of the most widely used longitudinal handling qualities criteria are presented in figure 38. Figure 38(a) shows the short-period frequency requirements of reference 12 and, as can be seen, the results predicted by the criterion agree reasonably well with the results obtained during the present simulation studies. Figure 38(b) shows the Shomber-Gertsen longitudinal handling qualities criterion of reference 16. This criterion relates the ability of the pilot to change flight path with normal acceleration to the factor L_{α} . By using this parameter and by recognizing that the pilot's mode of control is not constant for all flight regimes, a criterion for satisfactory short-period characteristics was developed that correlates well with current airplane experience and reasonably well with the results obtained during the present low-speed supersonic cruise transport simulation program. Figure 39 presents the longitudinal short-period criterion, for transport aircraft, of refer-

ence 17. In general, the results of the present study are said to be in good agreement with this criterion, particularly for the unaugmented and HSAS configurations. As noted in reference 17, the limit line for the "acceptable unaugmented area" of this criterion is subject to further research. It is believed, from the results obtained for the SCAS configurations during the present study, that the upper limit line for the "acceptable augmented area" could also be extended to higher values of the short-period damping ratio ζ_{sp} .

The low-speed pitch rate response criterion shown in figure 40, and reported in reference 18, was based on the Shomber-Gertsen criterion of reference 16. As can be seen, there is excellent agreement between the results obtained during the present study and this low-speed pitch response criterion when the normal operational augmentation (SCAS) was operative. The constraints imposed upon the use of the reference 18 criterion, however, negate its use for any of the other configurations evaluated during the present study. For the most part, the pitch divergence criterion of reference 10, with a time-to-double pitch attitude of 6 sec or greater for the most unstable root, was considered when the HSAS and unaugmented configurations were evaluated, and the subject simulation results agreed very well with the criterion. (For example, see fig. 13.)

The roll-acceleration and roll-rate capability criteria for transport aircraft are presented in figures 41 and 42, respectively. (These criteria were reported in refs. 12 and 17, respectively.) The various configurations evaluated during the present simulation study are indicated in these plots and, in general, would not be considered to be in agreement with results predicted by these criteria - particularly for the roll-acceleration capability criterion presented in figure 41. For example, the roll-control power available for the powered-lift concept was determined to be very satisfactory for landing in 90° crosswinds greater than 30 knots, which was the most demanding piloting task evaluated during the present low-speed simulation studies. (See fig. 30.)

The bank angle oscillation limitations criterion of reference 12 is presented in figure 43 and relates the phase angle of the Dutch roll component of sideslip (ψ_β) to the measure of the ratio of the oscillatory component of bank angle to the average component of bank angle ϕ_{osc}/ϕ_{av} . The various configurations evaluated during the present simulation study are indicated in this plot, and it can be seen that the simulated characteristics agree, reasonably well, with the aforementioned criterion - particularly, the fully augmented (SCAS) and unaugmented configurations.

In general, it is concluded that the results of the present simulation study agree with the established handling qualities criteria used for comparison in this paper, the major exception being the roll-acceleration capability criterion of reference 12.

Ride Quality Criteria

The ride quality criterion of reference 13 relates the root-mean-square values of a_n and a_y to the root-mean-square values of the gust intensity (level of turbulence). As discussed previously and shown in figure 25, the

response of the simulated supersonic cruise baseline concept to atmospheric turbulence compared favorably with the aforementioned criterion when the airframe flexibility effects were neglected - particularly, the criterion for the $(a_y)_{rms}$, which was equal to or less than 0.055g for acceptable passenger ride comfort. It should be noted, however, that the root-mean-square values of a_n and a_y presented in figure 25 for the SCAR and SJT airplanes were the values measured at the center of gravity of the aircraft, whereas the criterion of reference 13 pertains to the values at any passenger location. Also as discussed previously, the specific peak values (as opposed to the root-mean-square values) of a_y experienced at locations far removed from the center of gravity of the aircraft were found to be unsatisfactory during the in-flight simulation part of this study.

A criterion for the maximum allowable a_y at any passenger station as well as the pilot station (cockpit) has been proposed by the Boeing Company as a result of their analyses during the National SST Program and is reported in reference 11. This criterion states in part - "Lateral acceleration at the pilot station shall not exceed a level of $\pm 0.075g$ peak, and the critical passenger station shall not exceed $\pm 0.05g$ peak. These levels shall be met for all normal maneuvers including 30 degree bank and capture using an average roll rate of $5^\circ/\text{sec}$ in cruise and $10^\circ/\text{sec}$ at landing. If unpiloted time studies are conducted, the wheel input should be a 0.5-second ramp of magnitude sufficient to produce the specified average roll rates."

In order to compare the peak values of a_y that would be experienced on the baseline supersonic cruise transport concept with the aforementioned criterion, figure 44 was prepared. Figure 44 presents the peak values of a_y as a function of the longitudinal displacement from the aircraft center of gravity (\bar{x}). (The vertical displacement from the center of gravity was maintained constant as that representing the pilot station.) As can be seen, the proposed criterion for a_y cannot be satisfied even when no turn coordination is provided for any value of \bar{x} considered. That is, considering that an approximation of $(a_y)_{ps}$ is

$$(a_y)_{ps} \approx (a_y)_{cg} + \frac{\dot{r}(\bar{x}) - \dot{p}(\bar{z})}{32.17}$$

with no yaw acceleration (\dot{r}) for turn coordination, and even neglecting the $(a_y)_{cg}$ contribution, the $\dot{p}(\bar{z})/32.17$ term (roll acceleration times the vertical displacement of the pilot from the aircraft center of gravity) is 0.08g, which is larger than the acceptable level of the aforementioned criterion. In addition to no turn coordination (which is unrealistic), these values of $(a_y)_{ps}$ were obtained for a rigid airframe. It is believed that if airframe flexibility effects were included, the peak values of a_y would be even larger. It is also believed that some of the larger subsonic transports of today could not meet this proposed lateral acceleration criterion, simply because of the geometry of the problem. Therefore, it is concluded that the requirements of this proposed criterion must be relaxed or the roll maneuvers of all very large airplanes must be constrained in order to have acceptable low-speed ride qualities.

CONCLUDING REMARKS

Fixed-base simulator and in-flight simulator studies have been conducted to determine the low-speed flight characteristics of two advanced supersonic cruise transport concepts (a conventional concept and a powered-lift concept), each having an arrow wing, a horizontal tail, and four dry turbojets with variable geometry turbines. The primary piloting task was the approach and landing. This paper has attempted to summarize the results of these studies which support the following major conclusions.

The statically unstable (longitudinally) supersonic cruise transport concepts simulated had unacceptable (pilot rating of 10) low-speed handling qualities with no augmentation.

The longitudinal normal operational stability and control augmentation system, consisting of a high-gain pitch rate command/attitude hold system and an autothrottle, essentially eliminated the longitudinal control problems. The lateral-directional SCAS, consisting of a roll rate command/attitude hold system and of roll-rate, roll-angle, and roll-control surface deflection feedback signals to the rudder, made the lateral-directional handling characteristics satisfactory. With these augmentation systems operative, the average pilot rating for the instrument approach task was 2 for both the baseline and powered-lift concepts.

The hardened stability augmentation system (HSAS), designed to provide acceptable handling qualities with maximum simplicity (for reliability and ease of implementation) consisted of a filtered pitch rate feedback signal to the longitudinal control surface for additional pitch damping, and a roll-rate feedback signal to the roll-control surfaces, as well as to the rudder, for additional roll damping and improved turn-entry coordination. With this HSAS operative, the average pilot rating for the instrument approach task was 4 for both the baseline and powered-lift concepts.

In an effort to evaluate the effects of center-of-gravity location on the low-speed handling qualities, the baseline supersonic cruise transport concept was flown with increasing levels of negative static margin. It was determined that with the SCAS or HSAS operative, the landing-approach task could be performed with a negative static margin as high as 14 percent. (The pilot ratings assigned to the SCAS and HSAS configurations for the landing-approach task were 3.5 and 6.5, respectively.)

The available roll-control power required to meet the existing crosswind-landing requirements was found to be inadequate for the baseline concept but adequate for the powered-lift concept.

The response of the supersonic cruise transport concepts to atmospheric turbulence would not be expected to be any worse than the response of present-day subsonic transport airplanes, flexibility differences being neglected. However, the pilots commented that the rating for the landing-approach task on the transport concepts was degraded by one rating when the landing approach was made in the simulated heavy turbulence since the glide-slope tracking task required higher pilot workload.

The most apparent advantages of the powered-lift concept (over the baseline concept) were the ability to perform segmented-decelerating approaches (for community noise abatement), and the ability to perform landing approaches at reduced angles of attack; thereby, the possibility of eliminating the "drooped-nose" requirement for acceptable pilot field of view was increased.

The wave-off capabilities, as well as continued approaches and landings, were simulated after the failure of an outboard engine on both the baseline and powered-lift concepts. With the relatively high thrust-weight ratio available on both of these concepts (four-engine approach $T/W \approx 0.5$), the wave-off capability was no problem, from performance considerations, and met the established requirements with ease. The pilots commented that the loss of a critical engine during an instrument approach on either concept posed no problems insofar as tracking localizer and glide slope. The pilots further commented that they would probably choose to perform a wave-off on the powered-lift concept if the engine failure occurred below an altitude of approximately 91 m (300 ft), whereas they would probably continue the approach and landing on the baseline concept regardless of the altitude at which the engine failed.

In general, it was concluded that the results of the simulation study agree with the established handling qualities criteria used for comparison in this paper. However, it is believed from the results of this study that the proposed requirements for the maximum allowable peak values of lateral acceleration (a_y) at any passenger station, as well as the pilot station (cockpit) during coordinated turns must be relaxed or the roll maneuvers of all very large transport airplanes must be constrained in order to have satisfactory ride qualities.

It is further concluded that additional low-speed research is required to achieve satisfactory ride qualities and at the same time maintain satisfactory handling qualities on either of the subject supersonic cruise transport concepts.

Langley Research Center
National Aeronautics and Space Administration
Hampton, VA 23665
April 28, 1978

REFERENCES

1. Freeman, Delma C., Jr.: Low Subsonic Flight and Force Investigation of a Supersonic Transport Model With a Highly Swept Arrow Wing. NASA TN D-3887, 1967.
2. Grantham, William D.; and Deal, Perry L.: A Piloted Fixed-Base Simulator Study of Low-Speed Flight Characteristics of an Arrow-Wing Supersonic Transport Design. NASA TN D-4277, 1967.
3. Mach 2.7 Fixed Wing SST Model 969-336C (SCAT-15F). Doc. No. D6A11666-1 (Contract FA-SS-67-3), Boeing Co., July 1969.
4. Baber, Hal T., Jr.; and Swanson, E. E.: Advanced Supersonic Technology Concept AST-100 Characteristics Developed in a Baseline-Update Study. NASA TM X-72815, 1976.
5. Lockwood, Vernard E.: Effect of Trailing-Edge Flap Deflection on the Lateral and Longitudinal-Stability Characteristics of a Supersonic Transport Model Having a Highly-Swept Arrow Wing. NASA TM X-71936, 1974.
6. Coe, Paul L., Jr.; McLemore, H. Clyde; and Shivers, James P.: Effects of Upper-Surface Blowing and Thrust Vectoring on Low-Speed Aerodynamic Characteristics of a Large-Scale Supersonic Transport Model. NASA TM X-72792, 1975.
7. LTV Hampton Technical Center: Advanced Supersonic Technology Concept Study - Reference Characteristics. NASA CR-132374, 1973.
8. USAF Stability and Control Datcom. Contracts AF 33(616)-6460 and F33615-75-C-3067, McDonnell Douglas Corp., Oct. 1960. (Revised Apr. 1976.)
9. Coe, Paul L., Jr.; Smith, Paul M.; and Parlett, Lysle P.: Low-Speed Wind Tunnel Investigation of an Advanced Supersonic Cruise Arrow-Wing Configuration. NASA TM 74043, 1977.
10. Rising, J. J.: A Study of the Effects of Relaxed Static Stability on Stability Augmentation System Reliability Requirements. LR 26833, Lockheed California Co., Dec. 20, 1974.
11. Stability and Control, Flight Control, Hydraulic Systems and Related Structures Criteria. Doc. No. D6-6800-5, Boeing Co., Jan. 1970.
12. Chalk, C. R.; Neal, T. P.; Harris, T. M.; Pritchard, F. E.; and Woodcock, R. J.: Background Information and User Guide for MIL-F-8785B(ASG), "Military Specification - Flying Qualities of Piloted Airplanes." AFFDL-TR-69-72, U.S. Air Force, Aug. 1969. (Available from DDC as AD 860 856.)

13. Low-Wing-Loading STOL Transport Ride Smoothing Feasibility Study. D3-8514-2 (Contract NAS1-10410), Boeing Company, Feb. 8, 1971. (Available as NASA CR-111819.)
14. Tentative Airworthiness Standards for Supersonic Transports. Flight Standards Service, FAA, Nov. 1, 1965, Revision 7, Jan. 1, 1971.
15. Parlett, Lysle P.; Fink, Marvin P.; and Freeman, Delma C., Jr. (With appendix B by Marion O. McKinney and Joseph L. Johnson, Jr.): Wind-Tunnel Investigation of a Large Jet Transport Model Equipped With an External-Flow Jet Flap. NASA TN D-4928, 1968.
16. Shomber, H. A.; and Gertsen, W. M.: Longitudinal Handling Qualities Criteria: An Evaluation. AIAA Paper No. 65-780, Nov. 1965.
17. Aerospace Recommended Practice: Design Objectives for Flying Qualities of Civil Transport Aircraft. ARP 842B, Soc. Automot. Eng., Aug. 1, 1964. Revised Nov. 30, 1970.
18. Sudderth, Robert W.; Bohn, Jeff G.; Caniff, Martin A.; and Bennett, Gregory R.: Development of Longitudinal Handling Qualities Criteria for Large Advanced Supersonic Aircraft. NASA CR-137635, 1975.



TABLE I.- MASS AND DIMENSIONAL CHARACTERISTICS OF SIMULATED
SUPERSONIC CRUISE TRANSPORT AIRPLANES

(a) Baseline concept

Weight, N (lbf)	1 924 479 (432 640)
Reference wing area, m ² (ft ²)	784.75 (8447)
Wing span, m (ft)	38.66 (126.83)
Wing leading-edge sweep, deg (see fig. 2)	74.00/70.84/60.00
Reference mean aerodynamic chord, m (ft)	27.00 (88.59)
Center-of-gravity location, percent \bar{c}	56
Static margin, percent	-3.9
I _X , kg-m ² (slug-ft ²)	6 887 550 (5 080 000)
I _Y , kg-m ² (slug-ft ²)	67 994 260 (50 150 000)
I _Z , kg-m ² (slug-ft ²)	72 902 230 (53 770 000)
I _{XZ} , kg-m ² (slug-ft ²)	-2 833 660 (-2 090 000)

Maximum control surface deflections:

δ_t , deg	±20
δ_f , deg	0 to 40
δ_a , deg	±30
δ_{af} , deg	±22.5
δ_s , deg	±50
δ_r , deg	±35

Maximum control surface deflection rates:

$\dot{\delta}_t$, deg/sec	±50
$\dot{\delta}_f$, deg/sec	±10
$\dot{\delta}_a$, deg/sec	±70
$\dot{\delta}_{af}$, deg/sec	±40
$\dot{\delta}_s$, deg/sec	±50
$\dot{\delta}_r$, deg/sec	±50

Horizontal tail:

Gross horizontal-tail area, m ² (ft ²)	49.80 (536)
Mean aerodynamic chord, m (ft)	6.04 (19.80)
Distance from center of gravity to horizontal-tail 0.25 \bar{c} , m (ft)	32.90 (107.93)

Vertical tail:

Exposed vertical-tail area, m ² (ft ²)	16.72 (180)
Mean aerodynamic chord, m (ft)	6.35 (20.83)
Distance from center of gravity to vertical-tail 0.25 \bar{c} , m (ft)	36.41 (119.46)

TABLE I.- Concluded

(b) Powered-lift concept

Weight, N (lbf)	1 924 479 (432 640)
Reference wing area, m ² (ft ²)	784.75 (8447)
Wing span, m (ft)	38.66 (126.83)
Wing leading-edge sweep, deg (see fig. 3)	74.00/70.84/60.00
Reference mean aerodynamic chord, m (ft)	27.00 (88.59)
Center-of-gravity location, percent \bar{c}	66
Static margin, percent	-9.5
I _X , kg-m ² (slug-ft ²)	6 937 629 (5 117 000)
I _Y , kg-m ² (slug-ft ²)	65 860 697 (48 577 000)
I _Z , kg-m ² (slug-ft ²)	70 713 105 (52 156 000)
I _{XZ} , kg-m ² (slug-ft ²)	-2 779 390 (-2 050 000)

Maximum control surface deflections:

δ_t , deg	±20
δ_f , deg	0 to 40
δ_a , deg	±30
δ_{afo} , deg	±20
δ_{afi} , deg	±30
δ_r , deg	±25

Maximum control surface deflection rates:

$\dot{\delta}_t$, deg/sec	±50
$\dot{\delta}_f$, deg/sec	±10
$\dot{\delta}_a$, deg/sec	±70
$\dot{\delta}_{afo}$, deg/sec	±40
$\dot{\delta}_{afi}$, deg/sec	±40
$\dot{\delta}_r$, deg/sec	±50

Horizontal tail:

Gross horizontal-tail area, m ² (ft ²)	88.83 (956)
Mean aerodynamic chord, m (ft)	7.13 (23.39)
Distance from center of gravity to horizontal-tail 0.25 \bar{c} , m (ft)	29.76 (97.62)

Vertical tail:

Exposed vertical-tail area, m ² (ft ²)	34.84 (375)
Mean aerodynamic chord, m (ft)	9.16 (30.07)
Distance from center of gravity to vertical-tail 0.25 \bar{c} , m (ft)	33.27 (109.16)



TABLE II.- AERODYNAMIC INPUTS USED IN SIMULATION OF BASELINE CONCEPT

α , deg	Aerodynamic inputs for -								
	$C_{X,o}$	$C_{Z,o}$	$C_{X\delta_t}$, deg ⁻¹	$C_{Z\delta_t}$, deg ⁻¹	$C_{X\delta_f}$, deg ⁻¹	$C_{Z\delta_f}$, deg ⁻¹	$C_{m\delta_f}$, deg ⁻¹	C_{X1g}	C_{Z1g}
-4	-0.0484	0.0734	0.00059	-0.0038	-0.00039	-0.00769	-0.0019	-0.0085	0.00059
0	-.0340	-.0920	-.00085	-.0038	-.00045	-.00720	-.0018	-.0085	0
4	-.0203	-.2551	-.00031	-.0038	-.00053	-.00675	-.0017	-.0085	-.00059
8	-.0071	-.4159	.00018	-.0038	-.00061	-.00645	-.0016	-.0084	-.00119
12	.0031	-.5820	.00058	-.0037	-.00073	-.00619	-.0016	-.0083	-.00177
16	.0180	-.7414	.00095	-.0036	-.00096	-.00632	-.0014	-.0082	-.00235
20	.0235	-.9301	.00128	-.0035	-.00095	-.00588	-.0008	-.0080	-.00291

α , deg	$C_m(\delta_f=0)$ for tail deflections of -								
	-20°	-15°	-10°	-5°	0°	5°	10°	15°	20°
-4	0.1080	0.1060	0.1010	0.0843	0.0447	0.0073	-0.0237	-0.0478	-0.0645
0	.1318	.1255	.1113	.0858	.0460	.0083	-.0225	-.0465	-.0630
4	.1463	.1360	.1163	.0870	.0475	.0100	-.0213	-.0453	-.0615
8	.1530	.1403	.1193	.0880	.0487	.0117	-.0190	-.0425	-.0587
12	.1540	.1420	.1213	.0903	.0510	.0142	-.0160	-.0385	-.0535
16	.1570	.1473	.1275	.0977	.0580	.0200	-.0100	-.0305	-.0430
20	.1585	.1490	.1290	.0982	.0600	.0230	-.0057	-.0257	-.0370

TABLE II.- Continued

α , deg	Aerodynamic inputs for -								
	$C_{Y\delta_s}$, deg ⁻¹	$C_{Y\delta_{af}}$, deg ⁻¹	$C_{Y\delta_a}$, deg ⁻¹	$C_{l\delta_s}$, deg ⁻¹	$C_{l\delta_{af}}$, deg ⁻¹	$C_{l\delta_a}$, deg ⁻¹	$C_{n\delta_s}$, deg ⁻¹	$C_{n\delta_{af}}$, deg ⁻¹	$C_{n\delta_a}$, deg ⁻¹
				(a)	(a)	(a)			
-4	-0.00009	-0.00029	-0.00029	0.00019	0.00044	0.00039	0	0.00012	0.00017
0	-.00009	-.00029	-.00028	.00019	.00044	.00038	0	.00011	.00017
4	-.00008	-.00028	-.00028	.00017	.00042	.00038	0	.00011	.00016
8	-.00008	-.00026	-.00026	.00012	.00040	.00036	0	.00009	.00014
12	-.00007	-.00023	-.00023	.00004	.00036	.00033	0	.00007	.00010
16	-.00003	-.00008	-.00008	.00002	.00028	.00029	0	.00003	.00004
20	0	-.00007	0	.00001	.00016	.00022	0	.00002	-.00001

α , deg	Aerodynamic inputs for -					
	$C_{Y\delta_r}$, deg ⁻¹	$C_{l\delta_r}$, deg ⁻¹	$C_{n\delta_r}$, deg ⁻¹	$C_{Y\beta}$, deg ⁻¹	$C_{l\beta}$, deg ⁻¹	$C_{n\beta}$, deg ⁻¹
	(a)	(a)	(a)			
-4	0.00100	-0.00008	-0.00120	-0.00646	-0.00128	0.00183
0	.00100	0	-.00120	-.00654	-.00150	.00176
4	.00100	.00008	-.00120	-.00681	-.00179	.00169
8	.00100	.00017	-.00119	-.00723	-.00219	.00160
12	.00099	.00026	-.00116	-.00789	-.00191	.00131
16	.00091	.00044	-.00101	-.00649	-.00199	.00125
20	.00059	.00043	-.00059	-.00770	-.00200	.00119

^aRigid derivatives.

TABLE II.- Concluded

α , deg	Aerodynamic inputs for -							
	$C_{m\dot{q}}$, rad ⁻¹	$C_{m\dot{\alpha}}$, rad ⁻¹	C_{Yp} , rad ⁻¹	C_{lp} , rad ⁻¹	C_{np} , rad ⁻¹	C_{Yr} , rad ⁻¹	C_{lr} , rad ⁻¹	C_{nr} , rad ⁻¹
-4	-1.2716	-0.1621	0.1233	-0.1279	-0.1113	0.2291	0.0257	-0.3225
0	-1.2680	-.1528	.5094	-.1209	-.1074	.2402	.0879	-.3120
4	-1.2635	-.1404	.8368	-.1237	-.0985	.3016	.1432	-.3009
8	-1.2590	-.1184	1.1793	-.1389	-.0747	.4154	.1946	-.2941
12	-1.2555	-.0844	1.5157	-.1796	.0057	.5815	.2439	-.2712
16	-1.2475	.0165	1.8106	-.2256	.0287	.7817	.2848	-.2389
20	-1.2550	.0672	2.0982	-.2880	.0567	.9837	.3293	-.2003

TABLE III.- AERODYNAMIC INPUTS USED IN SIMULATION OF POWERED-LIFT CONCEPT

[Trailing-edge flaps deflected 40°]

(a) All engines operating

C_T	α , deg	C_x for tail deflections of -								
		-20°	-15°	-10°	-5°	0°	5°	10°	15°	20°
0	-4	-0.1307	-0.1106	-0.0949	-0.0837	-0.0750	-0.0692	-0.0722	-0.0802	-0.0900
0	0	-.1275	-.1072	-.0910	-.0792	-.0702	-.0651	-.0687	-.0772	-.0877
0	4	-.1216	-.1005	-.0840	-.0721	-.0630	-.0585	-.0624	-.0715	-.0822
0	8	-.1148	-.0937	-.0772	-.0653	-.0562	-.0522	-.0565	-.0662	-.0774
0	12	-.1070	-.0858	-.0696	-.0590	-.0517	-.0479	-.0524	-.0628	-.0749
0	16	-.1015	-.0808	-.0654	-.0559	-.0503	-.0468	-.0515	-.0623	-.0745
0	20	-.0983	-.0776	-.0633	-.0556	-.0521	-.0495	-.0536	-.0646	-.0772
.15	-4	-.0604	-.0403	-.0246	-.0134	-.0047	.0011	-.0019	-.0099	-.0197
.15	0	-.0565	-.0362	-.0200	-.0082	.0008	.0059	.0023	-.0062	-.0167
.15	4	-.0498	-.0287	-.0122	-.0003	.0088	.0133	.0094	.0003	-.0104
.15	8	-.0395	-.0184	-.0019	.0100	.0191	.0231	.0188	.0091	-.0021
.15	12	-.0241	-.0029	.0133	.0239	.0312	.0350	.0305	.0201	.0080
.15	16	-.0049	.0158	.0312	.0407	.0443	.0498	.0451	.0343	.0221
.15	20	.0137	.0344	.0487	.0564	.0599	.0625	.0584	.0474	.0348
.30	-4	.0399	.0600	.0757	.0869	.0956	.1014	.0984	.0904	.0806
.30	0	.0437	.0640	.0802	.0920	.1010	.1061	.1025	.0940	.0835
.30	4	.0498	.0709	.0874	.0993	.1084	.1129	.1090	.0999	.0892
.30	8	.0597	.0808	.0973	.1092	.1183	.1223	.1180	.1083	.0971
.30	12	.0762	.0974	.1136	.1242	.1315	.1353	.1308	.1204	.1083
.30	16	.0984	.1191	.1345	.1440	.1496	.1531	.1484	.1376	.1254
.30	20	.1210	.1417	.1560	.1637	.1672	.1698	.1657	.1547	.1421

TABLE III.- Continued

[Trailing-edge flaps deflected 40°]

(a) Continued

C_T	α , deg	C_Z for tail deflections of -								
		-20°	-15°	-10°	-5°	0°	5°	10°	15°	20°
0	-4	-0.0891	-0.0912	-0.0985	-0.1223	-0.1787	-0.2329	-0.2758	-0.3086	-0.3319
0	0	-.1995	-.2095	-.2291	-.2654	-.3216	-.3756	-.4192	-.4515	-.4745
0	4	-.3286	-.3450	-.3728	-.4133	-.4694	-.5235	-.5666	-.5987	-.6211
0	8	-.4610	-.4791	-.5092	-.5517	-.6074	-.6615	-.7044	-.7360	-.7577
0	12	-.6093	-.6271	-.6555	-.6970	-.7530	-.8079	-.8502	-.8806	-.9013
0	16	-.7691	-.7839	-.8104	-.8514	-.9078	-.9622	-1.0030	-1.0311	-1.0494
0	20	-.9410	-.9558	-.9814	-1.0207	-1.0751	-1.1276	-1.1666	-1.1944	-1.2123
.15	-4	-.4098	-.4119	-.4192	-.4430	-.4994	-.5536	-.5965	-.6293	-.6526
.15	0	-.5375	-.5475	-.5671	-.6034	-.6596	-.7136	-.7572	-.7895	-.8125
.15	4	-.6776	-.6940	-.7218	-.7623	-.8184	-.8725	-.9156	-.9477	-.9701
.15	8	-.8287	-.8468	-.8769	-.9194	-.9751	-1.0292	-1.0721	-1.1037	-1.1254
.15	12	-.9902	-1.0080	-1.0364	-1.0779	-1.1339	-1.1888	-1.2311	-1.2615	-1.2822
.15	16	-1.1453	-1.1601	-1.1866	-1.2276	-1.2840	-1.3384	-1.3792	-1.4073	-1.4256
.15	20	-1.3031	-1.3179	-1.3435	-1.3828	-1.4372	-1.4897	-1.5287	-1.5565	-1.5744
.30	-4	-.5305	-.5326	-.5399	-.5637	-.6201	-.6743	-.7172	-.7500	-.7733
.30	0	-.6675	-.6775	-.6971	-.7334	-.7896	-.8436	-.8872	-.9195	-.9425
.30	4	-.8209	-.8373	-.8651	-.9056	-.9617	-1.0158	-1.0589	-1.0910	-1.1134
.30	8	-.9762	-.9943	-1.0244	-1.0669	-1.1226	-1.1767	-1.2196	-1.2512	-1.2729
.30	12	-1.1388	-1.1566	-1.1850	-1.2265	-1.2825	-1.3374	-1.3797	-1.4101	-1.4308
.30	16	-1.3079	-1.3227	-1.3492	-1.3902	-1.4466	-1.5010	-1.5418	-1.5699	-1.5882
.30	20	-1.4737	-1.4885	-1.5141	-1.5534	-1.6078	-1.6603	-1.6993	-1.7271	-1.7450

TABLE III.- Continued

[Trailing-edge flaps deflected 40°]

(a) Concluded

C_T	α , deg	C_m for tail deflections of -								
		-20°	-15°	-10°	-5°	0°	5°	10°	15°	20°
0	-4	0.1173	0.1148	0.1063	0.0785	0.0126	-0.0508	-0.1009	-0.1393	-0.1665
0	0	.1712	.1595	.1366	.0941	.0284	-.0346	-.0856	-.1234	-.1503
0	4	.2087	.1896	.1571	.1097	.0441	-.0191	-.0694	-.1070	-.1332
0	8	.2326	.2114	.1762	.1266	.0615	-.0018	-.0519	-.0889	-.1142
0	12	.2476	.2268	.1936	.1451	.0797	.0155	-.0339	-.0695	-.0937
0	16	.2601	.2428	.2119	.1640	.0980	.0344	-.0132	-.0461	-.0675
0	20	.2717	.2544	.2245	.1785	.1150	.0536	.0080	-.0245	-.0454
.15	-4	.0623	.0598	.0513	.0235	-.0424	-.1058	-.1559	-.1943	-.2215
.15	0	.1159	.1042	.0813	.0388	-.0269	-.0899	-.1409	-.1787	-.2056
.15	4	.1528	.1337	.1012	.0538	-.0118	-.0750	-.1253	-.1629	-.1891
.15	8	.1770	.1558	.1206	.0710	.0059	-.0574	-.1075	-.1445	-.1698
.15	12	.1947	.1739	.1407	.0922	.0268	-.0374	-.0868	-.1224	-.1466
.15	16	.2076	.1903	.1594	.1115	.0455	-.0181	-.0657	-.0986	-.1280
.15	20	.2244	.2071	.1772	.1312	.0677	.0063	-.0393	-.0718	-.0927
.30	-4	.0462	.0437	.0352	.0074	-.0585	-.1219	-.1720	-.2104	-.2376
.30	0	.0966	.0849	.0620	.0195	-.0462	-.1092	-.1602	-.1980	-.2249
.30	4	.1323	.1132	.0807	.0333	-.0323	-.0955	-.1458	-.1834	-.2096
.30	8	.1545	.1333	.0981	.0485	-.0166	-.0799	-.1300	-.1670	-.1923
.30	12	.1709	.1501	.1169	.0684	.0030	-.0612	-.1106	-.1462	-.1704
.30	16	.1839	.1666	.1357	.0878	.0218	-.0418	-.0894	-.1223	-.1437
.30	20	.2012	.1839	.1540	.1080	.0445	-.0169	-.0625	-.0950	-.1159

TABLE III.- Continued

[Trailing-edge flaps deflected 40°]

(b) Number 3 engine failed

C _T	α, deg	C _x for tail deflections of -								
		-20°	-15°	-10°	-5°	0°	5°	10°	15°	20°
0	-4	-0.1307	-0.1106	-0.0949	-0.0837	-0.0750	-0.0692	-0.0722	-0.0802	-0.0900
0	0	-.1275	-.1072	-.0910	-.0792	-.0702	-.0651	-.0687	-.0772	-.0877
0	4	-.1216	-.1005	-.0840	-.0721	-.0630	-.0585	-.0624	-.0715	-.0822
0	8	-.1148	-.0937	-.0772	-.0653	-.0562	-.0522	-.0565	-.0662	-.0774
0	12	-.1070	-.0858	-.0696	-.0590	-.0517	-.0479	-.0524	-.0628	-.0749
0	16	-.1015	-.0808	-.0654	-.0559	-.0503	-.0468	-.0515	-.0623	-.0745
0	20	-.0983	-.0776	-.0633	-.0556	-.0521	-.0495	-.0536	-.0646	-.0772
.15	-4	-.0425	-.0224	-.0067	.0045	.0132	.0190	.0160	.0080	-.0018
.15	0	-.0394	-.0191	-.0029	.0089	.0179	.0230	.0194	.0109	.0004
.15	4	-.0337	-.0126	.0039	.0158	.0249	.0294	.0255	.0164	.0057
.15	8	-.0250	-.0039	.0126	.0245	.0336	.0376	.0333	.0236	.0124
.15	12	-.0115	.0097	.0259	.0365	.0438	.0476	.0431	.0327	.0206
.15	16	.0055	.0262	.0416	.0511	.0567	.0602	.0555	.0447	.0325
.15	20	.0222	.0429	.0572	.0649	.0684	.0710	.0669	.0559	.0433
.30	-4	.0988	.1189	.1346	.1458	.1545	.1603	.1573	.1493	.1395
.30	0	.0992	.1195	.1357	.1475	.1565	.1616	.1580	.1495	.1390
.30	4	.1024	.1235	.1400	.1519	.1610	.1655	.1616	.1525	.1418
.30	8	.1069	.1280	.1445	.1564	.1655	.1695	.1652	.1555	.1443
.30	12	.1137	.1349	.1511	.1617	.1690	.1728	.1683	.1579	.1458
.30	16	.1229	.1436	.1590	.1685	.1741	.1776	.1729	.1621	.1499
.30	20	.1342	.1549	.1692	.1769	.1804	.1830	.1789	.1679	.1553

TABLE III.- Continued

[Trailing-edge flaps deflected 40°]

(b) Continued

C_T	α , deg	C_Z for tail deflections of -								
		-20°	-15°	-10°	-5°	0°	5°	10°	15°	20°
0	-4	-0.0891	-0.0912	-0.0985	-0.1223	-0.1787	-0.2329	-0.2758	-0.3086	-0.3319
0	0	-.1995	-.2095	-.2291	-.2654	-.3216	-.3756	-.4192	-.4515	-.4745
0	4	-.3286	-.3450	-.3728	-.4133	-.4694	-.5235	-.5666	-.5987	-.6211
0	8	-.4610	-.4791	-.5092	-.5517	-.6074	-.6615	-.7044	-.7360	-.7577
0	12	-.6093	-.6271	-.6555	-.6970	-.7530	-.8079	-.8502	-.8806	-.9013
0	16	-.7691	-.7839	-.8104	-.8514	-.9078	-.9622	-1.0030	-1.0311	-1.0494
0	20	-.9410	-.9558	-.9814	-1.0207	-1.0751	-1.1276	-1.1666	-1.1944	-1.2123
.15	-4	-.3390	-.3411	-.3484	-.3722	-.4286	-.4828	-.5257	-.5585	-.5818
.15	0	-.4725	-.4825	-.5021	-.5384	-.5946	-.6486	-.6922	-.7245	-.7475
.15	4	-.6164	-.6328	-.6606	-.7011	-.7572	-.8113	-.8544	-.8865	-.9089
.15	8	-.7692	-.7873	-.8174	-.8599	-.9156	-.9697	-1.0126	-1.0442	-1.0659
.15	12	-.9324	-.9502	-.9786	-1.0201	-1.0761	-1.1310	-1.1733	-1.2037	-1.2244
.15	16	-1.0901	-1.1049	-1.1314	-1.1724	-1.2288	-1.2832	-1.3240	-1.3521	-1.3704
.15	20	-1.2496	-1.2644	-1.2900	-1.3293	-1.3837	-1.4362	-1.4752	-1.5030	-1.5209
.30	-4	-.3120	-.3141	-.3214	-.3452	-.4016	-.4558	-.4987	-.5315	-.5548
.30	0	-.4565	-.4665	-.4861	-.5224	-.5786	-.6326	-.6702	-.7085	-.7315
.30	4	-.6154	-.6318	-.6596	-.7001	-.7562	-.8103	-.8534	-.8855	-.9079
.30	8	-.7742	-.7923	-.8224	-.8649	-.9206	-.9747	-1.0176	-1.0492	-1.0709
.30	12	-.9372	-.9550	-.9834	-1.0249	-1.0809	-1.1358	-1.1781	-1.2035	-1.2292
.30	16	-1.1157	-1.1305	-1.1570	-1.1980	-1.2544	-1.3088	-1.3496	-1.3777	-1.3969
.30	20	-1.2898	-1.3046	-1.3302	-1.3695	-1.4239	-1.4764	-1.5154	-1.5432	-1.5600

TABLE III.- Continued

[Trailing-edge flaps deflected 40°]

(b) Concluded

C _T	α, deg	C _m for tail deflections of -								
		-20°	-15°	-10°	-5°	0°	5°	10°	15°	20°
0	-4	0.1173	0.1148	0.1063	0.0785	0.0126	-0.0508	-0.1009	-0.1393	-0.1665
0	0	.1712	.1595	.1366	.0941	.0284	-.0346	-.0856	-.1234	-.1503
0	4	.2087	.1896	.1571	.1097	.0441	-.0191	-.0694	-.1070	-.1332
0	8	.2326	.2114	.1762	.1266	.0615	-.0018	-.0519	-.0889	-.1142
0	12	.2476	.2268	.1936	.1451	.0797	.0155	-.0339	-.0695	-.0937
0	16	.2601	.2428	.2119	.1640	.0980	.0344	-.0132	-.0461	-.0675
0	20	.2717	.2544	.2245	.1785	.1150	.0536	.0080	-.0245	-.0454
.15	-4	.0831	.0806	.0721	.0443	-.0216	-.0850	-.1351	-.1735	-.2007
.15	0	.1357	.1240	.1011	.0586	-.0071	-.0701	-.1211	-.1589	-.1858
.15	4	.1725	.1534	.1209	.0735	.0079	-.0553	-.1056	-.1432	-.1694
.15	8	.1948	.1736	.1384	.0888	.0237	-.0396	-.0897	-.1267	-.1520
.15	12	.2131	.1923	.1591	.1106	.0452	-.0190	-.0684	-.1040	-.1282
.15	16	.2272	.2099	.1790	.1311	.0651	.0015	-.0461	-.0790	-.1004
.15	20	.2443	.2270	.1971	.1511	.0876	.0262	-.0194	-.0519	-.0728
.30	-4	.0961	.0936	.0851	.0573	-.0086	-.0720	-.1221	-.1605	-.1877
.30	0	.1452	.1335	.1106	.0681	.0024	-.0606	-.1116	-.1494	-.1763
.30	4	.1798	.1607	.1282	.0808	.0152	-.0480	-.0983	-.1359	-.1621
.30	8	.1991	.1779	.1427	.0931	.0280	-.0353	-.0854	-.1224	-.1477
.30	12	.2155	.1947	.1615	.1130	.0476	-.0166	-.0660	-.1016	-.1258
.30	16	.2304	.2131	.1822	.1343	.0683	.0047	-.0429	-.0758	-.0972
.30	20	.2490	.2317	.2018	.1558	.0923	.0309	-.0147	-.0472	-.0631

TABLE III.- Continued

[Trailing-edge flaps deflected 40°]

(c) Number 4 engine failed

C_T	α , deg	C_X for tail deflections of -								
		-20°	-15°	-10°	-5°	0°	5°	10°	15°	20°
0	-4	-0.1307	-0.1106	-0.0949	-0.0837	-0.0750	-0.0692	-0.0722	-0.0802	-0.0900
0	0	-.1275	-.1072	-.0910	-.0792	-.0702	-.0651	-.0687	-.0772	-.0877
0	4	-.1216	-.1005	-.0840	-.0721	-.0630	-.0585	-.0624	-.0715	-.0822
0	8	-.1148	-.0937	-.0772	-.0653	-.0562	-.0522	-.0565	-.0662	-.0774
0	12	-.1070	-.0858	-.0696	-.0590	-.0517	-.0479	-.0524	-.0628	-.0749
0	16	-.1015	-.0808	-.0654	-.0559	-.0503	-.0468	-.0515	-.0623	-.0745
0	20	-.0983	-.0776	-.0633	-.0556	-.0521	-.0495	-.0536	-.0646	-.0772
.15	-4	-.0798	-.0597	-.0440	-.0328	-.0241	-.0183	-.0213	-.0293	-.0391
.15	0	-.0762	-.0559	-.0397	-.0279	-.0189	-.0138	-.0174	-.0259	-.0304
.15	4	-.0694	-.0483	-.0318	-.0199	-.0108	-.0063	-.0102	-.0193	-.0300
.15	8	-.0586	-.0375	-.0210	-.0091	0	.0040	-.0003	-.0100	-.0212
.15	12	-.0414	-.0202	-.0040	.0060	.0139	.0177	.0132	.0028	-.0093
.15	16	-.0192	.0015	.0169	.0264	.0320	.0355	.0308	.0200	.0078
.15	20	.0032	.0239	.0382	.0459	.0494	.0520	.0479	.0369	.0243
.30	-4	.0240	.0441	.0598	.0710	.0797	.0855	.0825	.0745	.0647
.30	0	.0257	.0460	.0622	.0740	.0830	.0881	.0845	.0760	.0655
.30	4	.0307	.0518	.0683	.0802	.0893	.0938	.0899	.0808	.0701
.30	8	.0397	.0608	.0773	.0892	.0983	.1023	.0980	.0883	.0771
.30	12	.0538	.0750	.0912	.1018	.1091	.1129	.1084	.0980	.0859
.30	16	.0733	.0940	.1094	.1189	.1245	.1280	.1233	.1125	.1003
.30	20	.0962	.1169	.1312	.1389	.1424	.1450	.1409	.1299	.1173

TABLE III.- Continued

[Trailing-edge flaps deflected 40°]

(c) Continued

C_T	α , deg	C_Z for tail deflections of -								
		-20°	-15°	-10°	-5°	0°	5°	10°	15°	20°
0	-4	-0.0891	-0.0912	-0.0985	-0.1223	-0.1787	-0.2329	-0.2758	-0.3086	-0.3319
0	0	-.1995	-.2095	-.2291	-.2654	-.3216	-.3756	-.4192	-.4515	-.4745
0	4	-.3286	-.3450	-.3728	-.4133	-.4694	-.5235	-.5666	-.5987	-.6211
0	8	-.4610	-.4791	-.5092	-.5517	-.6074	-.6615	-.7044	-.7360	-.7577
0	12	-.6093	-.6271	-.6555	-.6970	-.7530	-.8079	-.8502	-.8806	-.9013
0	16	-.7691	-.7839	-.8104	-.8514	-.9078	-.9622	-1.0030	-1.0311	-1.0494
0	20	-.9410	-.9558	-.9814	-1.0207	-1.0751	-1.1276	-1.1666	-1.1944	-1.2123
.15	-4	-.4645	-.4666	-.4739	-.4977	-.5541	-.6083	-.6512	-.6840	-.7073
.15	0	-.5945	-.6045	-.6241	-.6604	-.7166	-.7706	-.8142	-.8465	-.8695
.15	4	-.7349	-.7513	-.7791	-.8196	-.8757	-.9298	-.9729	-1.0050	-1.0274
.15	8	-.8843	-.9024	-.9325	-.9750	-1.0307	-1.0848	-1.1277	-1.1593	-1.1810
.15	12	-1.0440	-1.0618	-1.0902	-1.1317	-1.1877	-1.2426	-1.2849	-1.3153	-1.3360
.15	16	-1.1984	-1.2132	-1.2397	-1.2807	-1.3371	-1.3915	-1.4323	-1.4604	-1.4787
.15	20	-1.3545	-1.3693	-1.3949	-1.4342	-1.4886	-1.5411	-1.5801	-1.6079	-1.6258
.30	-4	-.5630	-.5651	-.5724	-.5962	-.6526	-.7068	-.7497	-.7825	-.8058
.30	0	-.7005	-.7105	-.7301	-.7664	-.8226	-.8766	-.9202	-.9525	-.9755
.30	4	-.8524	-.8688	-.8966	-.9371	-.9932	-1.0473	-1.0904	-1.1225	-1.1449
.30	8	-1.0042	-1.0223	-1.0524	-1.0949	-1.1506	-1.2047	-1.2476	-1.2792	-1.3009
.30	12	-1.1604	-1.1782	-1.2066	-1.2481	-1.3041	-1.3590	-1.4013	-1.4317	-1.4524
.30	16	-1.3321	-1.3469	-1.3734	-1.4144	-1.4708	-1.5252	-1.5660	-1.5941	-1.6124
.30	20	-1.4996	-1.5144	-1.5400	-1.5793	-1.6337	-1.6862	-1.7252	-1.7530	-1.7709

TABLE III.- Continued

[Trailing-edge flaps deflected 40°]

(c) Concluded

C_T	α , deg	C_m for tail deflections of -								
		-20°	-15°	-10°	-5°	0°	5°	10°	15°	20°
0	-4	0.1173	0.1148	0.1063	0.0785	0.0126	-0.0508	-0.1009	-0.1393	-0.1665
0	0	.1712	.1595	.1366	.0941	.0284	-.0346	-.0856	-.1234	-.1503
0	4	.2087	.1896	.1571	.1097	.0441	-.0191	-.0694	-.1070	-.1332
0	8	.2326	.2114	.1762	.1266	.0615	-.0018	-.0519	-.0889	-.1142
0	12	.2476	.2268	.1936	.1451	.0797	.0155	-.0339	-.0695	-.0937
0	16	.2601	.2428	.2119	.1640	.0980	.0344	-.0132	-.0461	-.0675
0	20	.2717	.2544	.2245	.1785	.1150	.0536	.0080	-.0245	-.0454
.15	-4	.0535	.0510	.0425	.0147	-.0512	-.1146	-.1647	-.2031	-.2303
.15	0	.1061	.0944	.0715	.0290	-.0367	-.0997	-.1507	-.1885	-.2154
.15	4	.1431	.1240	.0915	.0441	-.0215	-.0847	-.1350	-.1726	-.1988
.15	8	.1664	.1452	.1100	.0604	-.0047	-.0680	-.1181	-.1551	-.1804
.15	12	.1849	.1641	.1309	.0824	.0170	-.0472	-.0966	-.1322	-.1564
.15	16	.1994	.1821	.1512	.1033	.0373	-.0263	-.0739	-.1068	-.1282
.15	20	.2167	.1994	.1695	.1235	.0600	-.0014	-.0470	-.0795	-.1004
.30	-4	.0369	.0344	.0259	-.0019	-.0678	-.1312	-.1813	-.2197	-.2469
.30	0	.0859	.0742	.0513	.0088	-.0569	-.1199	-.1709	-.2087	-.2356
.30	4	.1211	.1020	.0695	.0221	-.0435	-.1067	-.1570	-.1946	-.2208
.30	8	.1422	.1210	.0858	.0362	-.0289	-.0922	-.1423	-.1793	-.2046
.30	12	.1591	.1383	.1051	.0566	-.0088	-.0730	-.1224	-.1580	-.1822
.30	16	.1747	.1574	.1265	.0786	.0126	-.0510	-.0986	-.1315	-.1529
.30	20	.1939	.1766	.1467	.1007	.0372	-.0242	-.0698	-.1023	-.1232

TABLE III.- Continued

[Trailing-edge flaps deflected 40°]

(d) Aerodynamic inputs

C_T	α , deg	Aerodynamic inputs for -					
		$C_{Y\beta}$	$C_{l\beta}$	$C_{n\beta}$	$C_{Y\delta_r}$ (a)	$C_{l\delta_r}$ (a)	$C_{n\delta_r}$ (a)
0	-4	-0.00616	-0.00038	0.00176	0.00161	0.00019	-0.00173
0	0	-.00510	-.00140	.00206	.00160	.00013	-.00179
0	4	-.00420	-.00212	.00217	.00155	.00009	-.00179
0	8	-.00359	-.00278	.00206	.00144	.00007	-.00170
0	12	-.00324	-.00329	.00167	.00106	.00007	-.00150
0	16	-.00191	-.00382	.00223	.00061	.00012	-.00119
0	20	.00189	-.00408	.00376	.00045	.00020	-.00105
.15	-4	-.00649	-.00035	.00176	.00194	.00016	-.00173
.15	0	-.00544	-.00140	.00207	.00194	.00013	-.00180
.15	4	-.00453	-.00214	.00219	.00188	.00011	-.00181
.15	8	-.00389	-.00280	.00211	.00174	.00009	-.00175
.15	12	-.00346	-.00330	.00175	.00128	.00008	-.00158
.15	16	-.00203	-.00380	.00231	.00073	.00010	-.00127
.15	20	.00188	-.00404	.00383	.00047	.00016	-.00112
.30	-4	-.00681	-.00033	.00176	.00226	.00014	-.00173
.30	0	-.00578	-.00140	.00208	.00228	.00013	-.00181
.30	4	-.00487	-.00216	.00220	.00222	.00013	-.00182
.30	8	-.00420	-.00282	.00216	.00205	.00011	-.00180
.30	12	-.00368	-.00331	.00183	.00150	.00009	-.00166
.30	16	-.00215	-.00378	.00238	.00085	.00008	-.00134
.30	20	.00186	-.00401	.00390	.00048	.00013	-.00119

^aRigid derivatives.

TABLE III.- Continued
 [Trailing-edge flaps deflected 40°]

(d) Continued

C_T	α , deg	Input due to No. 3 engine failure			C_T	α , deg	Input due to No. 4 engine failure		
		ΔC_Y	ΔC_L	ΔC_N			ΔC_Y	ΔC_L	ΔC_N
0	-4	0	0	0	0	-4	0	0	0
0	0	0	0	0	0	0	0	0	0
0	4	0	0	0	0	4	0	0	0
0	8	0	0	0	0	8	0	0	0
0	12	0	0	0	0	12	0	0	0
0	16	0	0	0	0	16	0	0	0
0	20	0	0	0	0	20	0	0	0
.15	-4	-.0030	.0153	.0034	.15	-4	0	.0018	.0267
.15	0	-.0042	.0154	.0034	.15	0	0	.0001	.0269
.15	4	-.0048	.0160	.0033	.15	4	0	-.0015	.0267
.15	8	-.0052	.0170	.0033	.15	8	0	-.0033	.0264
.15	12	-.0071	.0182	.0034	.15	12	0	-.0048	.0259
.15	16	-.0122	.0199	.0034	.15	16	0	-.0063	.0250
.15	20	-.0204	.0217	.0046	.15	20	0	-.0077	.0241
.30	-4	-.0060	.0307	.0068	.30	-4	0	.0032	.0535
.30	0	-.0084	.0309	.0067	.30	0	0	.0002	.0537
.30	4	-.0097	.0321	.0066	.30	4	0	-.0028	.0535
.30	8	-.0103	.0340	.0066	.30	8	0	-.0058	.0529
.30	12	-.0142	.0365	.0067	.30	12	0	-.0087	.0519
.30	16	-.0244	.0399	.0068	.30	16	0	-.0114	.0505
.30	20	-.0409	.0434	.0091	.30	20	0	-.0139	.0487

TABLE III.- Continued

[Trailing-edge flaps deflected 40°]

(d) Continued

C_T α , deg		Aerodynamic inputs for -								
		$C_{Y\delta_a}$, deg ⁻¹	$C_{l\delta_a}$, deg ⁻¹	$C_{n\delta_a}$, deg ⁻¹	C_{Yafi} , deg ⁻¹	C_{lafi} , deg ⁻¹	C_{nafi} , deg ⁻¹	C_{Yafo} , deg ⁻¹	C_{lafo} , deg ⁻¹	C_{nafo} , deg ⁻¹
		(a)			(a)			(a)		
0	-4	-0.00038	0.00042	0.00009	-0.00015	0.00050	0.00007	-0.00008	0.00036	0.00005
0	0	-0.00040	.00046	.00009	-.00027	.00049	.00008	-.00007	.00033	.00009
0	4	-.00041	.00046	.00009	-.00033	.00048	.00008	-.00006	.00029	.00013
0	8	-.00041	.00043	.00009	-.00035	.00047	.00007	-.00006	.00024	.00014
0	12	-.00039	.00036	.00008	-.00033	.00048	.00006	-.00005	.00018	.00012
0	16	-.00035	.00028	.00007	-.00029	.00048	.00006	-.00004	.00014	.00004
0	20	-.00013	.00024	.00010	-.00025	.00041	.00008	-.00004	.00013	.00002
.15	-4	-0.00038	.00042	.00009	-.00015	.00050	.00007	-.00038	.00087	.00021
.15	0	-0.00040	.00046	.00009	-.00027	.00049	.00008	-.00036	.00085	.00024
.15	4	-.00041	.00046	.00009	-.00033	.00048	.00008	-.00035	.00082	.00028
.15	8	-.00041	.00043	.00009	-.00035	.00047	.00007	-.00042	.00078	.00029
.15	12	-.00039	.00036	.00008	-.00033	.00048	.00006	-.00045	.00072	.00026
.15	16	-.00035	.00028	.00007	-.00029	.00048	.00006	-.00042	.00065	.00016
.15	20	-.00013	.00024	.00010	-.00025	.00041	.00008	-.00040	.00061	.00014
.30	-4	-0.00038	.00042	.00009	-.00015	.00050	.00007	-.00068	.00137	.00037
.30	0	-0.00040	.00046	.00009	-.00027	.00049	.00008	-.00065	.00137	.00039
.30	4	-.00041	.00046	.00009	-.00033	.00048	.00008	-.00065	.00134	.00041
.30	8	-.00041	.00043	.00009	-.00035	.00047	.00007	-.00078	.00131	.00043
.30	12	-.00039	.00036	.00008	-.00033	.00048	.00006	-.00085	.00125	.00039
.30	16	-.00035	.00028	.00007	-.00029	.00048	.00006	-.00080	.00116	.00029
.30	20	-.00013	.00024	.00010	-.00025	.00041	.00008	-.00077	.00110	.00027

^aRigid derivatives.

TABLE III.- Concluded

[Trailing-edge flaps deflected 40°]

(d) Concluded

C_T	α , deg	Aerodynamic inputs for -							
		$C_{m\dot{q}}$, rad ⁻¹	$C_{m\dot{\alpha}}$, rad ⁻¹	C_{Yp} , rad ⁻¹	C_{l_p} , rad ⁻¹	C_{n_p} , rad ⁻¹	C_{Yr} , rad ⁻¹	C_{l_r} , rad ⁻¹	C_{n_r} , rad ⁻¹
0	-4	-1.5641	-0.4239	0.0897	-0.1206	-0.1150	0.2328	0.0117	-0.3848
0	0	-1.5604	-.4146	.5094	-.1209	-.1074	.2339	.0917	-.4057
0	4	-1.5560	-.4022	.8682	-.1204	-.0909	.2823	.1373	-.3899
0	8	-1.5515	-.3749	1.2427	-.1171	-.0661	.3959	.1822	-.3227
0	12	-1.5480	-.3257	1.6091	-.0922	-.0065	.5518	.2048	-.1692
0	16	-1.5400	-.2049	1.9096	-.0970	.0868	.7052	.2740	-.3599
0	20	-1.5475	-.1279	2.0000	.0112	-.1388	.7511	.2076	.2884
.15	-4	-1.5641	-.4239	.4429	-.1876	-.2575	.2328	.1292	-.3467
.15	0	-1.5604	-.4146	.8637	-.2243	-.2652	.2339	.2080	-.3510
.15	4	-1.5560	-.4022	1.2102	-.2595	-.2688	.2823	.2424	-.3198
.15	8	-1.5515	-.3749	1.5630	-.2930	-.2761	.3959	.2704	-.2384
.15	12	-1.5480	-.3257	1.8732	-.3004	-.2538	.5518	.2664	-.0754
.15	16	-1.5400	-.2049	2.0663	-.3212	-.1921	.7052	.3002	-.2668
.15	20	-1.5475	-.1279	2.1070	-.1863	-.4454	.7511	.1947	.3722
.30	-4	-1.5641	-.4239	.5691	-.2216	-.3099	.2328	.1747	-.3237
.30	0	-1.5604	-.4146	1.0000	-.2755	-.3259	.2339	.2527	-.3199
.30	4	-1.5560	-.4022	1.3601	-.3315	-.3437	.2823	.2837	-.2795
.30	8	-1.5515	-.3749	1.7161	-.3801	-.3642	.3959	.3020	-.1927
.30	12	-1.5480	-.3257	2.0255	-.3984	-.3566	.5518	.2841	-.0271
.30	16	-1.5400	-.2049	2.2301	-.4373	-.3226	.7052	.3016	-.2148
.30	20	-1.5475	-.1279	2.2750	-.3433	-.6023	.7511	.1761	.4222

TABLE IV.- PILOT RATING SYSTEM

<p>CONTROLLABLE</p> <p>Capable of being controlled or managed in context of mission, with available pilot attention.</p>	<p>ACCEPTABLE</p> <p>May have deficiencies which warrant improvement, but adequate for mission.</p> <p>Pilot compensation, if required to achieve acceptable performance, is feasible.</p>	<p>SATISFACTORY</p> <p>Meets all requirements and expectations; good enough without improvement.</p>	<p>Excellent, highly desirable.</p> <p>Good, pleasant, well behaved.</p>	<p>1</p> <p>2</p>
		<p>Clearly adequate for mission.</p>	<p>Fair. Some mildly unpleasant characteristics. Good enough for mission without improvement.</p>	<p>3</p>
		<p>UNSATISFACTORY</p> <p>Reluctantly acceptable. Deficiencies which warrant improvement. Performance adequate for mission with feasible pilot compensation.</p>	<p>Some minor but annoying deficiencies. Improvement is requested. Effect on performance is easily compensated for by pilot.</p>	<p>4</p>
		<p>Moderately objectionable deficiencies. Improvement is needed. Reasonable performance requires considerable pilot compensation.</p>	<p>5</p>	
		<p>Very objectionable deficiencies. Major improvements are needed. Requires best available pilot compensation to achieve acceptable performance.</p>	<p>6</p>	
		<p>UNACCEPTABLE</p> <p>Deficiencies which require improvement. Inadequate performance for mission even with maximum feasible pilot compensation.</p>	<p>Major deficiencies which require improvement for acceptance. Controllable. Performance inadequate for mission, or pilot compensation required for minimum acceptable performance in mission is too high.</p>	<p>7</p>
		<p>Controllable with difficulty. Requires substantial pilot skill and attention to retain control and continue mission.</p>	<p>8</p>	
		<p>Marginally controllable in mission. Requires maximum available pilot skill and attention to retain control.</p>	<p>9</p>	
		<p>UNCONTROLLABLE</p> <p>Control will be lost during some portion of mission.</p>	<p>Uncontrollable in mission.</p>	<p>10</p>

TABLE V.- DYNAMIC STABILITY CHARACTERISTICS OF SIMULATED SUPERSONIC CRUISE

TRANSPORT AIRPLANES

[Approach speed was 153 knots]

(a) Baseline concept

Parameters	Augmentation				Satisfactory criterion	Acceptable criterion
	None	HSAS (a)	SCAS (a)	Modified SCAS (a)		
Short-period mode						
ω_{sp} , rad/sec	0.171	0.751	1.534	1.534	See figure 38	See figure 38
P_{sp} , sec	42.72	8.71	15.12	15.12	-----	-----
ζ_{sp}	0.507	0.693	1.036	1.036	0.35 to 1.30	0.25 to 2.00
L_{α}/ω_{sp}	2.32	0.529	0.259	0.259	See figure 38	See figure 38
n/α , g units/rad	3.19	3.19	3.19	3.19	See figure 38	See figure 38
Long-period (aperiodic) mode						
t_2 , sec	4.79	43.86	∞	∞	-----	>6
Long-period (periodic) mode						
ω_{ph} , rad/sec	-----	0.067	0.080	0.080	-----	-----
P_{ph} , sec	-----	125.2	98.9	98.9	-----	-----
ζ_{ph}	-----	0.649	0.609	0.609	≥ 0.04	≥ 0
Roll mode						
τ_R , sec	1.689	0.850	0.270	0.241	≤ 1.4	≤ 3.0
Spiral mode						
$t_{1/2}$, sec	23.1	15.5	∞	∞	-----	-----
Dutch roll mode						
ω_d , rad/sec	0.805	0.522	0.741	0.562	≥ 0.4	≥ 0.4
ζ_d	0.079	0.450	0.266	0.259	≥ 0.08	≥ 0.02
$\zeta_d \omega_d$, rad/sec	0.064	0.235	0.197	0.146	≥ 0.15	≥ 0.05
P_d , sec	7.83	13.47	8.79	11.58	-----	-----
ϕ/β	2.5	2.10	0.80	0.71	-----	-----
Roll-control parameters						
ω_{ϕ}/ω_d	0.565	0.874	1.004	1.025	0.80 to 1.15	0.65 to 1.35
ζ_{ϕ}/ζ_d	3.12	0.589	0.962	0.987	-----	-----

^aAutothrottle on.

TABLE V.- Concluded

[Approach speed was 153 knots]

(b) Powered-lift concept

Parameters	Augmentation				Satisfactory criterion	Acceptable criterion
	None	HSAS (a)	SCAS (a)	Modified SCAS (a)		
Short-period mode						
ω_{sp} , rad/sec	0.185	0.962	0.756	0.756	See figure 38	See figure 38
P_{sp} , sec	45.14	9.09	34.70	34.70	-----	-----
ζ_{sp}	0.259	0.697	0.971	0.971	0.35 to 1.30	0.25 to 2.00
L_{α}/ω_{sp}	2.25	0.432	0.550	0.550	See figure 38	See figure 38
n/α , g units/rad	3.34	3.34	3.34	3.34	See figure 38	See figure 38
Long-period (aperiodic) mode						
t_2 , sec	2.98	90.94	∞	∞	-----	>6
Long-period (periodic) mode						
ω_{ph} , rad/sec	-----	0.066	0.066	0.066	-----	-----
P_{ph} , sec	-----	110.32	106.12	106.12	-----	-----
ζ_{ph}	-----	0.506	0.444	0.444	≥ 0.04	≥ 0
Roll mode						
T_R , sec	1.017	0.351	0.238	0.218	≤ 1.4	≤ 3.0
Spiral mode						
$t_{1/2}$, sec	128.6	178.2	∞	∞	-----	-----
Dutch roll mode						
ω_d , rad/sec	0.685	0.524	0.617	0.528	≥ 0.4	≥ 0.4
ζ_d	0.051	0.205	0.269	0.254	≥ 0.08	≥ 0.02
$\zeta_d \omega_d$, rad/sec	0.035	0.107	0.166	0.134	≥ 0.15	≥ 0.05
P_d , sec	9.18	12.24	10.57	12.01	-----	-----
ϕ/β	2.0	1.1	≈ 0	≈ 0	-----	-----
Roll-control parameters						
ω_{ϕ}/ω_d	0.695	0.908	0.994	0.996	0.80 to 1.15	0.65 to 1.35
P_{ϕ}/P_d	4.65	1.16	0.970	0.961	-----	-----

^aAutothrottle on.

TABLE VI.- CONTROL RESPONSE CHARACTERISTICS OF SIMULATED SUPERSONIC CRUISE

TRANSPORT AIRPLANES

[Approach speed was 153 knots]

(a) Baseline concept

Parameters	Augmentation				Satisfactory criterion	Acceptable criterion
	None	HSAS (a)	SCAS (a)	Modified SCAS (a)		
Longitudinal						
$\ddot{\Theta}_{\max}$, rad/sec ²	b-0.06	b-0.05	b-0.06	Same as SCAS ^a	b-0.08	b-0.05
$\dot{\Theta}/\dot{\Theta}_{ss}$	-----	-----	See figure 40		See figure 40	-----
$\Delta a_n/\ddot{\Theta}$, g/deg/sec ²	-----	-----	See figure 15		-----	See figure 15
Lateral						
$\ddot{\phi}_{\max}$, rad/sec ²	0.211	0.188	0.190	0.190	See figure 41	See figure 41
$\dot{\phi}_{\max}$, deg/sec	14.94	9.3	19.9	15.7	-----	See figure 42
p_2/p_1	-0.155	0.803	0.940	0.992	≥ 0.60	≥ 0.25
ϕ_{osc}/ϕ_{av}	0.801	0.012	0.011	0.015	See figure 43	See figure 43
$t_{\phi=30^\circ}$, sec	2.9	4.0	2.7	2.9	≤ 2.5	≤ 3.2

^aAutothrottle on.^bMinimum demonstrated speed of 125 knots.

TABLE VI.- Concluded

[Approach speed was 153 knots]

(b) Powered-lift concept

Parameters	Augmentation				Satisfactory criterion	Acceptable criterion
	None	HSAS (a)	SCAS (a)	Modified SCAS (a)		
Longitudinal						
$\ddot{\Theta}_{max}$, rad/sec ²	b-0.13	b-0.10	b-0.13	Same as SCAS ^a	b-0.08	b-0.05
$\dot{\Theta}/\dot{\Theta}_{ss}$	-----	-----	See figure 40		See figure 40	-----
$\Delta a_n/\ddot{\Theta}$, g/deg/sec ² . . .	-----	-----	See figure 15		-----	See figure 15
Lateral						
$\ddot{\phi}_{max}$, rad/sec ²	0.470	0.400	0.433	0.299	See figure 41	See figure 41
$\dot{\phi}_{max}$, deg/sec	>30	25.9	25.0	17.0	-----	See figure 42
P ₂ /P ₁	0.792	0.196	0.995	0.988	≥0.60	≥0.25
ϕ_{osc}/ϕ_{av}	0.531	0.037	~0	0.004	See figure 43	See figure 43
t _{φ=30°} , sec	1.78	2.07	1.88	2.54	≤2.5	≤3.2

^aAutothrottle on.

^bMinimum demonstrated speed of 125 knots.

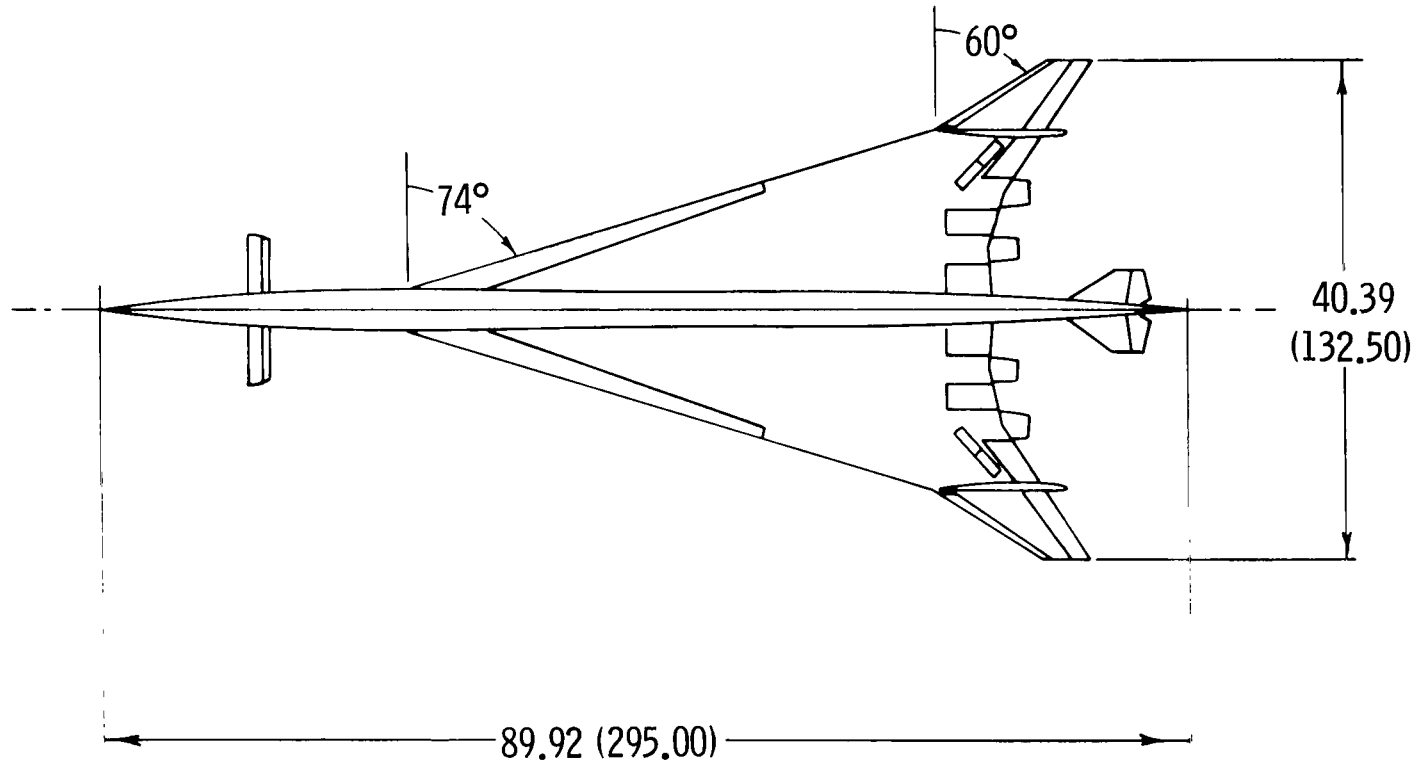


Figure 1.- Boeing model 969-336C based on NASA SCAT-15F configuration.
All linear dimensions are in meters (feet).

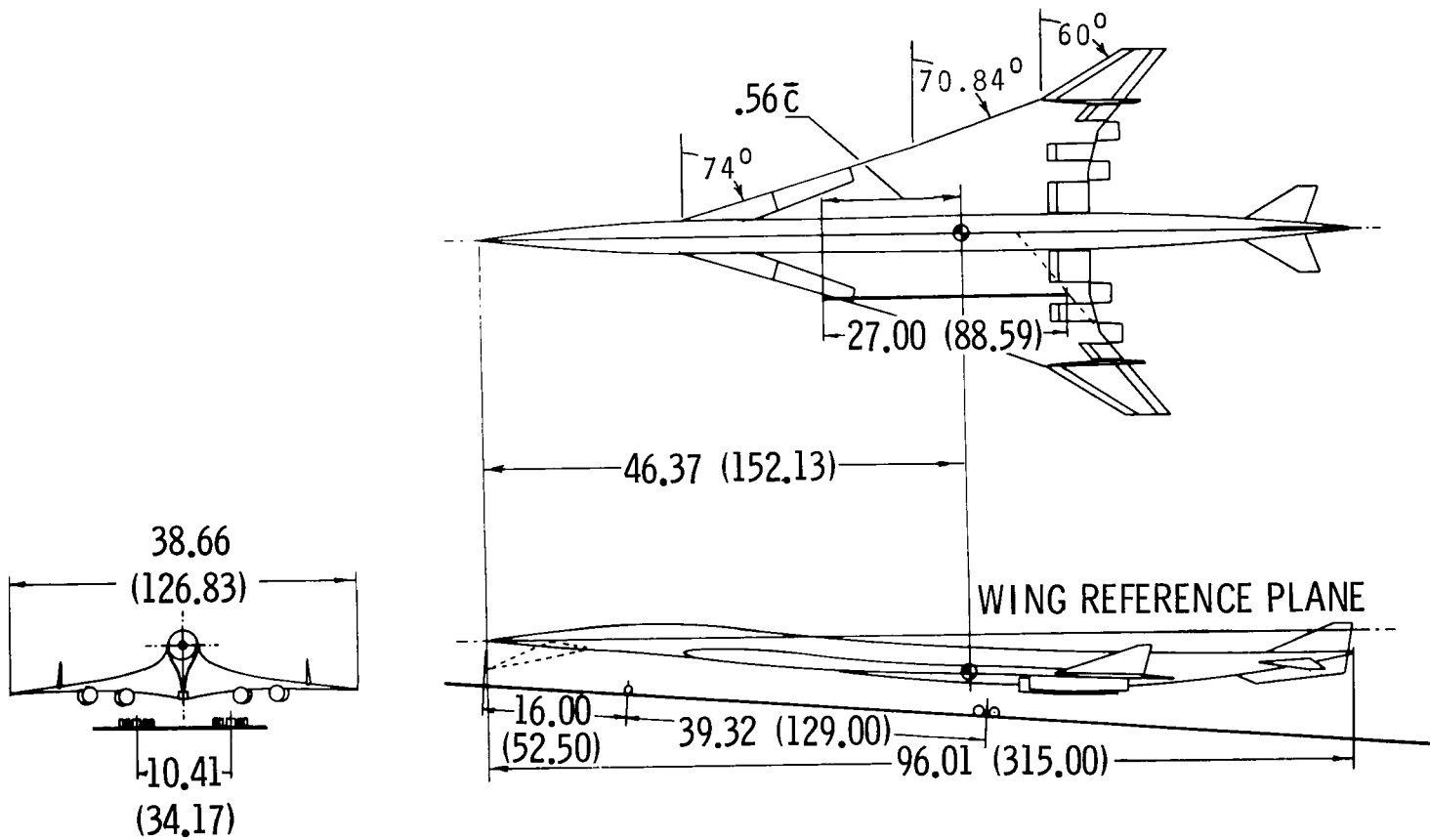


Figure 2.- Baseline supersonic cruise transport simulated.
All linear dimensions are in meters (feet).

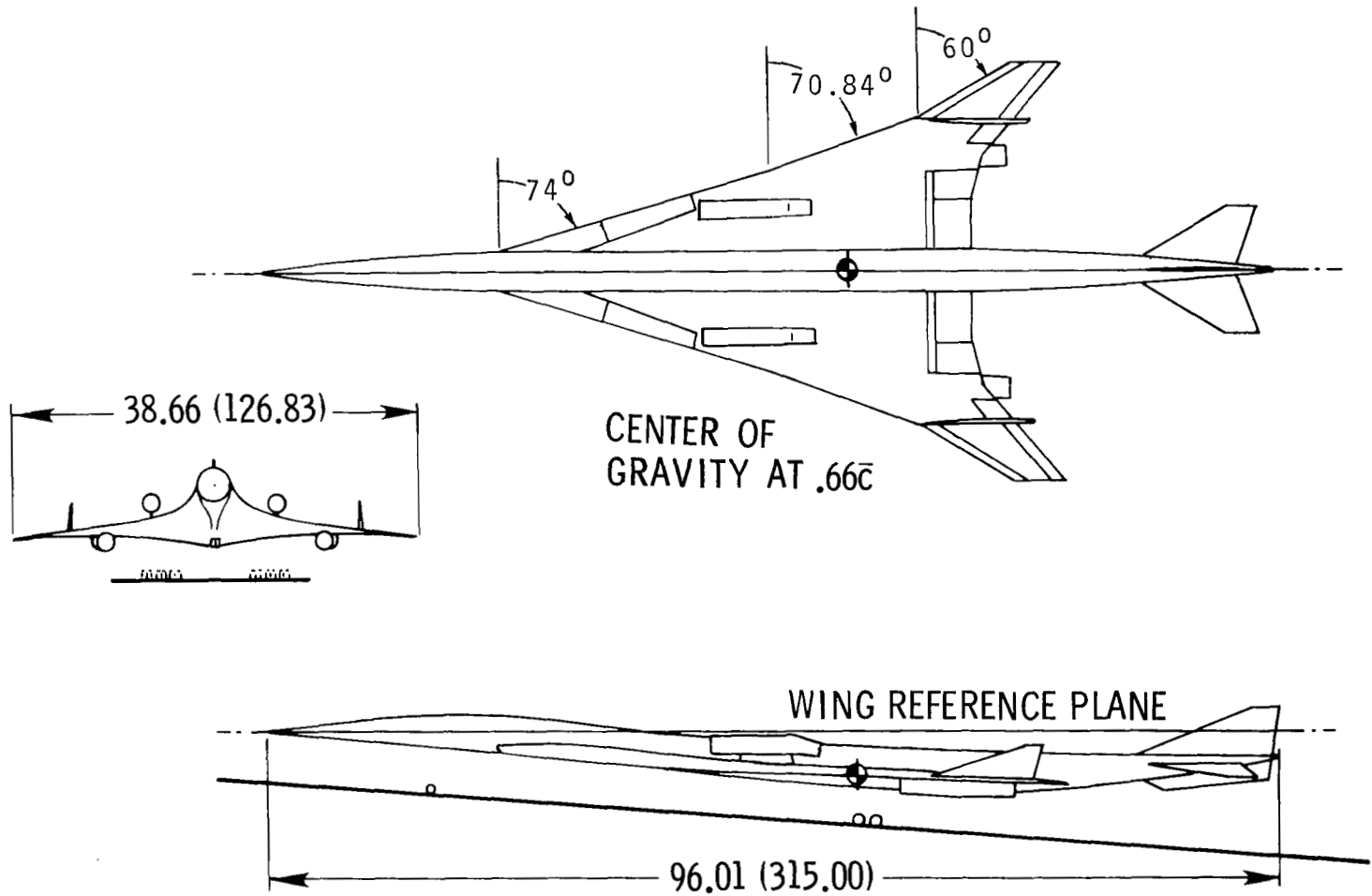
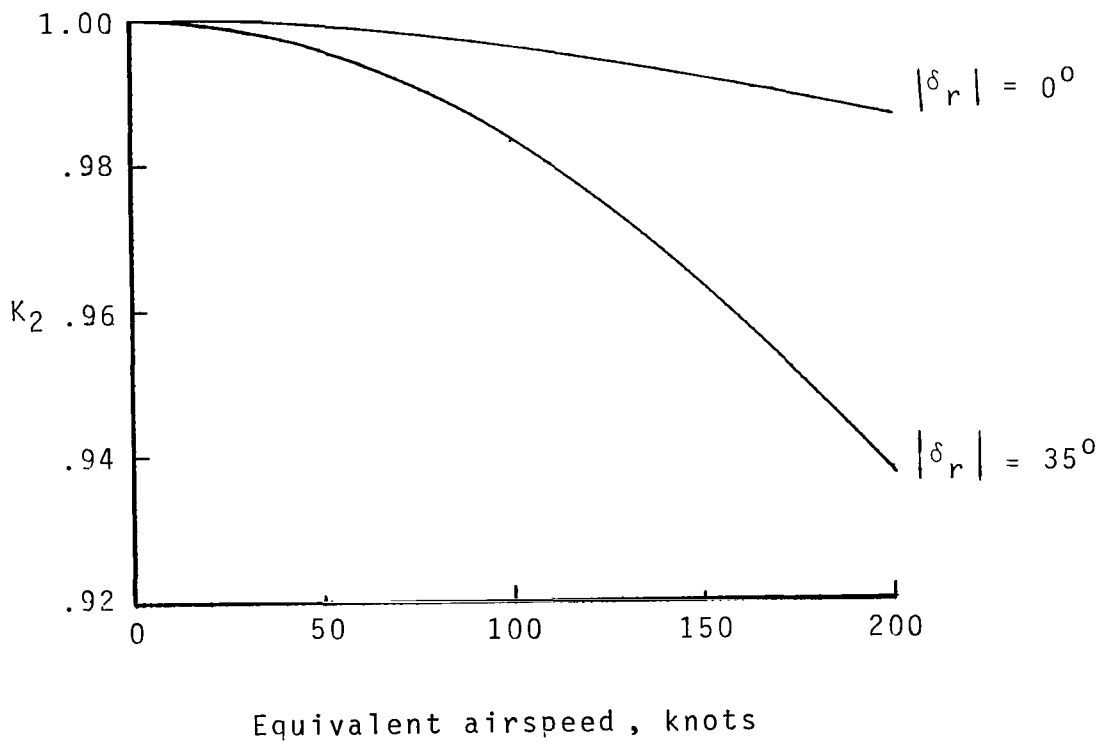
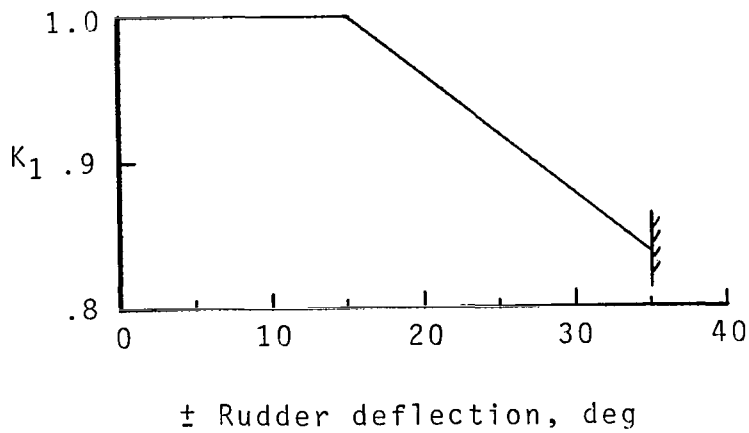
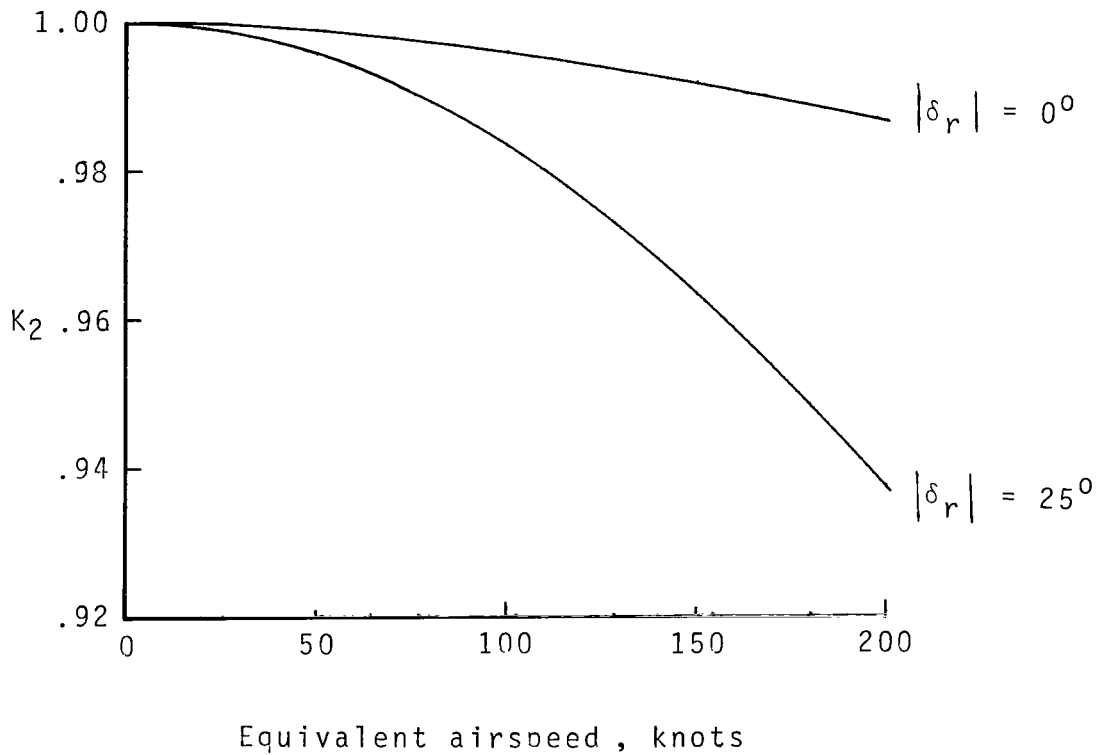
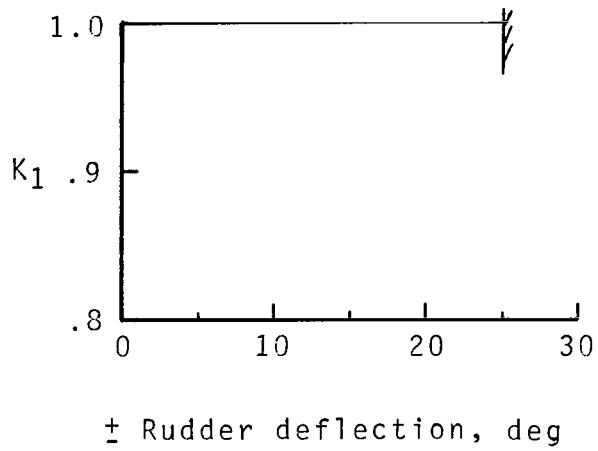


Figure 3.- Powered-lift supersonic cruise transport simulated.
All linear dimensions are in meters (feet).



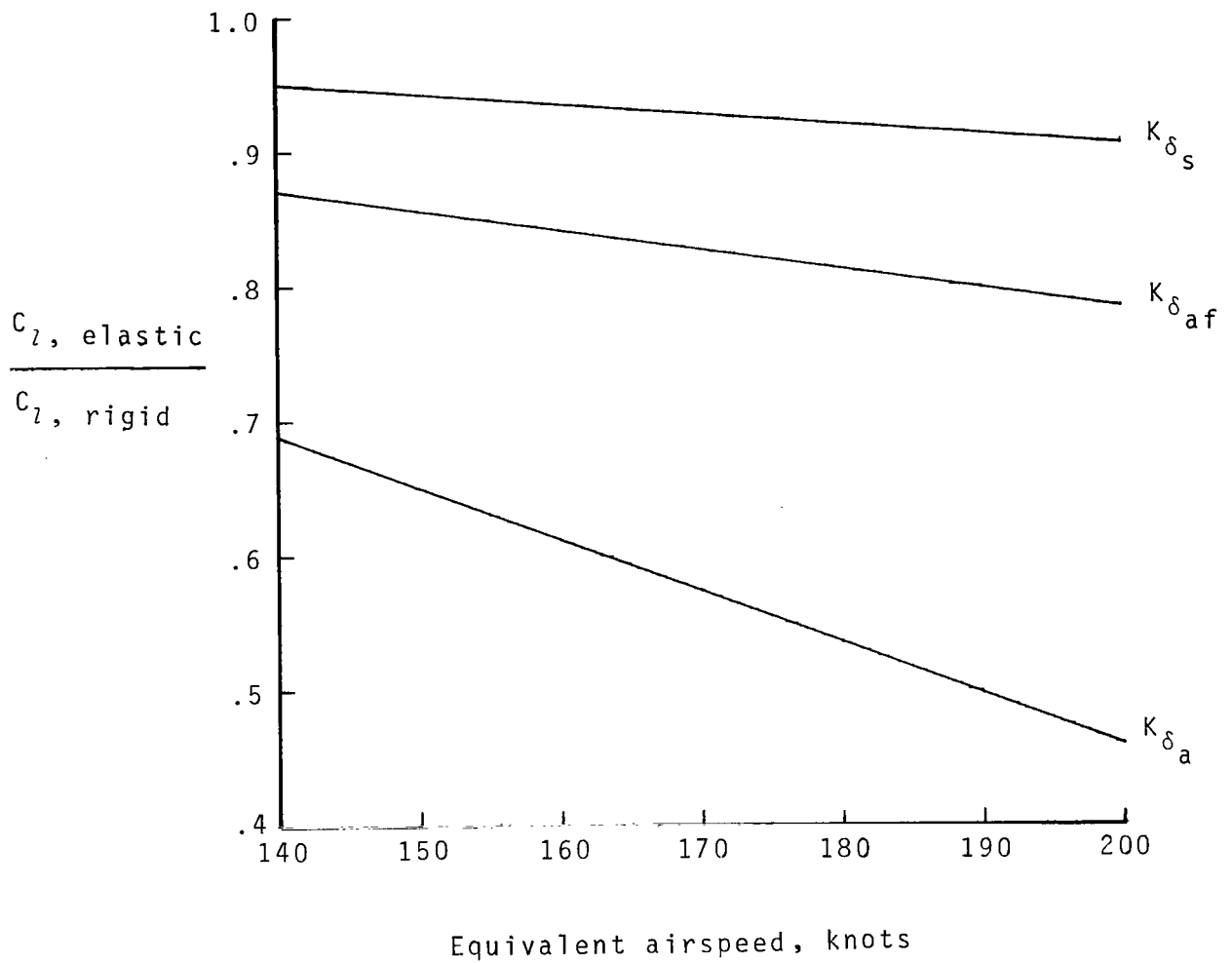
(a) Flexibility effects and rudder effectiveness for baseline concept.

Figure 4.- Flexibility effects on lateral and directional control effectiveness.



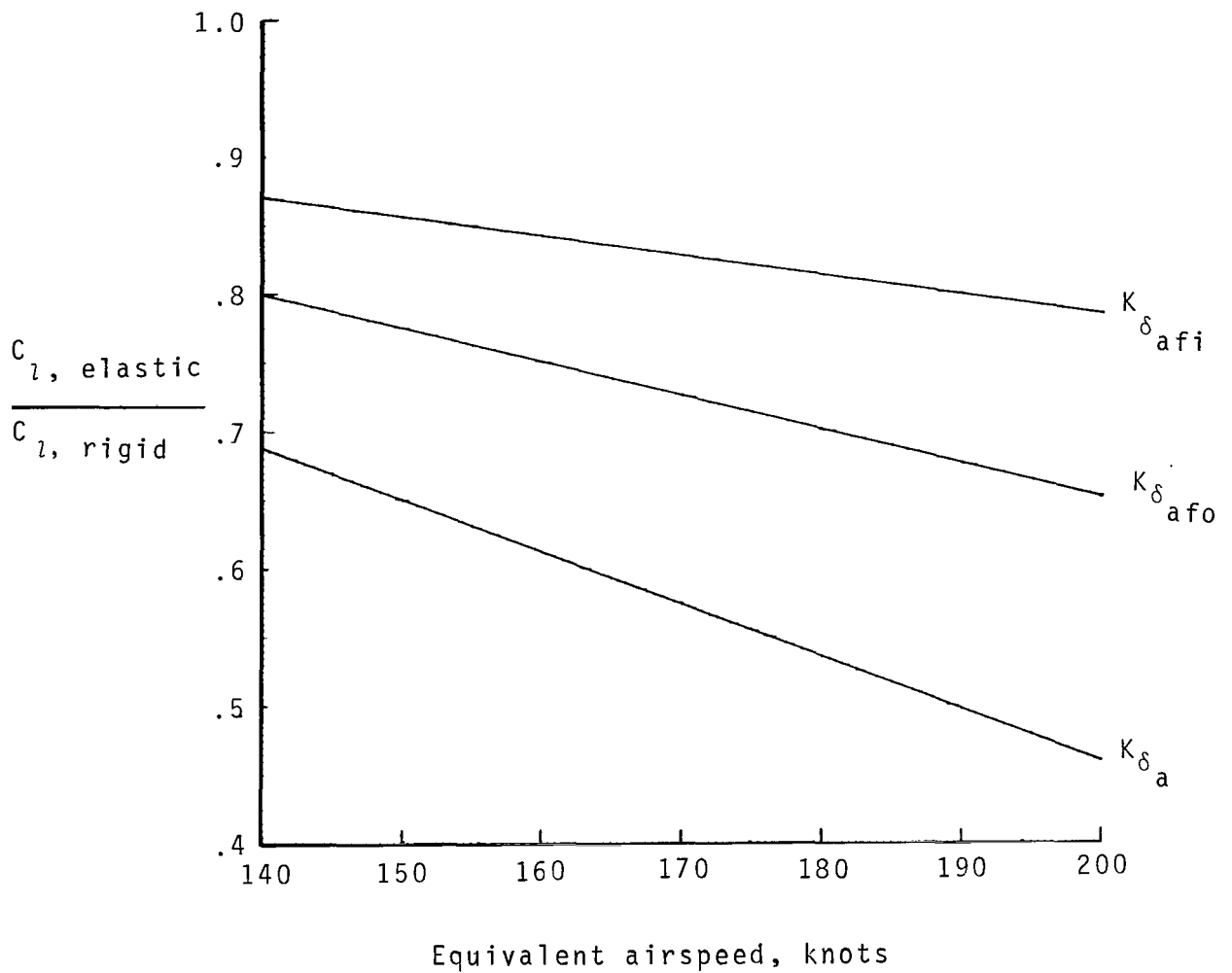
(b) Flexibility effects and rudder effectiveness for powered-lift concept.

Figure 4.- Continued.



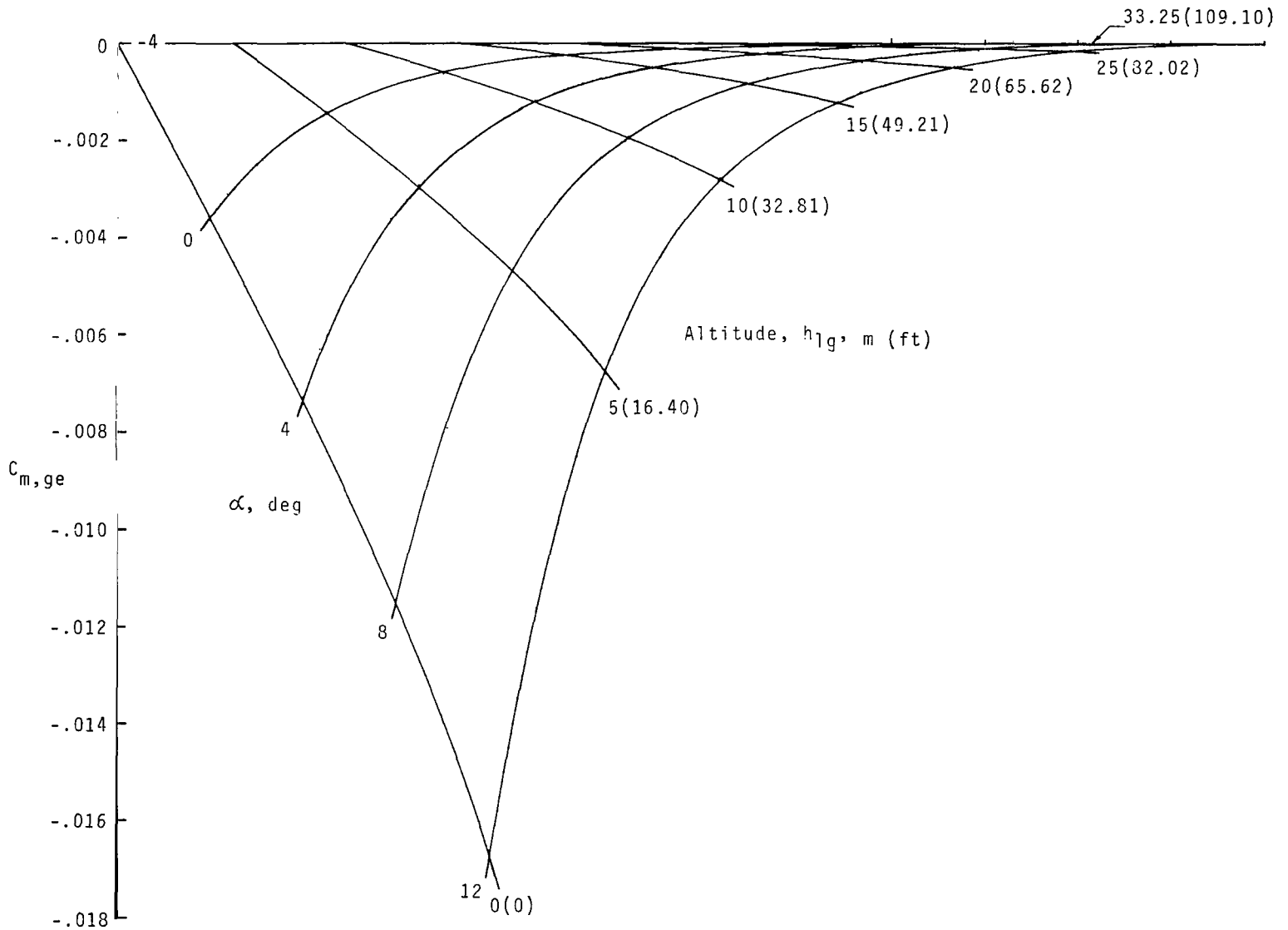
(c) Flexibility effects on roll-control effectiveness for baseline concept.

Figure 4.- Continued.



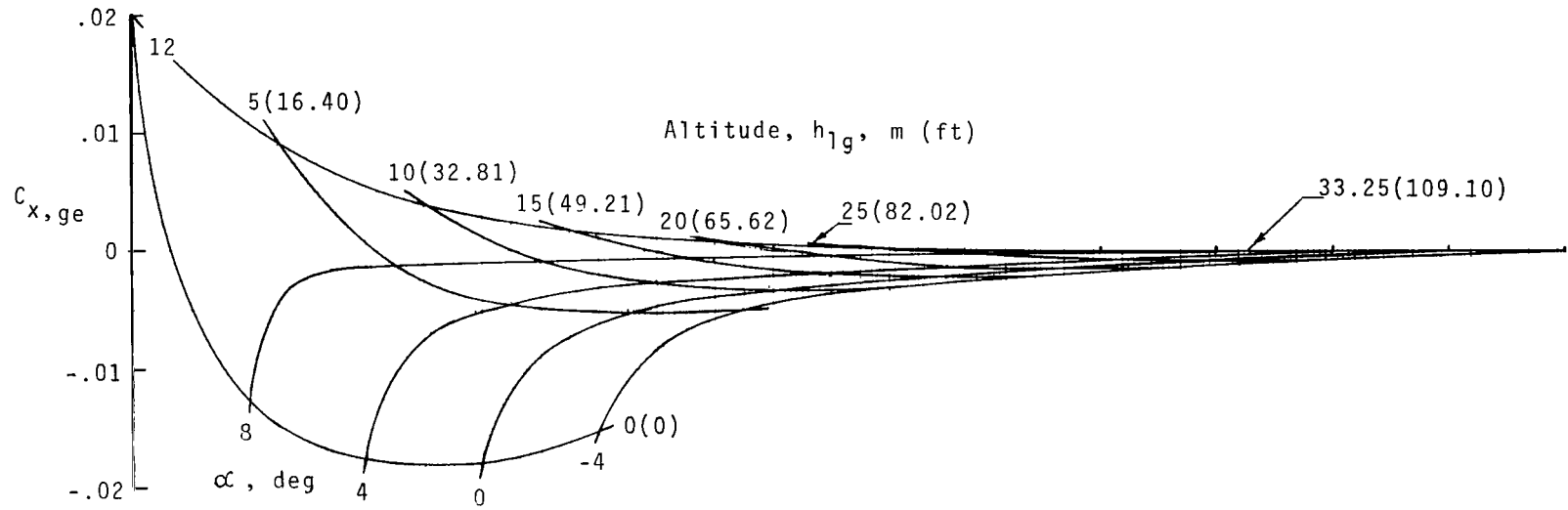
(d) Flexibility effects on roll-control effectiveness for powered-lift concept.

Figure 4.- Concluded.



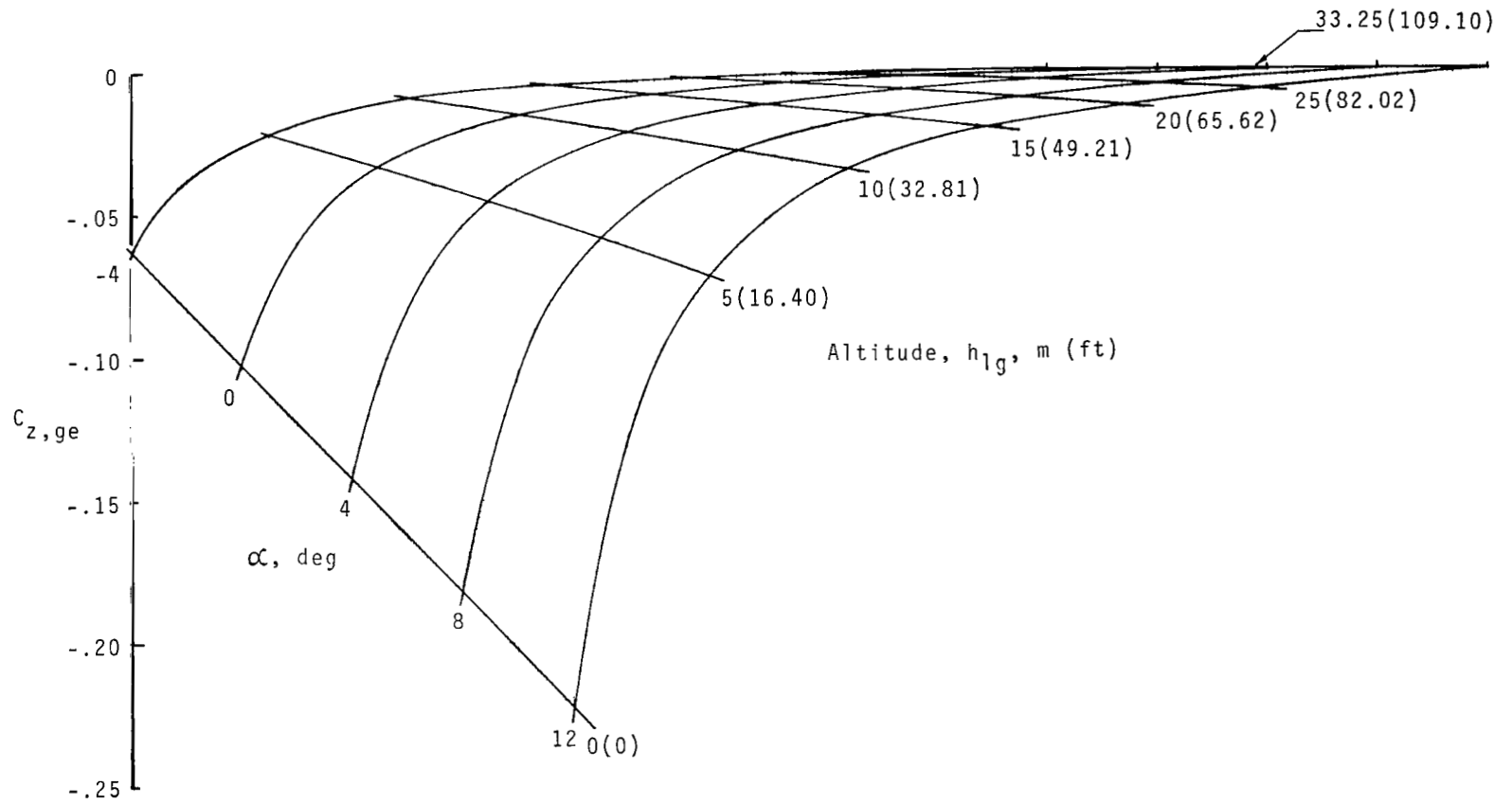
(a) Incremental changes in pitching-moment coefficient due to ground effects.

Figure 5.- Incremental changes in pitching-moment, longitudinal-force, and vertical-force coefficients due to ground effects.



(b) Incremental changes in longitudinal-force coefficient due to ground effects.

Figure 5.- Continued.



(c) Incremental changes in vertical-force coefficient due to ground effects.

Figure 5.- Concluded.

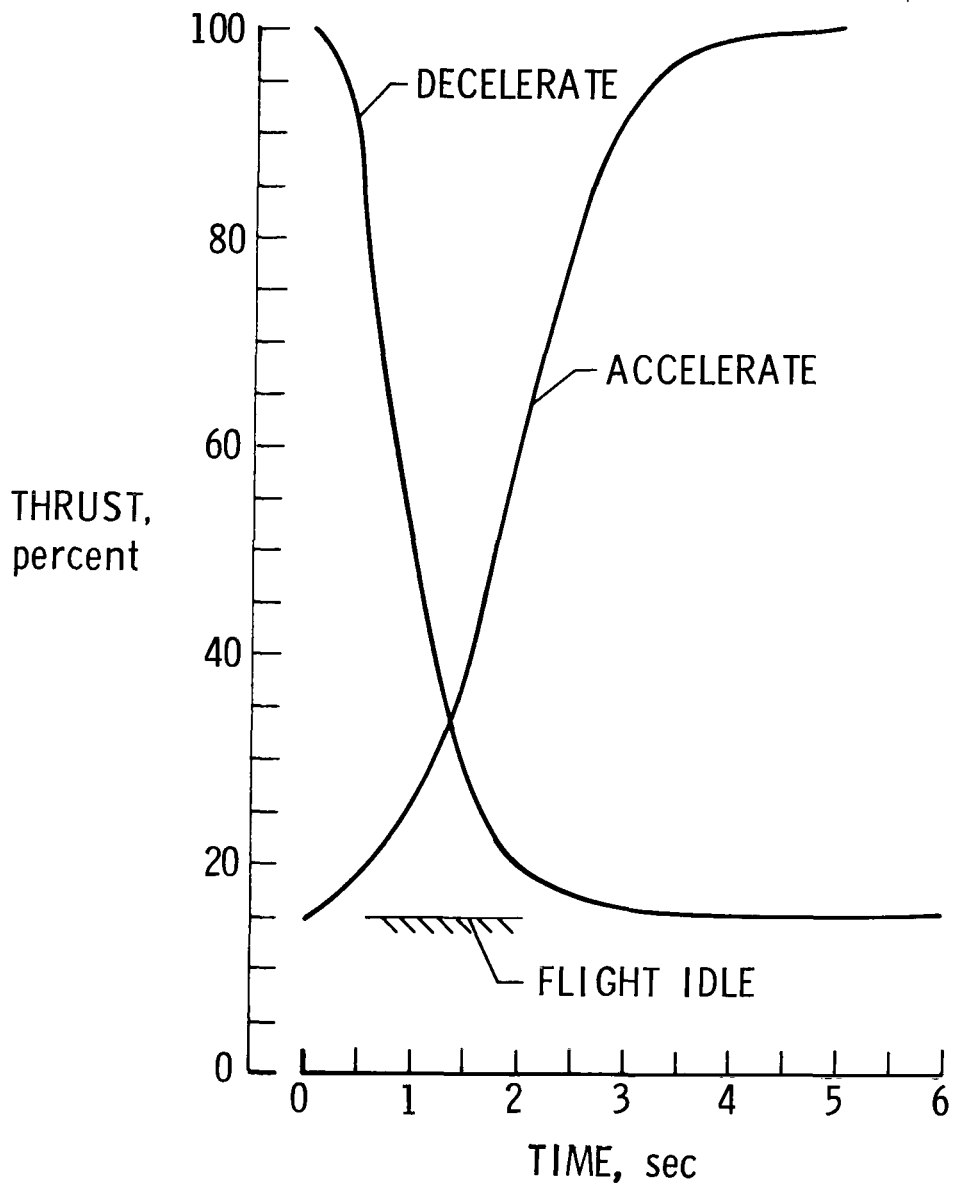
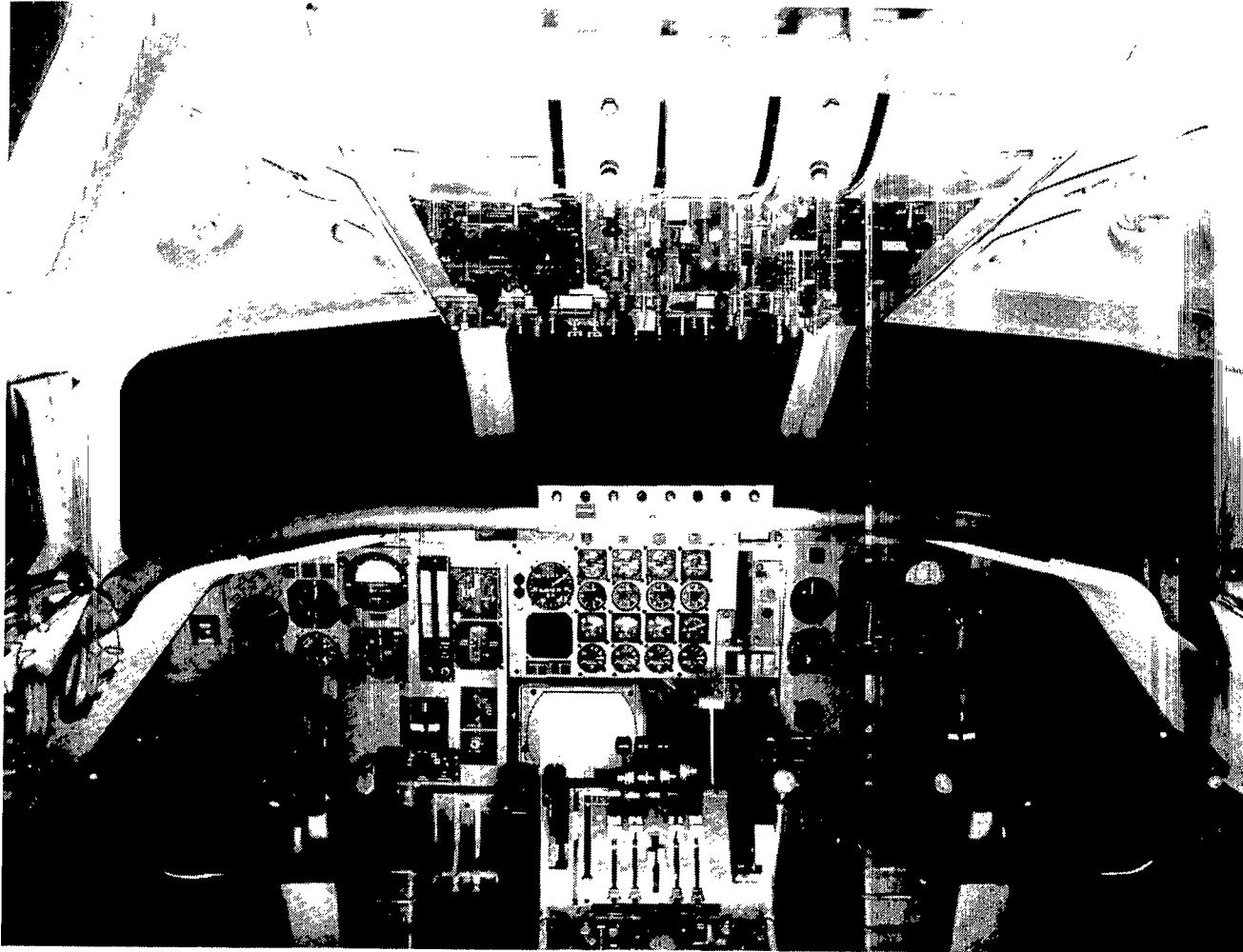


Figure 6.- Example of engine response characteristics.





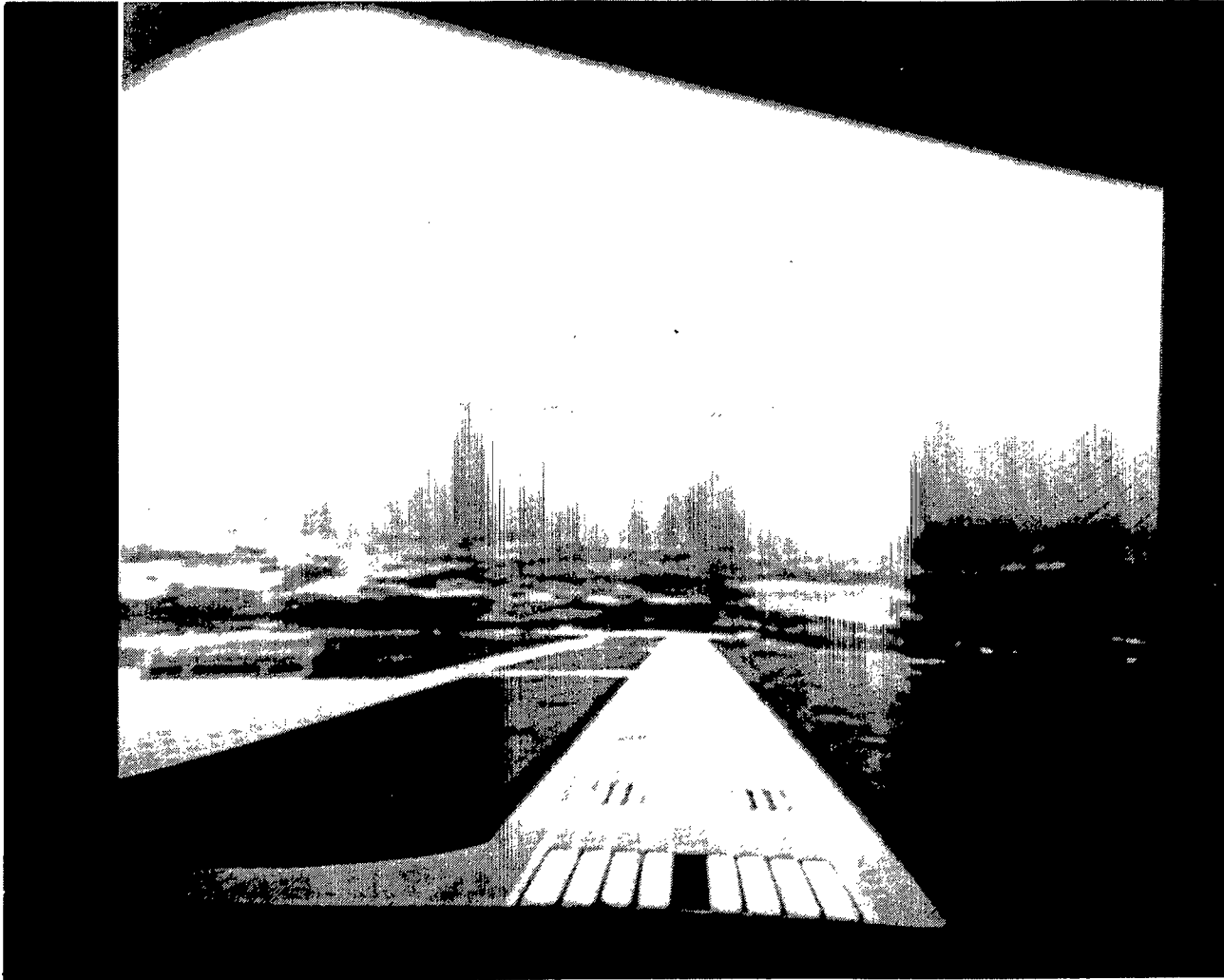
L-78-78

Figure 7.- Fixed-base simulator cockpit and instrument display.



L-78-79

Figure 8.- Photograph of landing scene equipment and airport model.



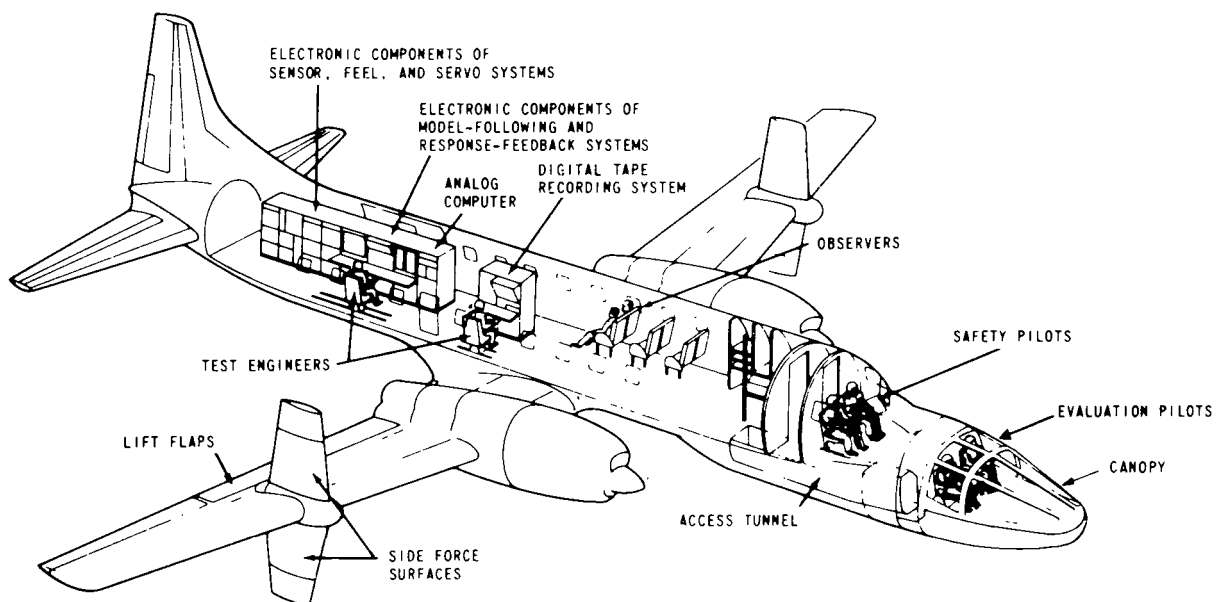
L-78-80

Figure 9.- View of runway as seen by pilot prior to touchdown.



L-78-81

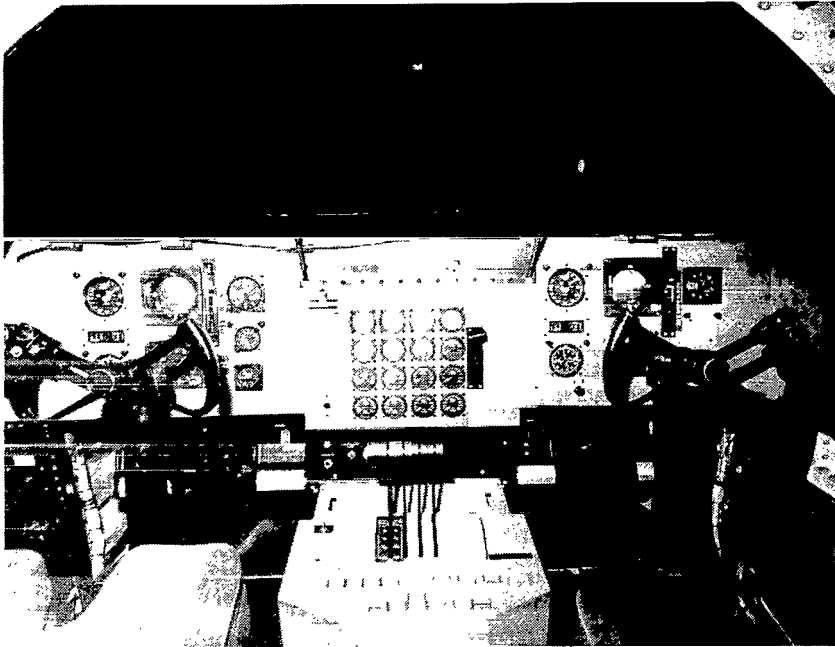
(a) TIFS airplane.



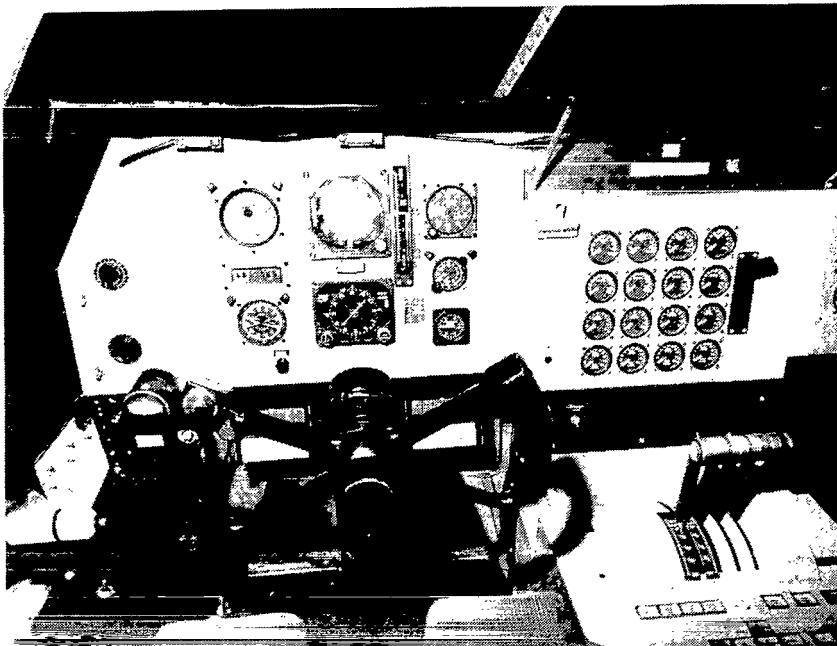
(b) Layout of TIFS.

Figure 10.- Photograph and layout diagram of Total In-Flight Simulator (TIFS).





(a) Overall view of TIFS cockpit.



(b) Closeup view of TIFS instrumentation.

L-78-82

Figure 11.- TIFS cockpit and instrument display.

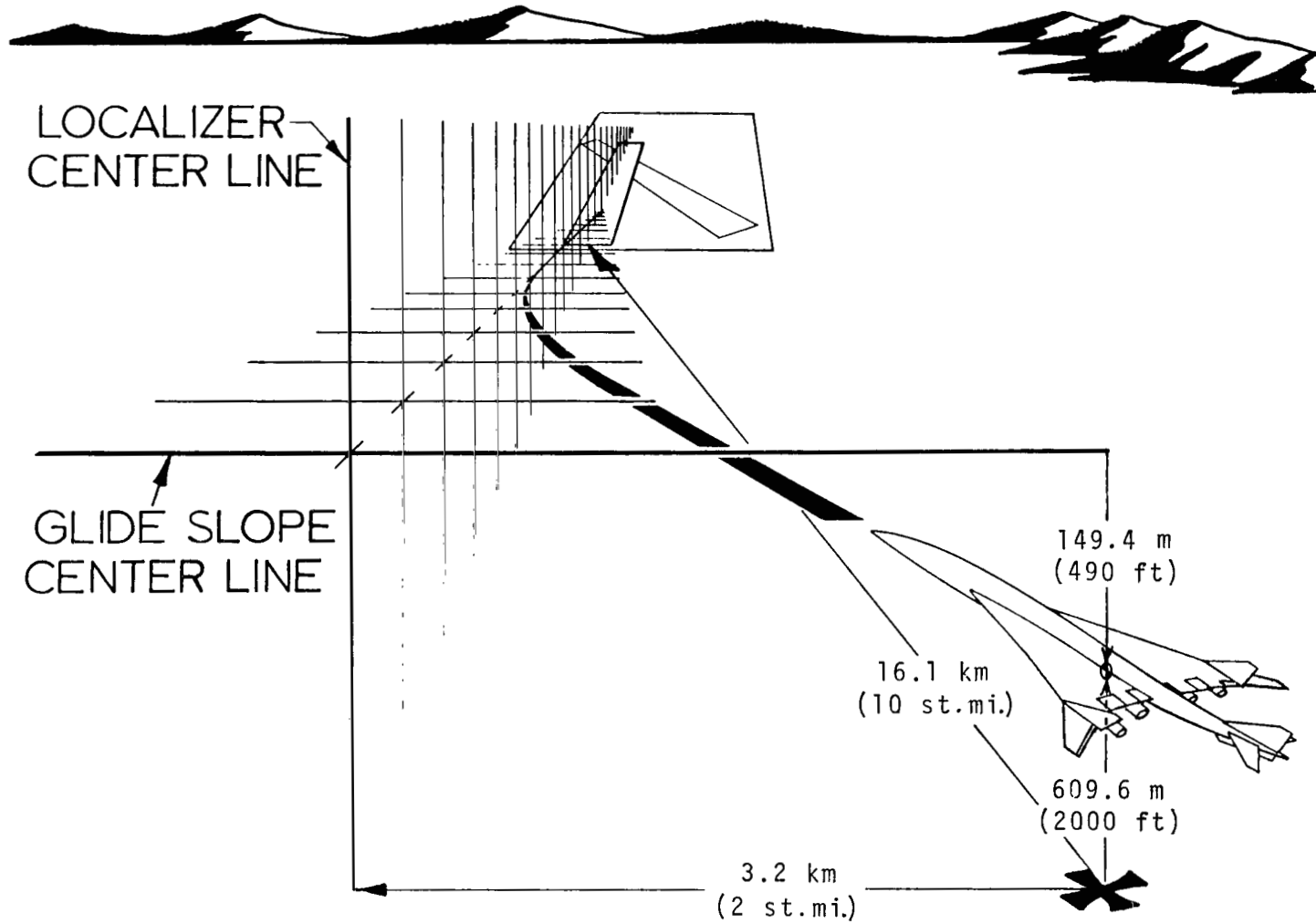


Figure 12.- Sketch indicating aircraft position relative to localizer and glide slope at time zero.

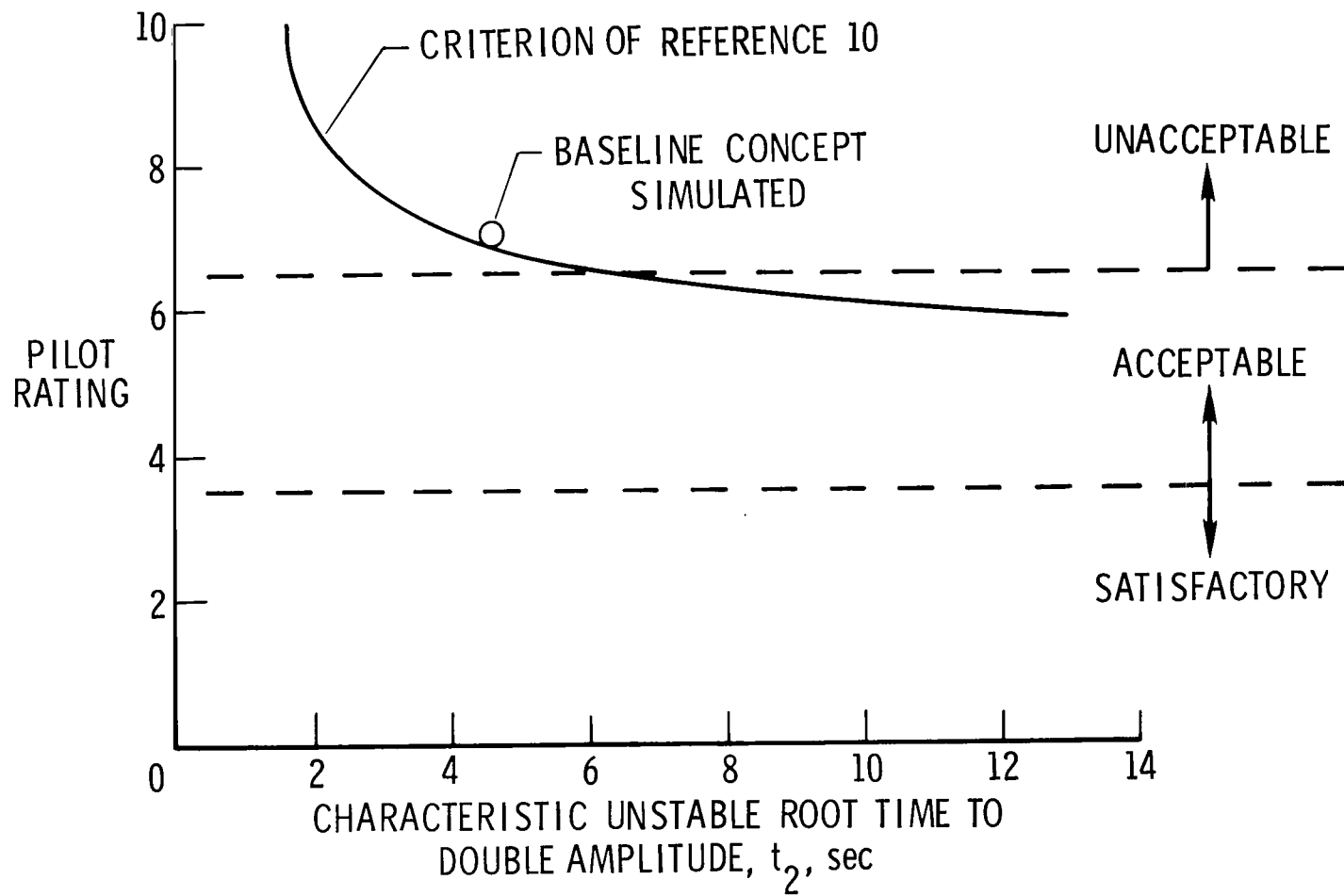


Figure 13.- Comparison of unaugmented baseline concept with criterion of reference 10.

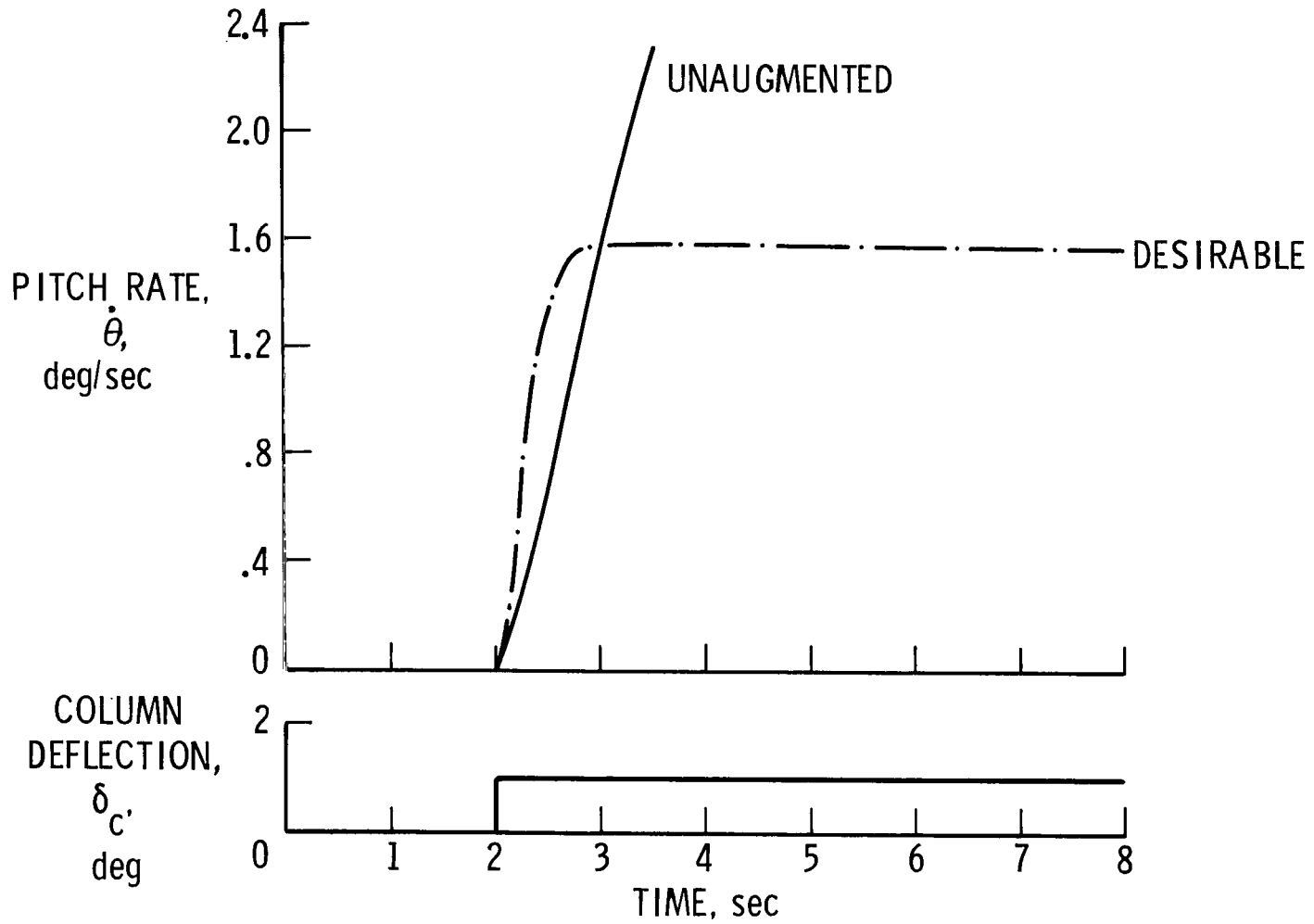


Figure 14.- Comparison of desirable pitch rate response characteristics with those of unaugmented airplane.

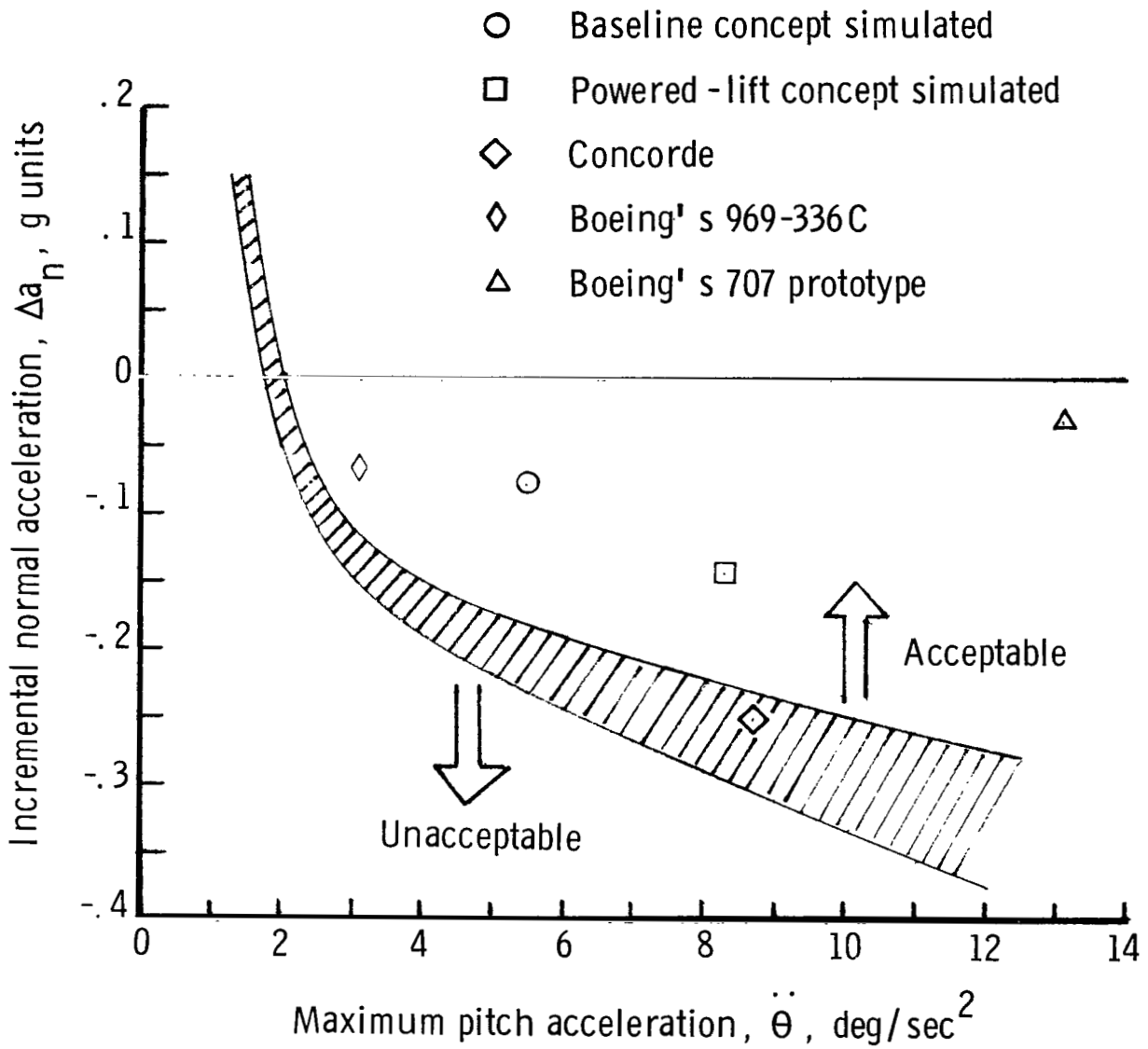


Figure 15.- Comparison of longitudinal control characteristics of simulated SCAR concepts with control requirements of reference 11.

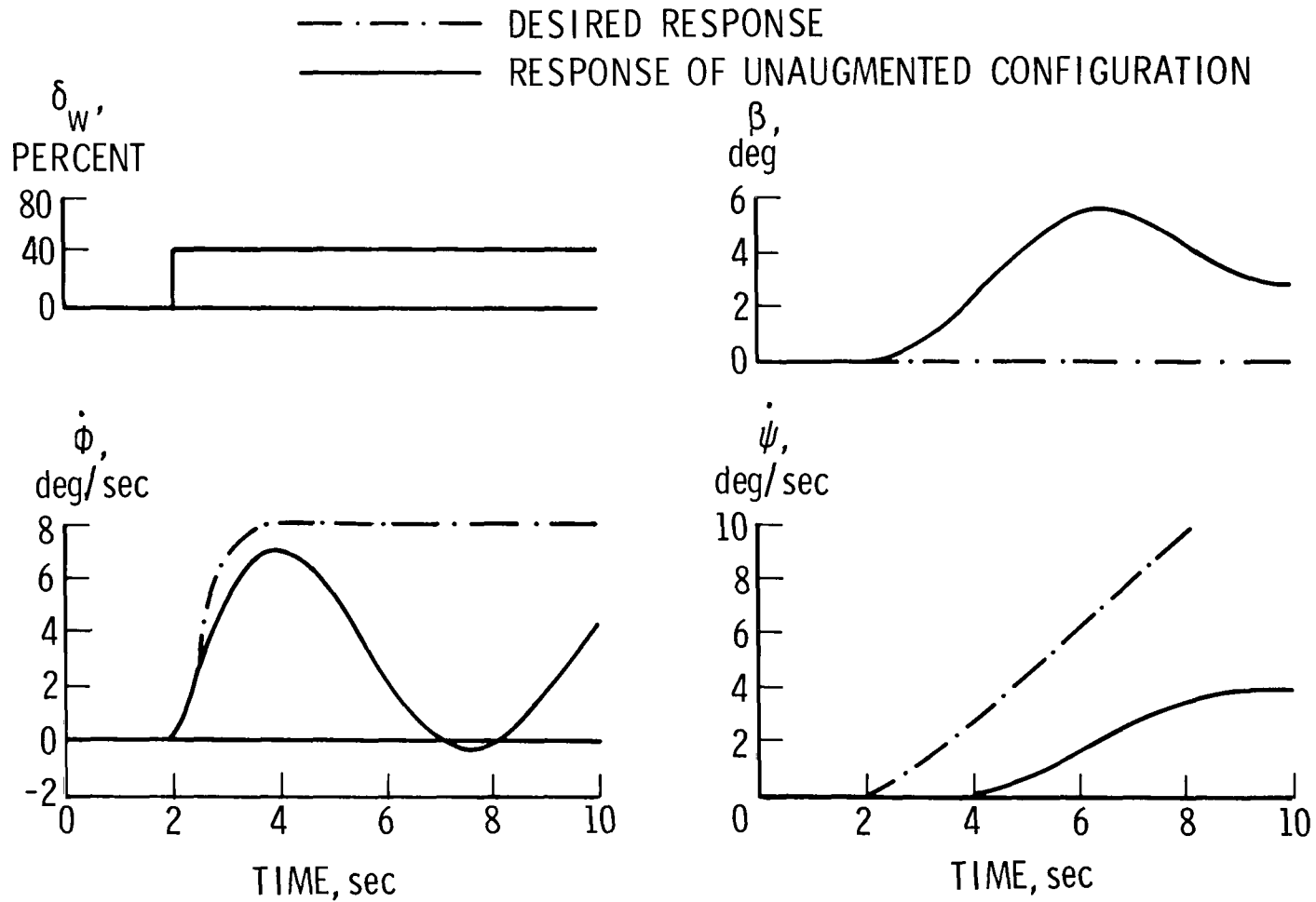


Figure 16.- Comparison of desired lateral-directional response characteristics and those obtained for unaugmented airplane.

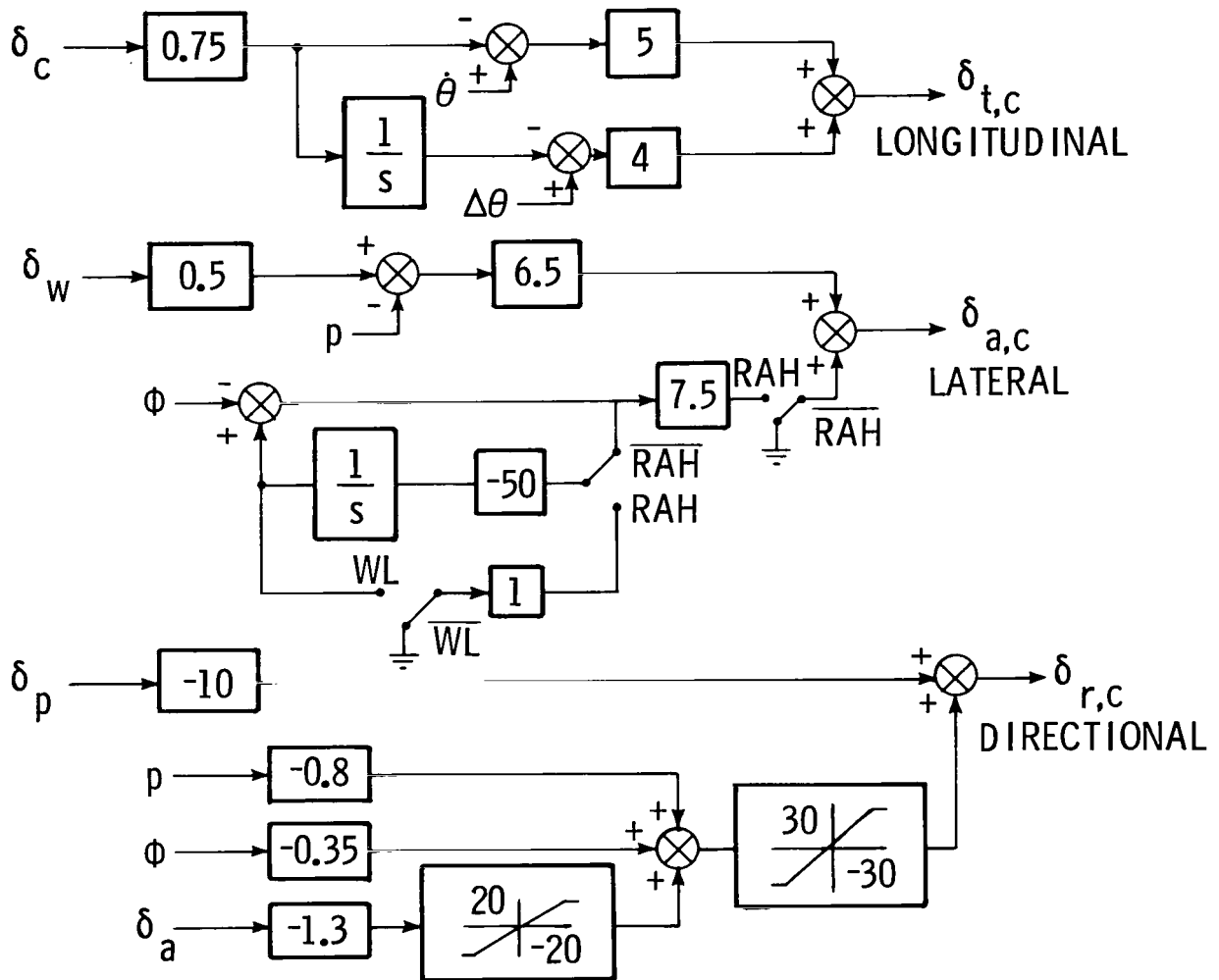


Figure 17.- Normal operational stability and control augmentation system (SCAS).
 (All control-surface deflections had 0.1-second lag due to actuator servo.)

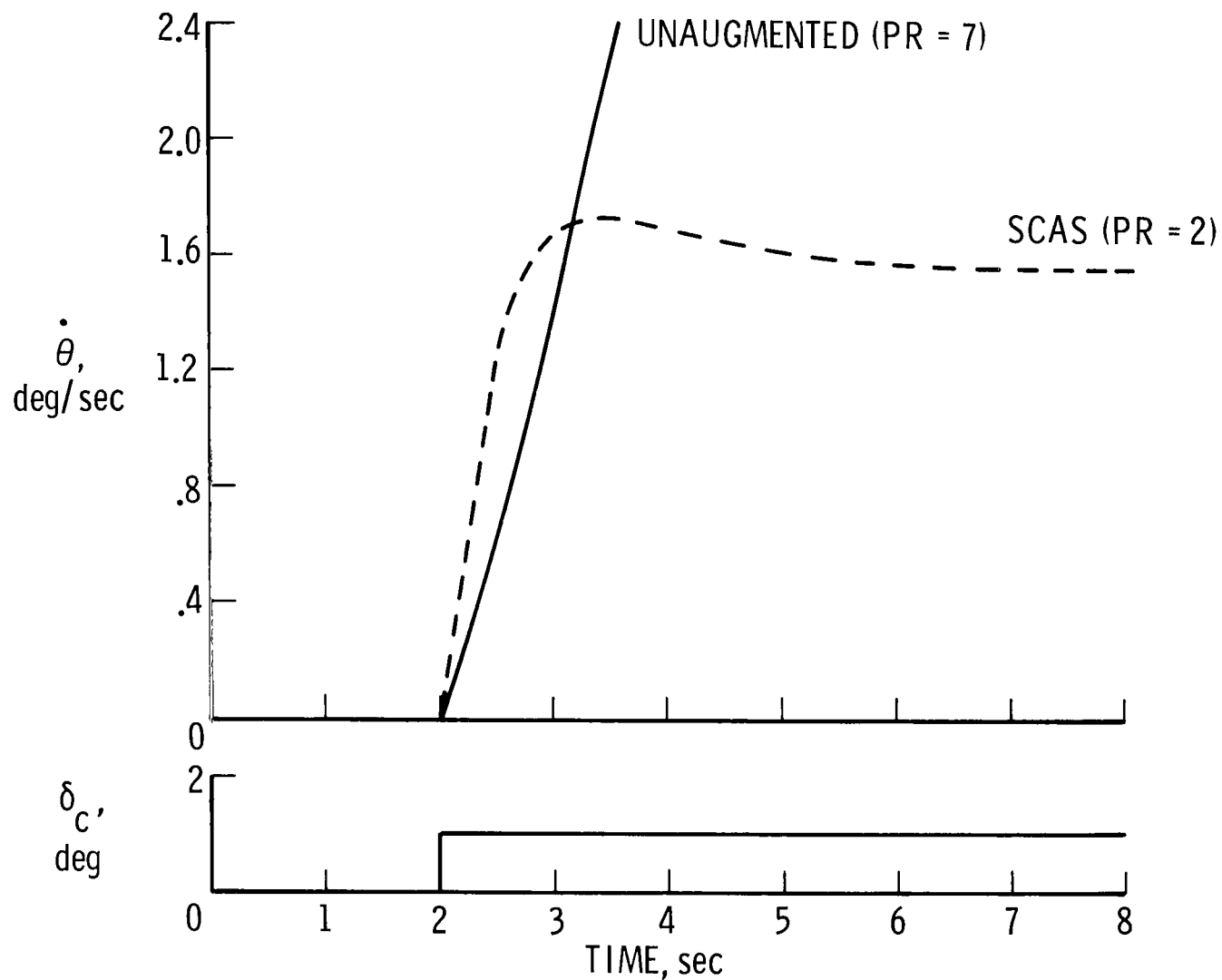


Figure 18.- Comparison of pitch rate response for unaugmented and SCAS configurations.

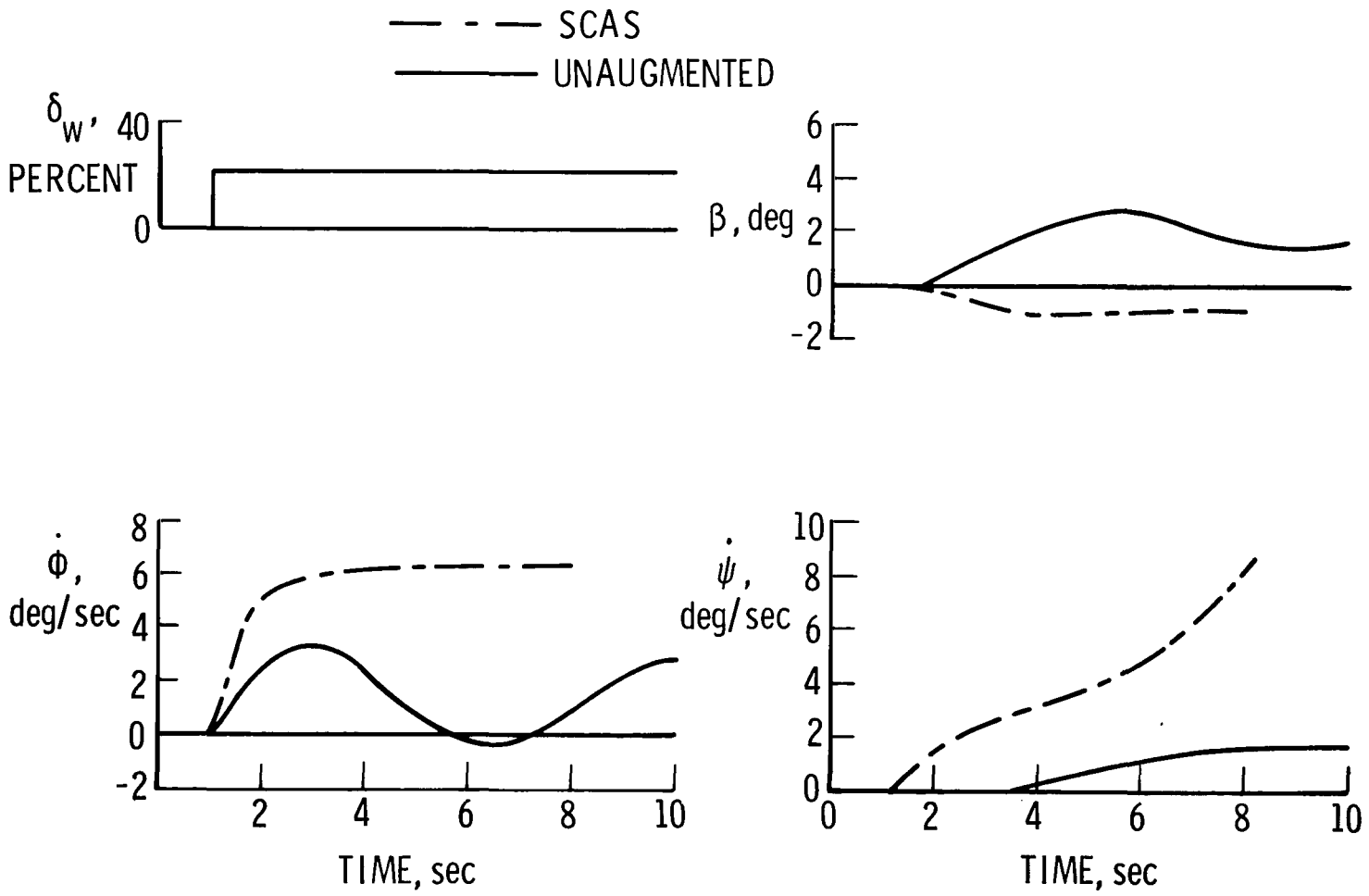


Figure 19.- Comparison of lateral-directional response characteristics for unaugmented and SCAS configurations.

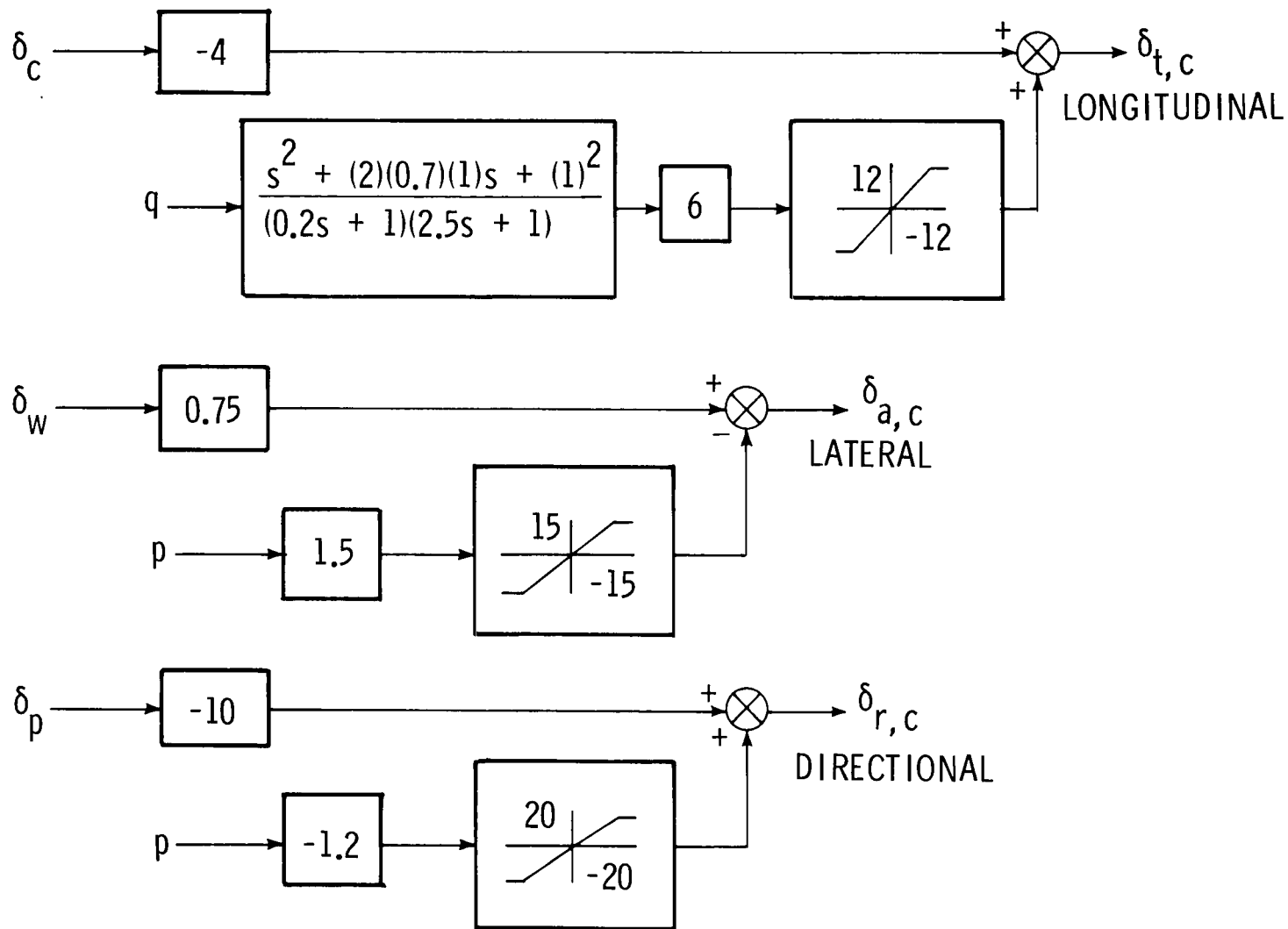


Figure 20.- Hardened stability augmentation system (HSAS). (All control-surface deflections had 0.1-second lag due to actuator servo.)

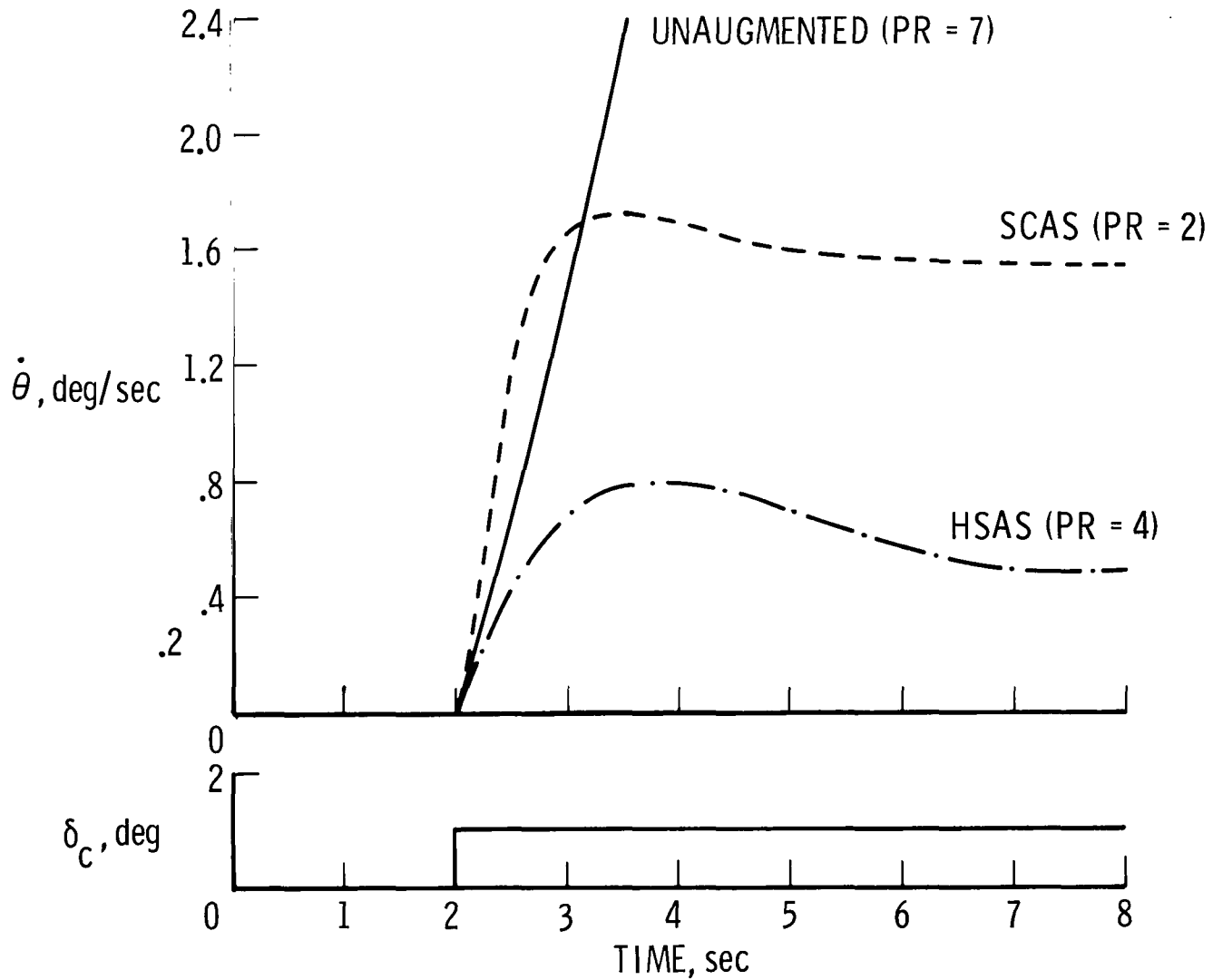


Figure 21.- Comparison of pitch rate response characteristics for various control systems.

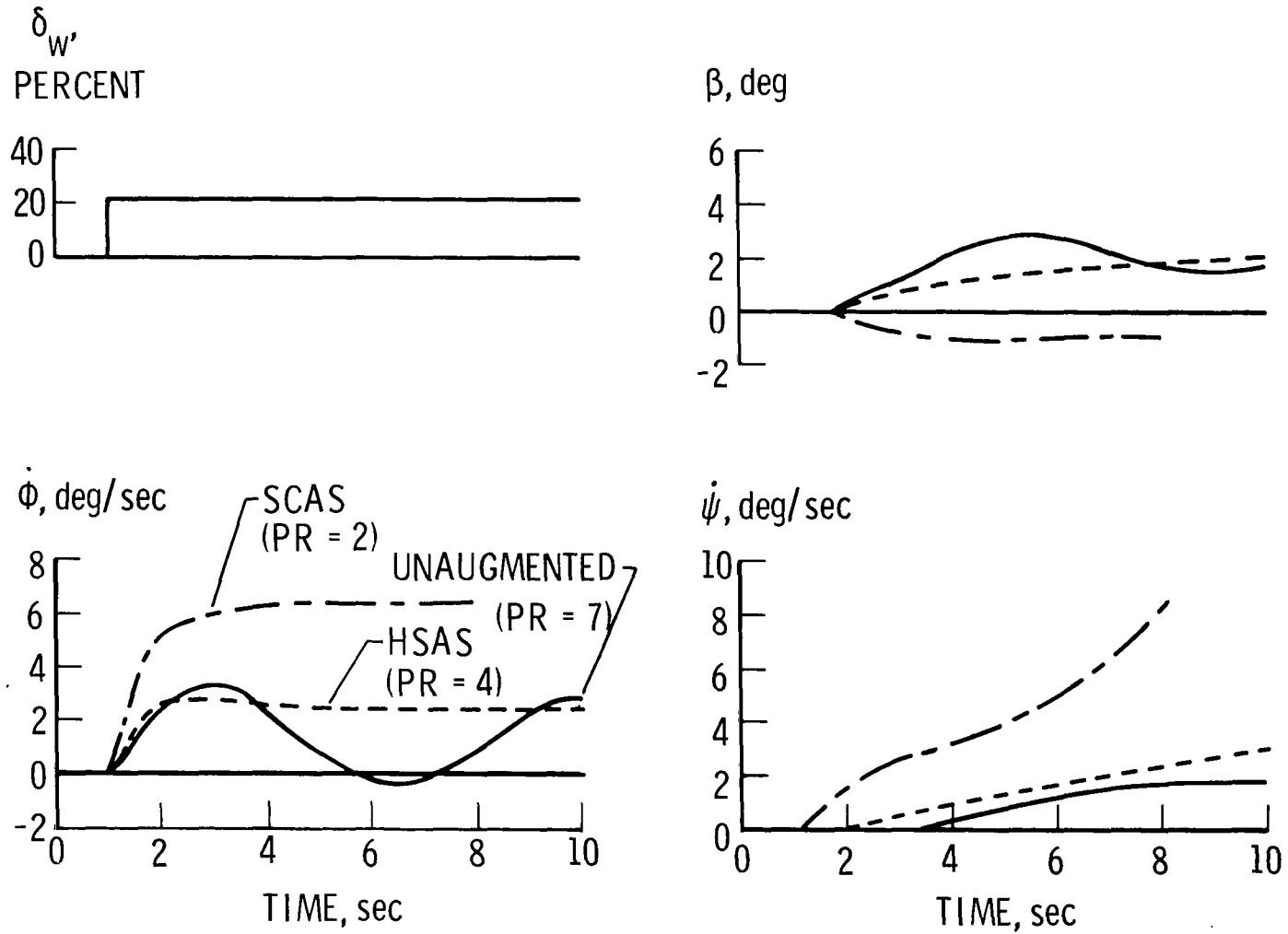


Figure 22.- Comparison of lateral-directional response to a lateral control step input for various control systems.

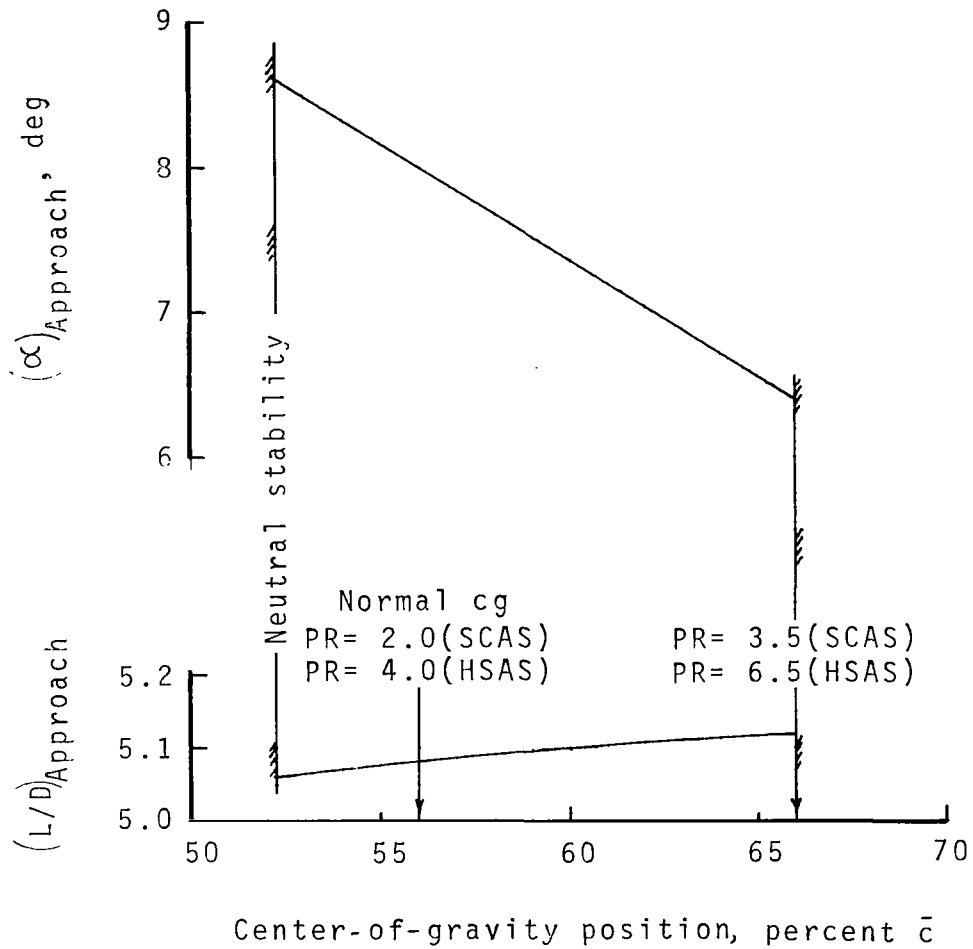


Figure 23.- Indication of effects of center-of-gravity variation on low-speed airplane performance.

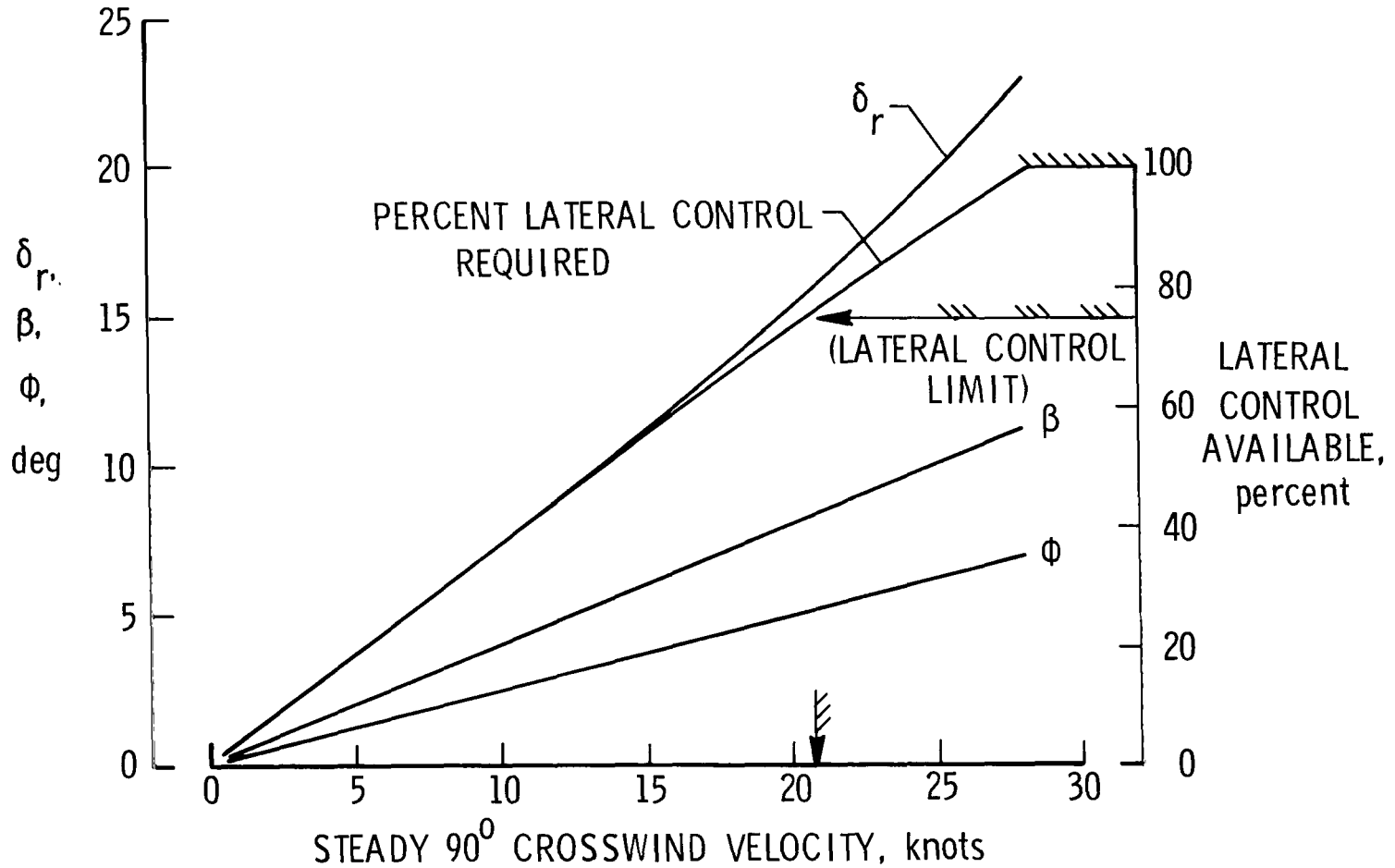


Figure 24.- Indication of crosswind trim capability of simulated baseline SCAR concept.

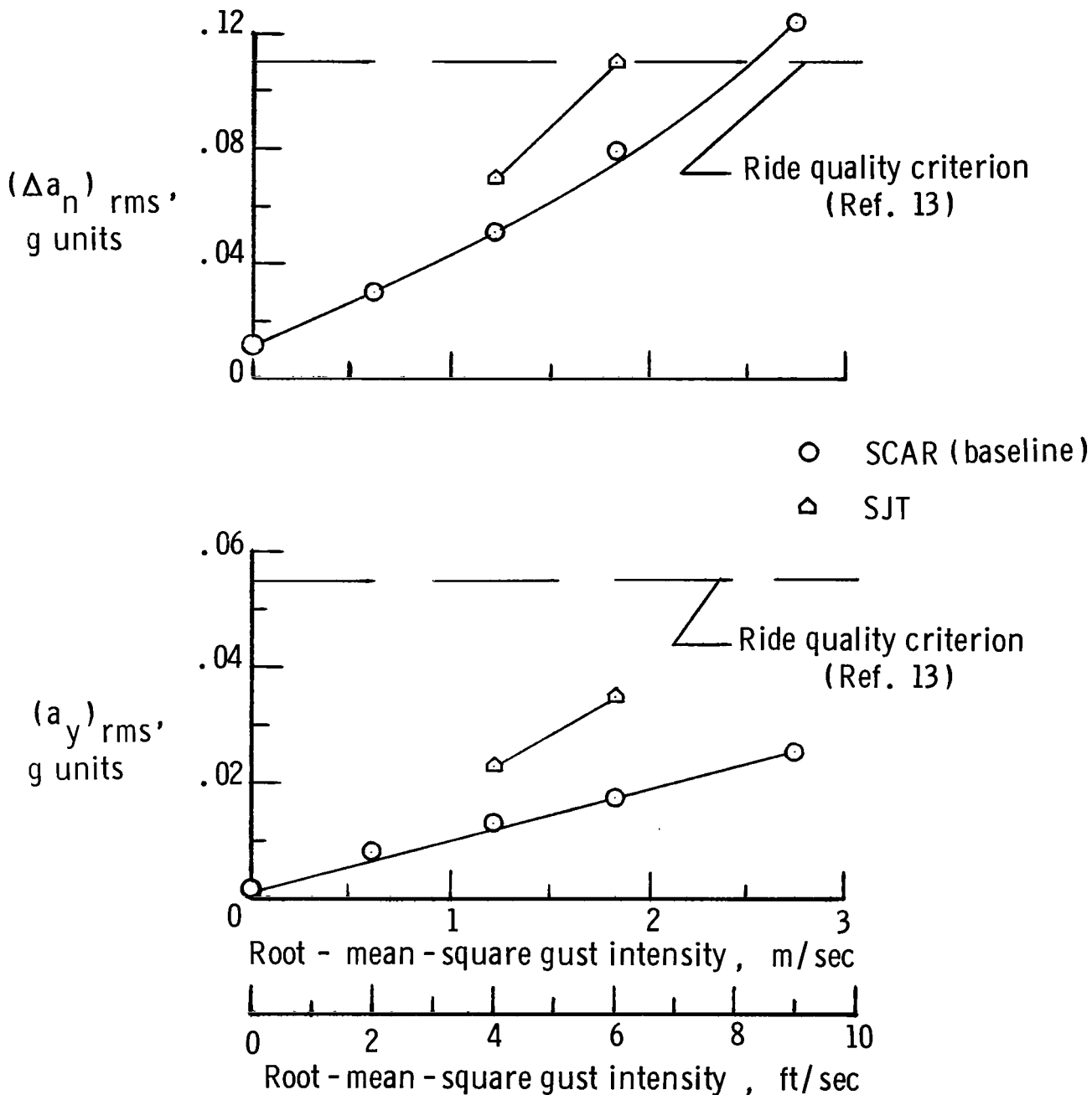


Figure 25.- Acceleration responses during landing approaches in various levels of turbulence. (Accelerations measured at aircraft center of gravity.)

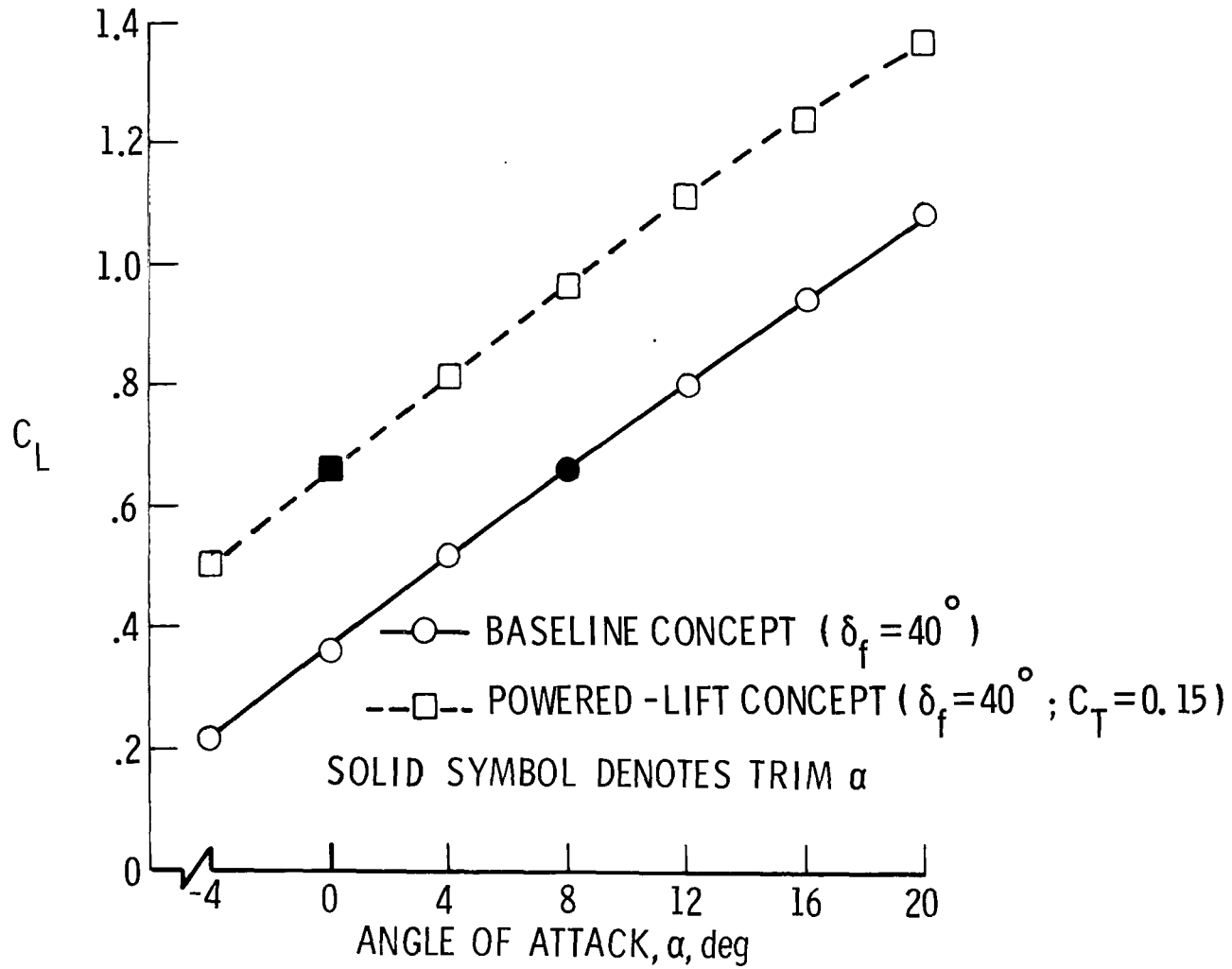
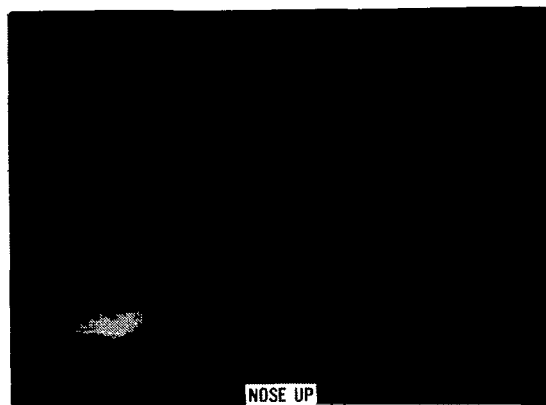
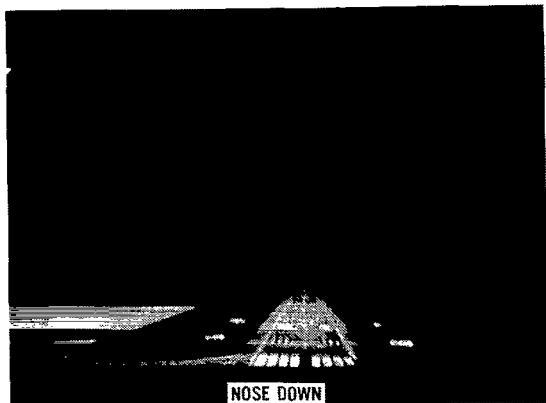
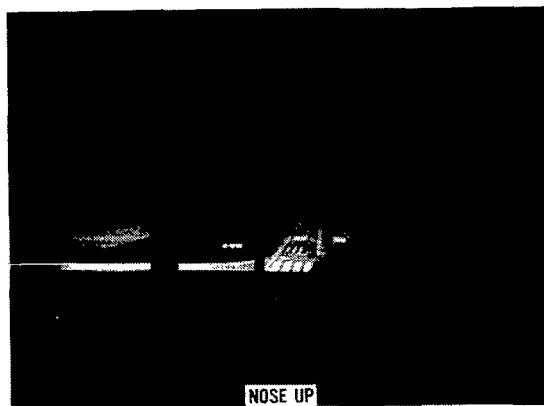
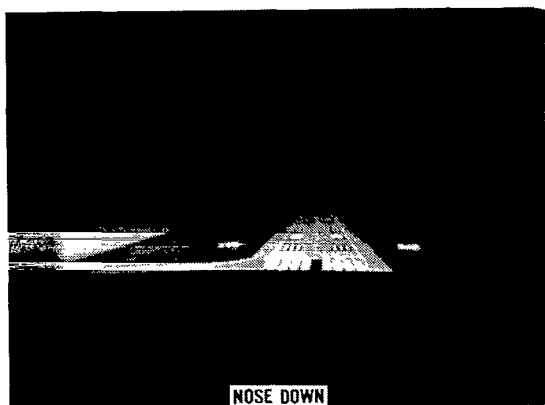


Figure 26.- Comparison of lift coefficient characteristics for baseline and powered-lift concepts simulated.



(a) Baseline SCAR concept.



(b) Powered-lift SCAR concept.

Figure 27.- View of runway as seen by pilot prior to touchdown. L-78-83
($h_{lg} = 30.5$ meters (100 feet); $\gamma = -2.7^\circ$.)

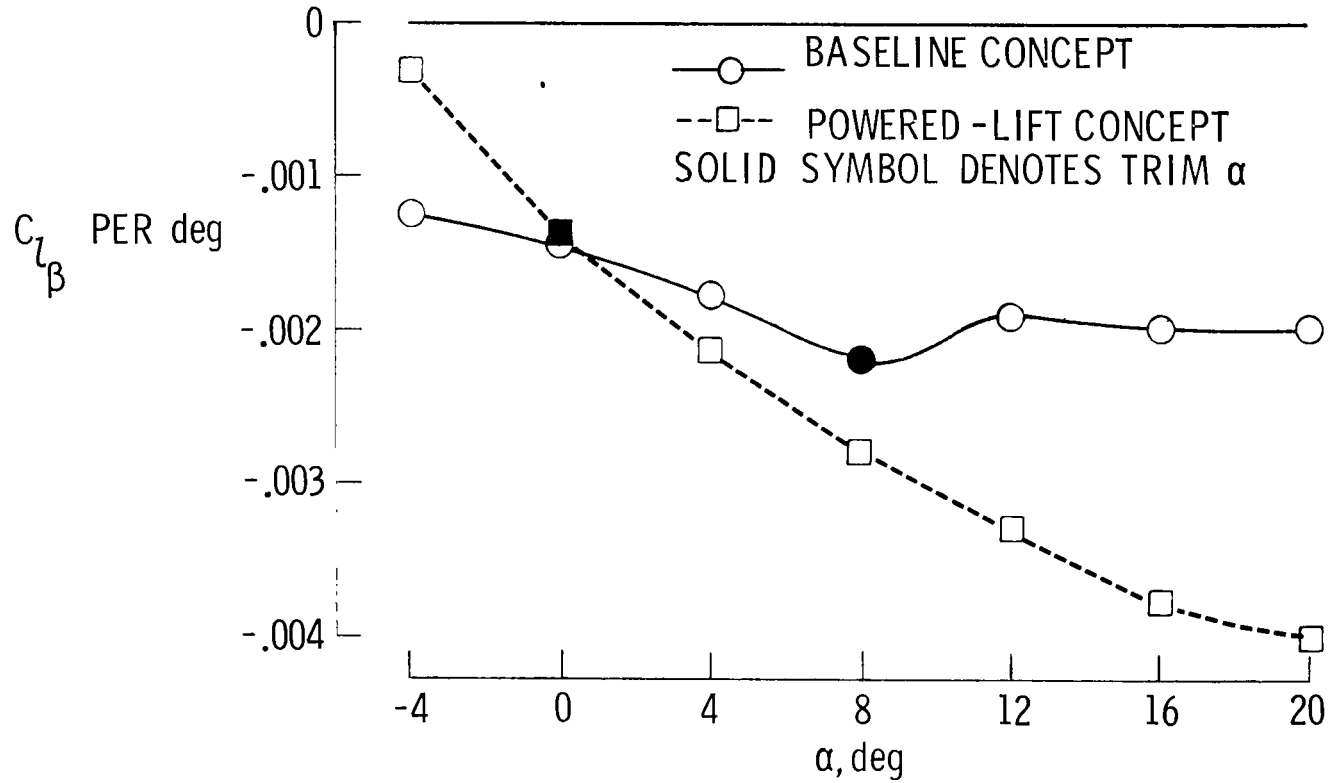


Figure 28.- Comparison of effective dihedral coefficient characteristics for baseline and powered-lift concepts simulated.

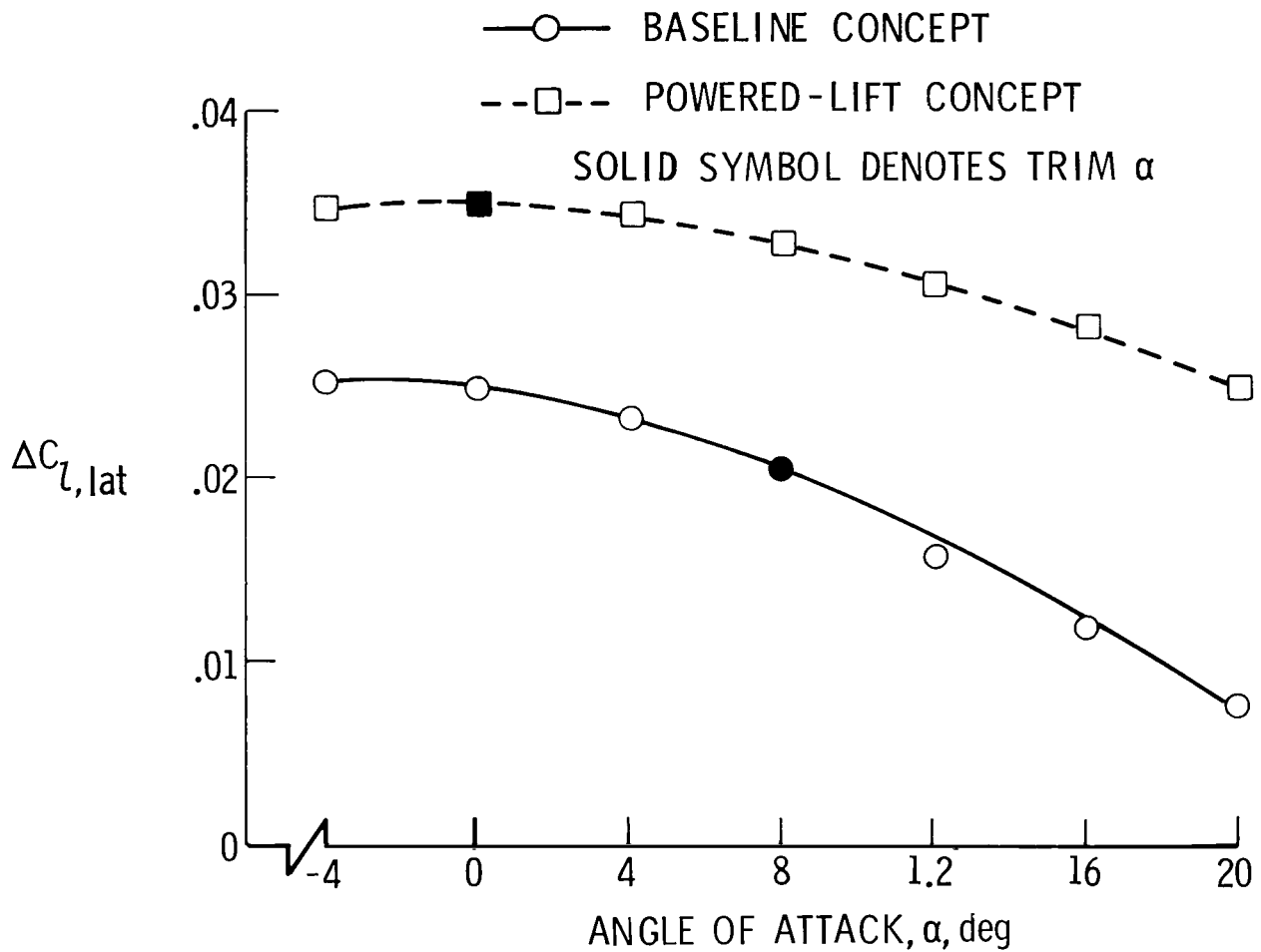


Figure 29.- Comparison of maximum lateral control effectiveness for baseline and powered-lift concepts.

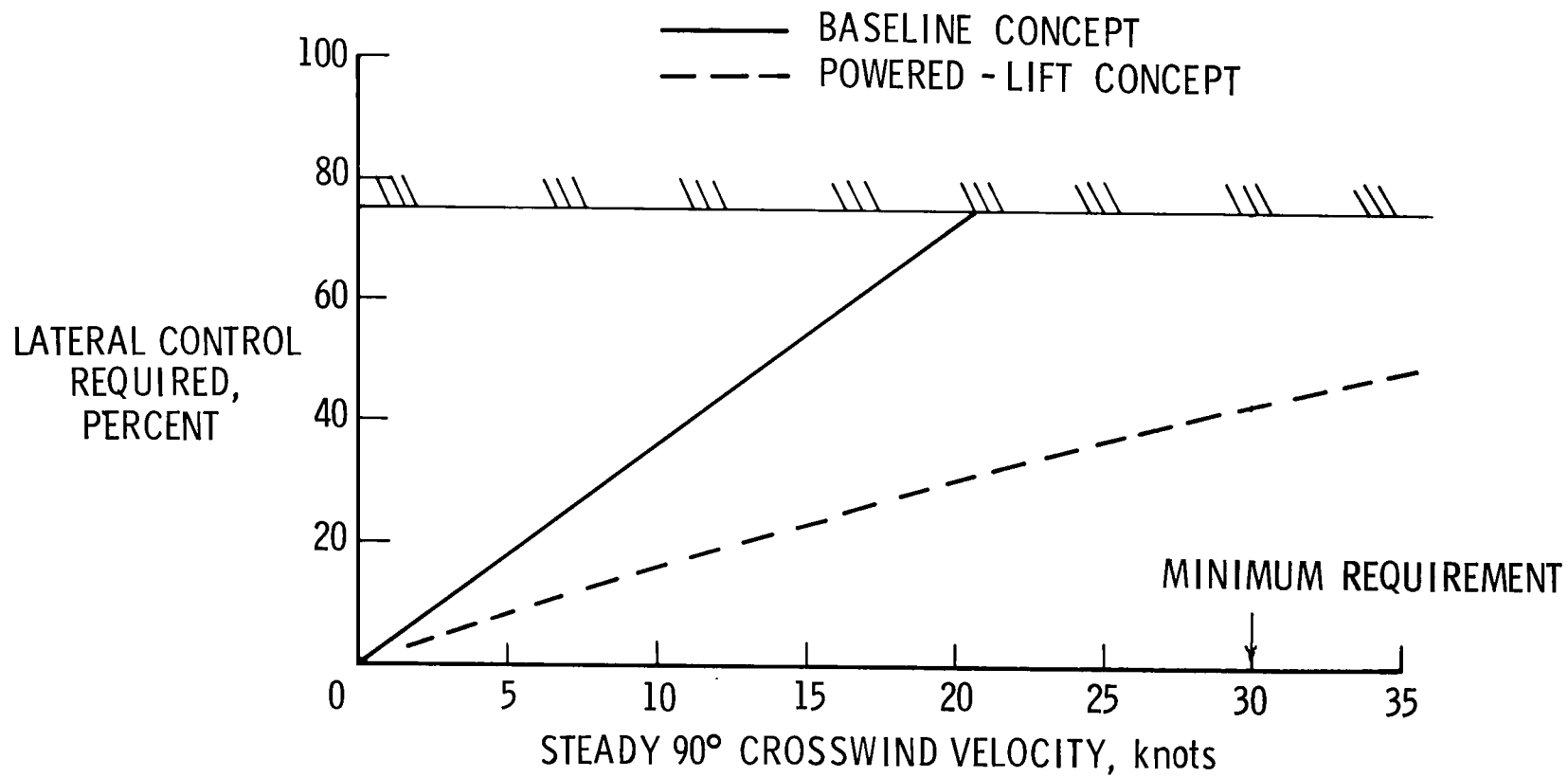


Figure 30.- Comparison of crosswind trim capability for baseline and powered-lift concepts.

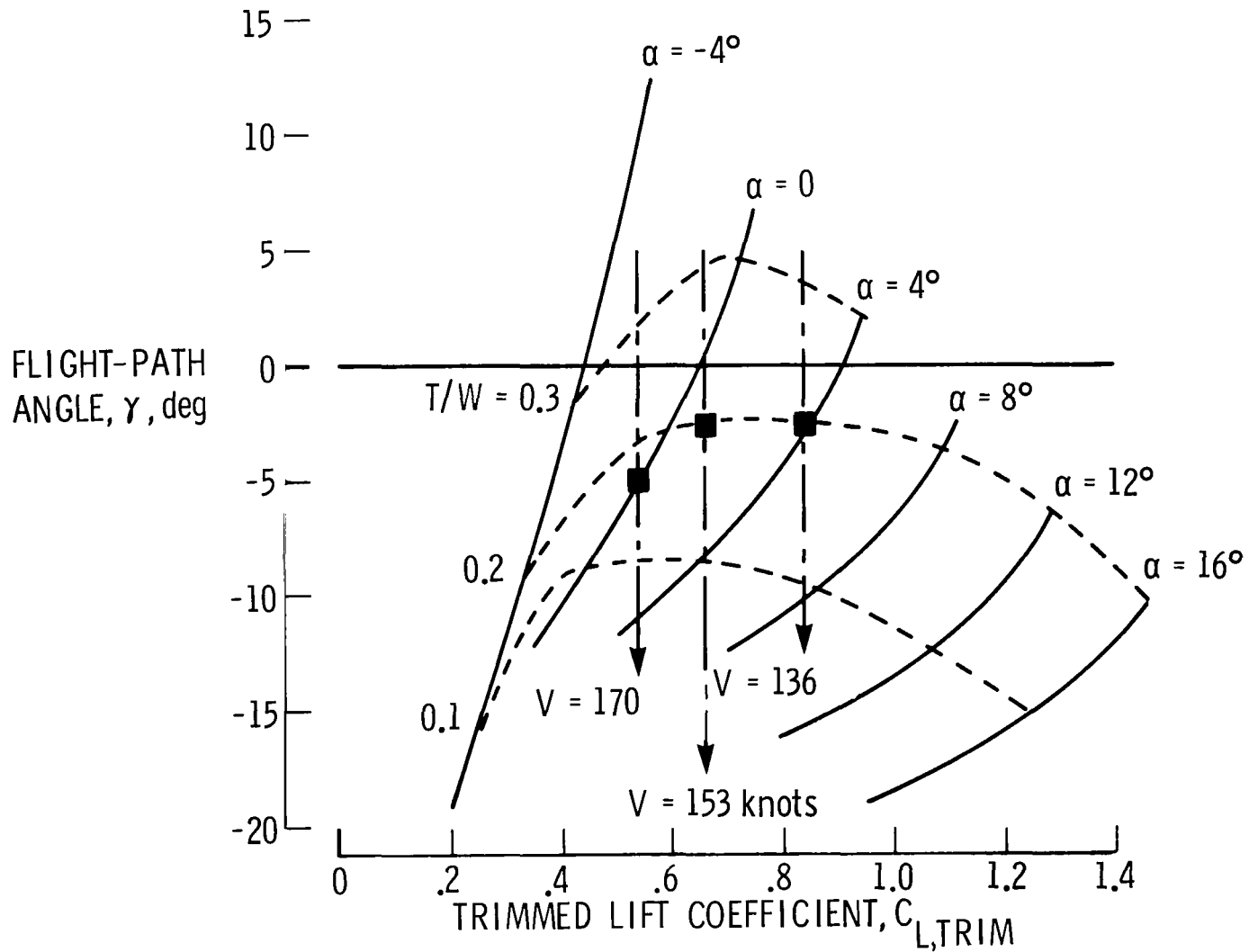
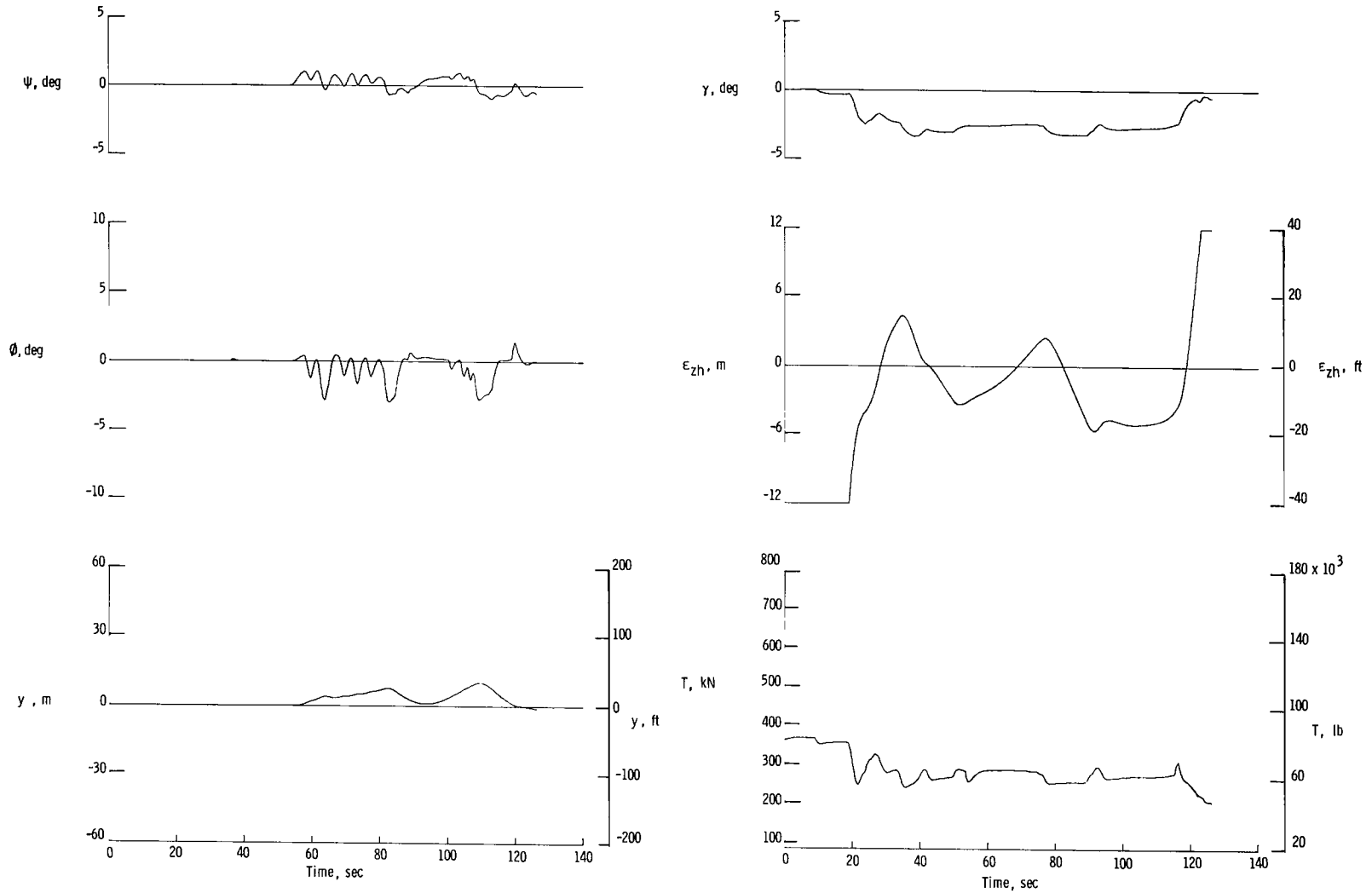
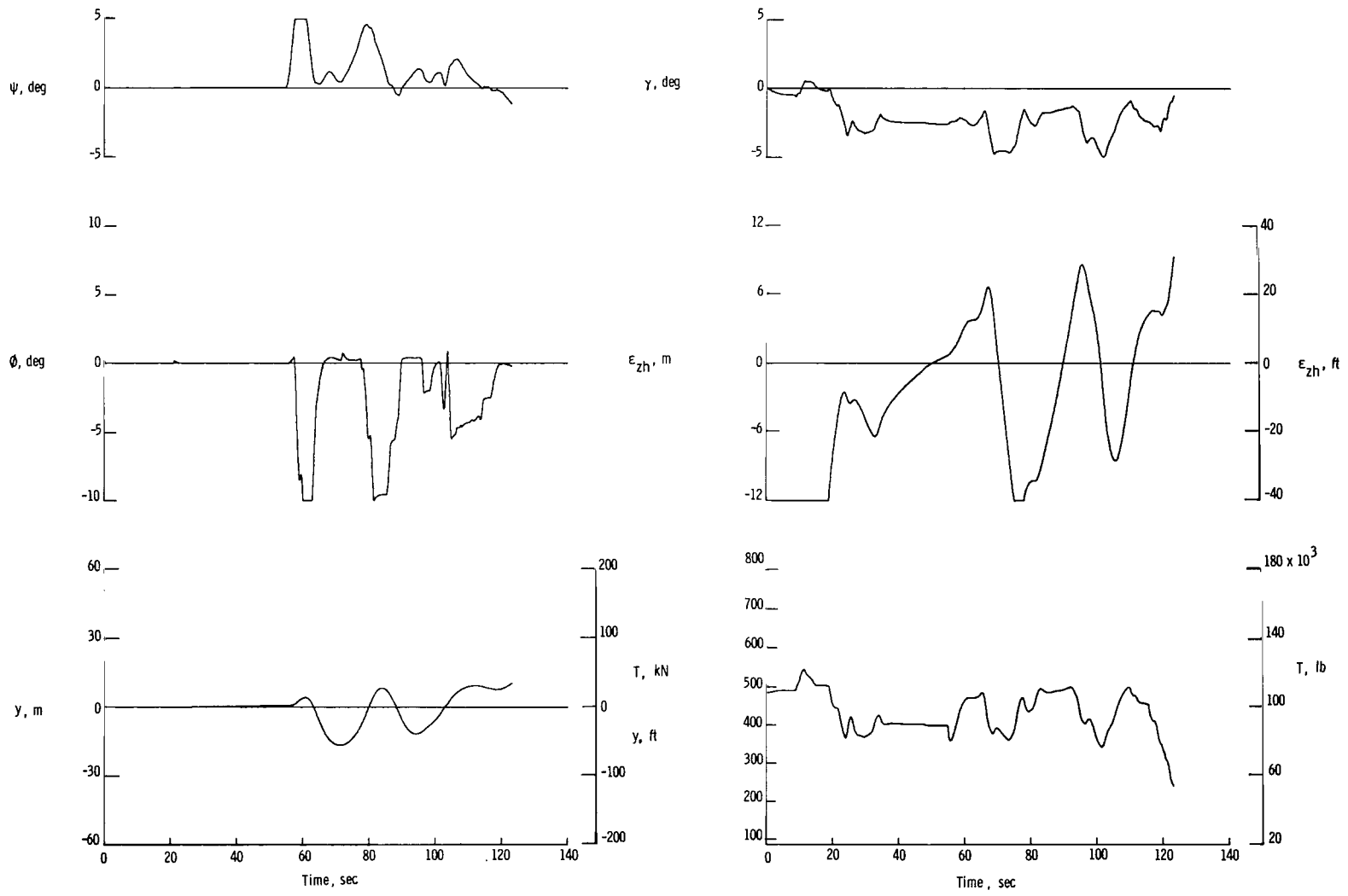


Figure 31.- Indication of effects of engine thrust on trim lift coefficient and flight-path angle for powered-lift concept.



(a) Baseline concept.

Figure 32.- Indication of lateral and vertical excursions experienced following failure of number four engine. (Engine failed at $t = 55$ seconds.)



(b) Powered-lift concept.

Figure 32.- Concluded.

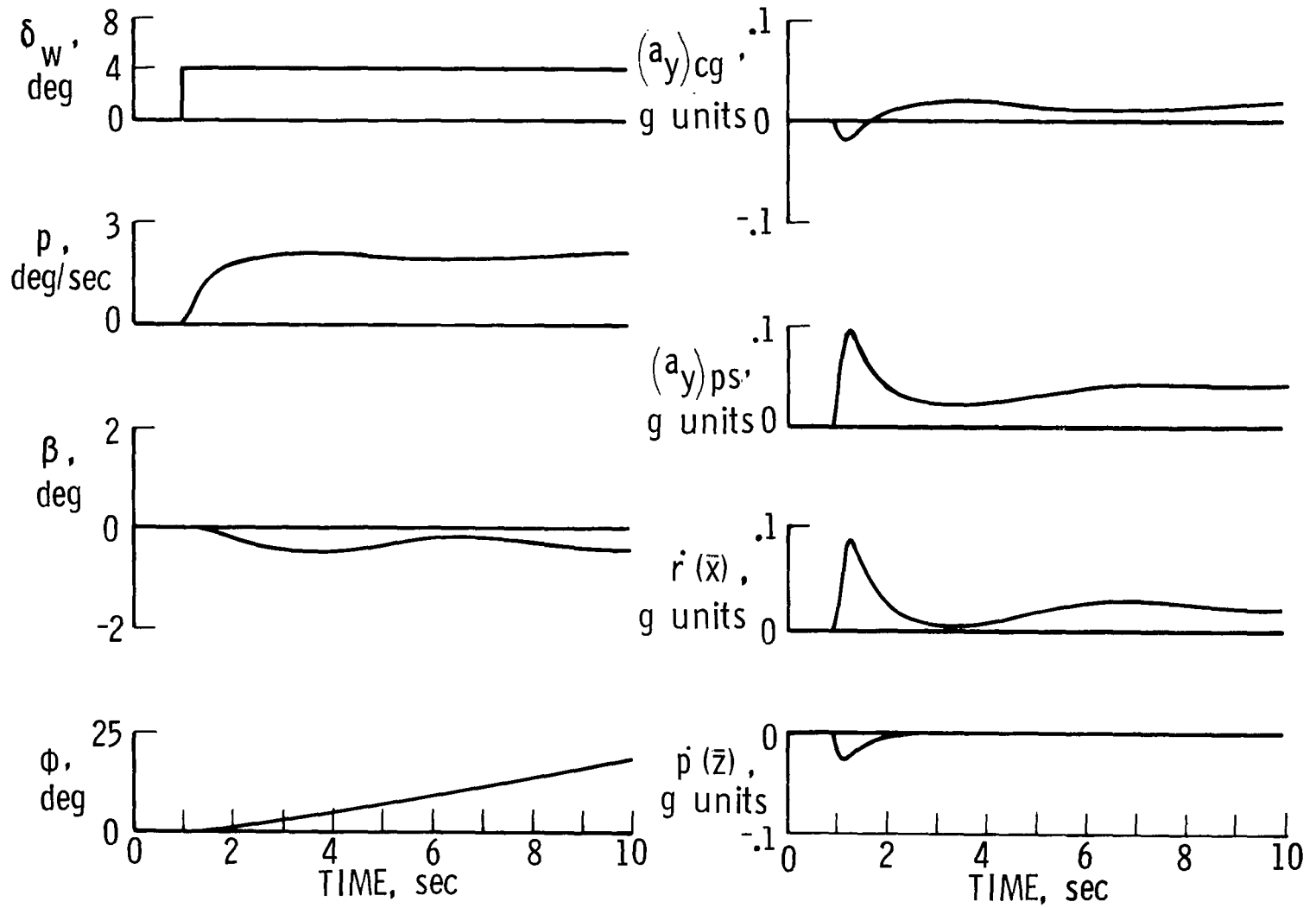


Figure 33.- Calculated lateral response to a wheel step input with SCAS operative.

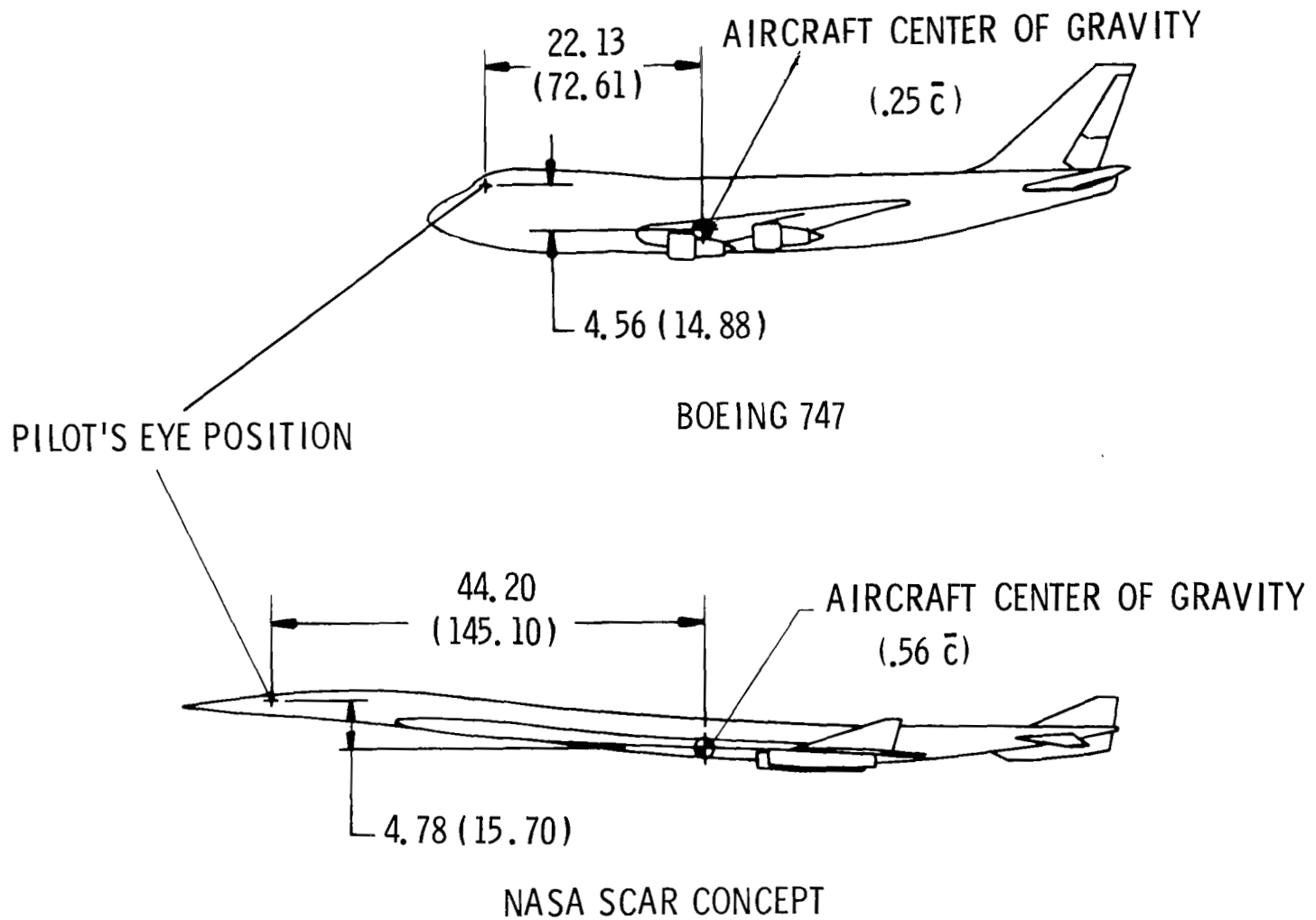


Figure 34.- Comparison of pilot location relative to airplane center of gravity for simulated SCAR and Boeing 747 airplanes. All linear dimensions are in meters (feet).

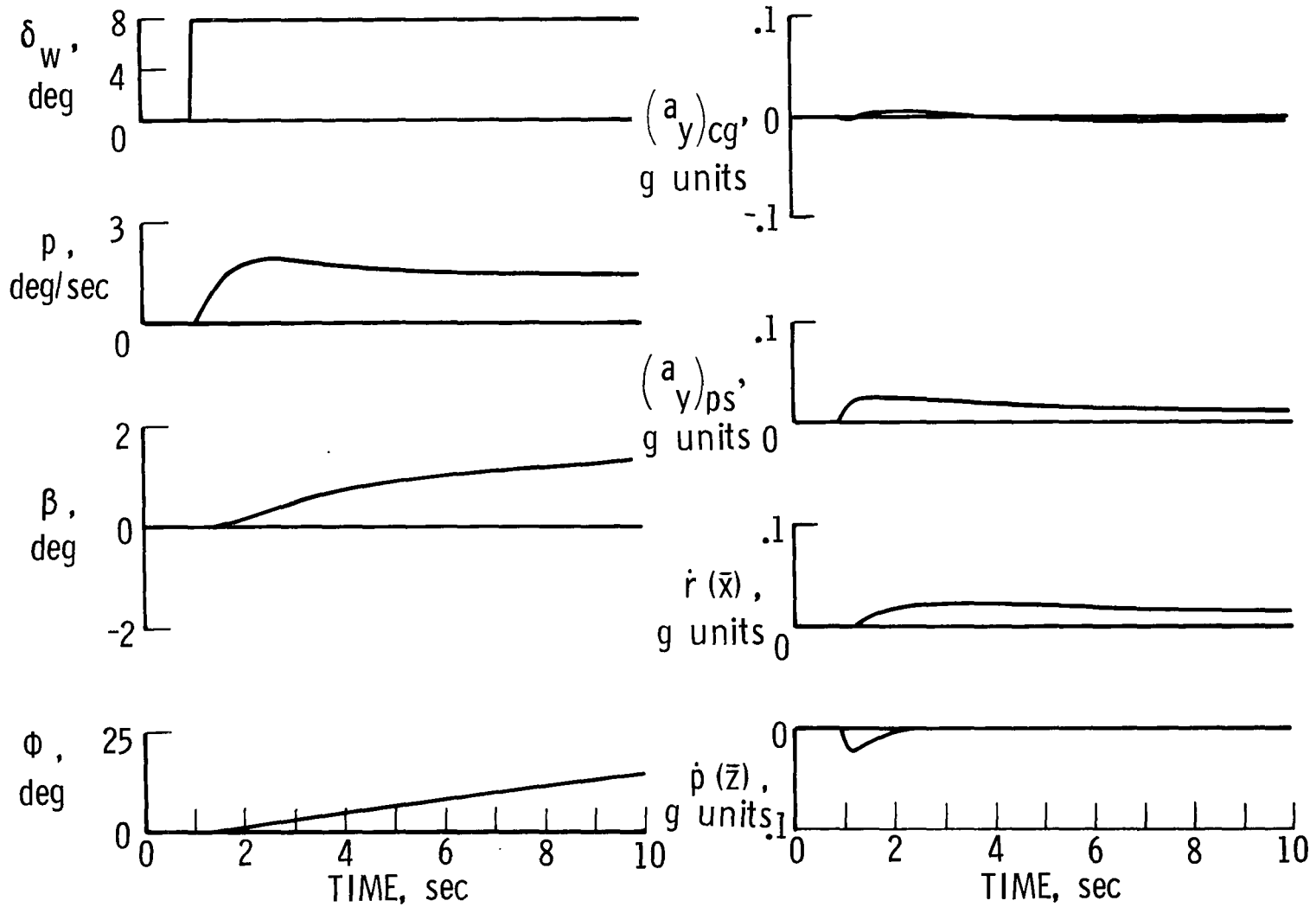


Figure 35.- Calculated lateral response to a wheel step input with HSAS operative.

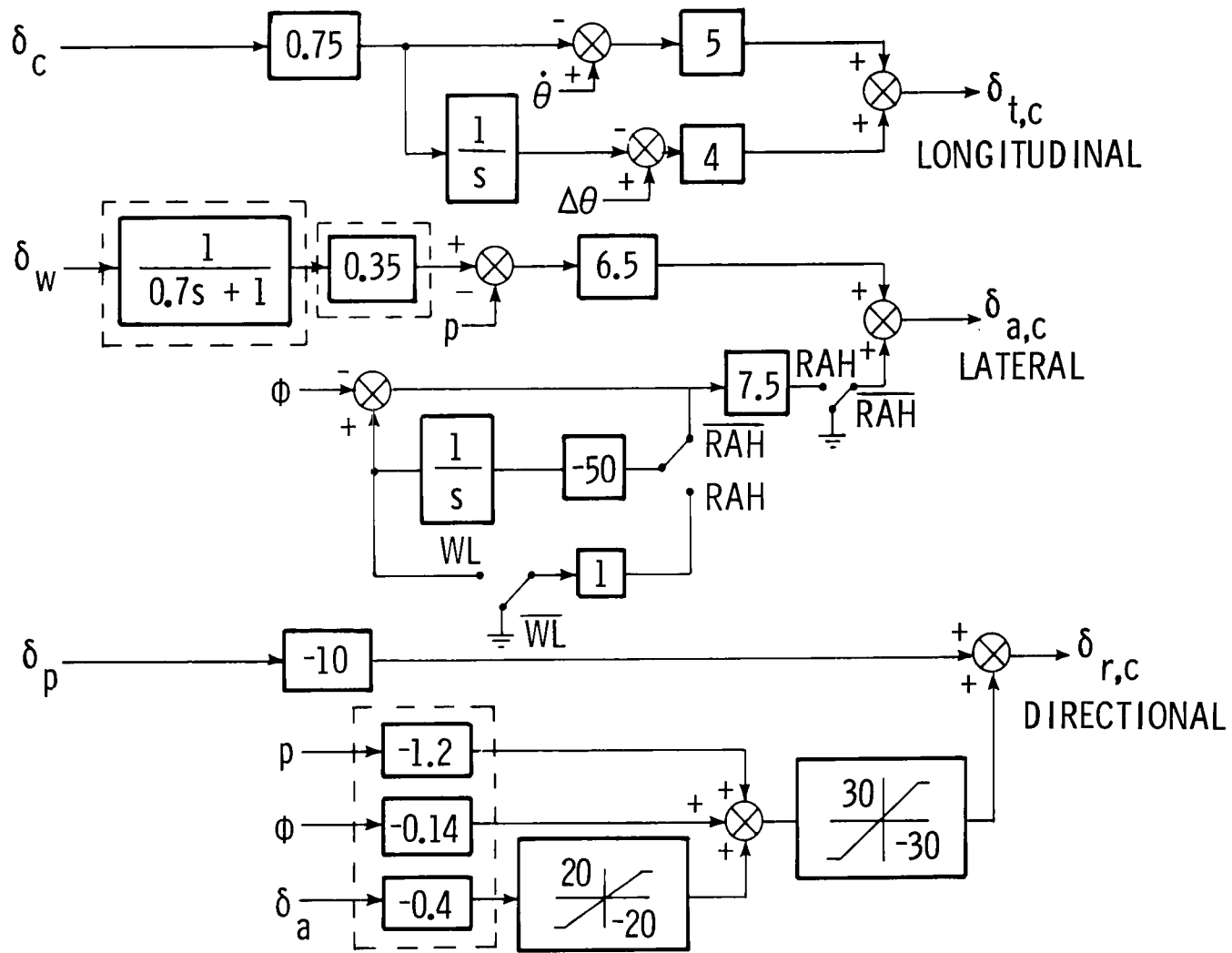


Figure 36.- Modified SCAS. Modifications to initial SCAS of figure 17 indicated within dashed lines. (All control-surface deflections had 0.1-second lag due to actuator servo.)

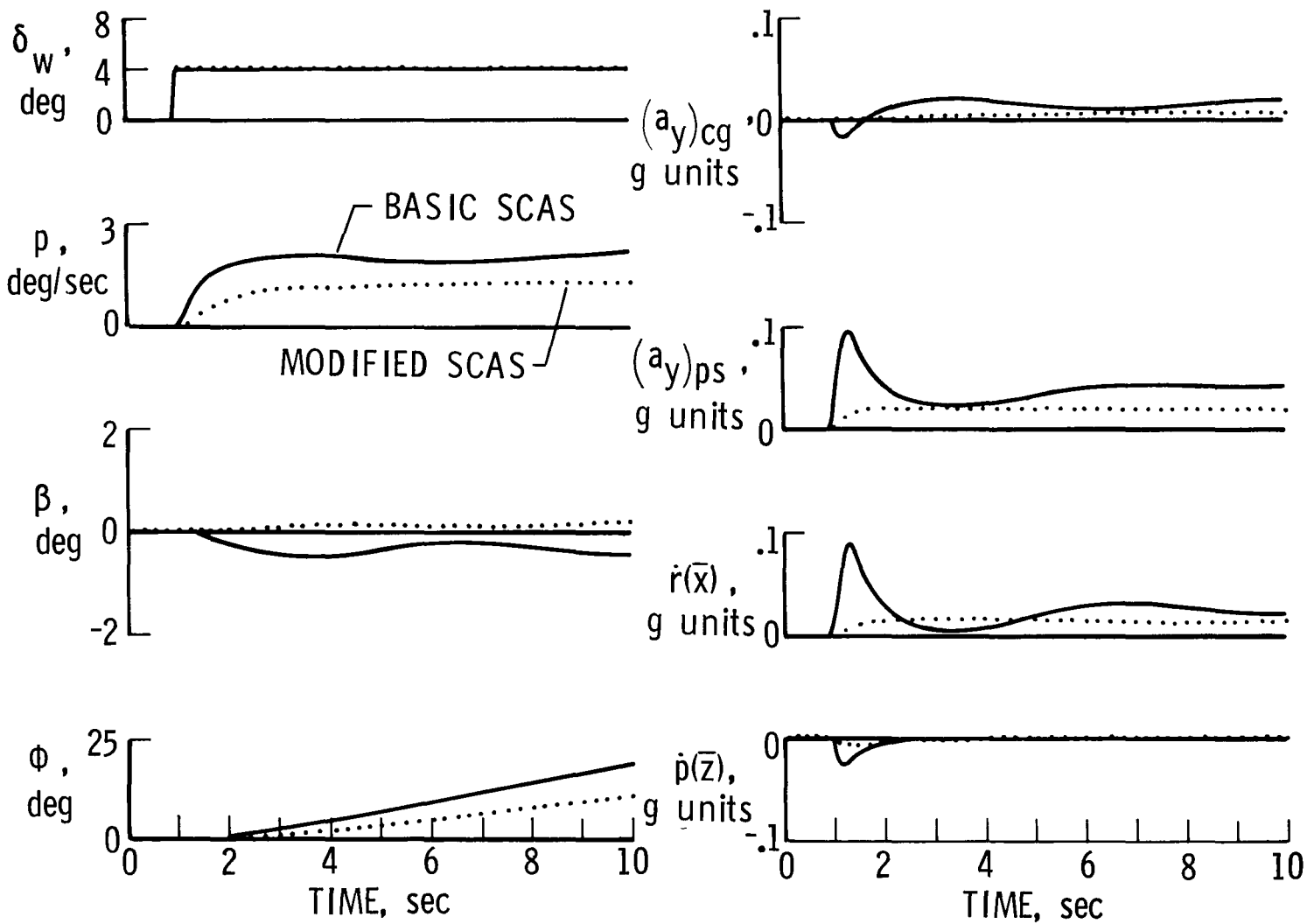
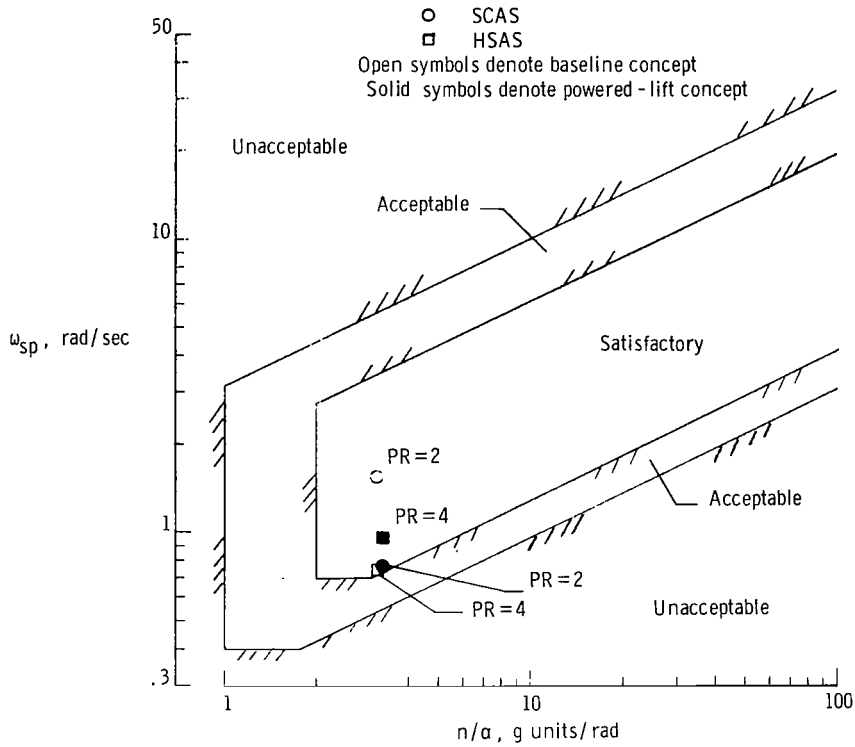
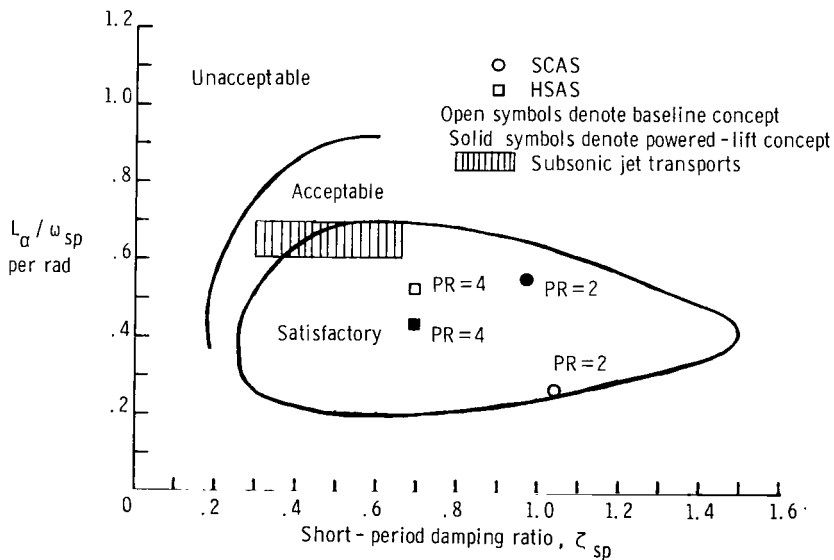


Figure 37.- Comparison of lateral response to a wheel step input for SCAS and modified SCAS configurations.



(a) Longitudinal short-period frequency requirements of reference 12. (Unaugmented configurations fell outside of plotted range.)



(b) Shomber-Gertsen longitudinal handling qualities criteria of reference 16. (Unaugmented configurations fell outside of plotted range.)

Figure 38.- Longitudinal handling qualities criteria.

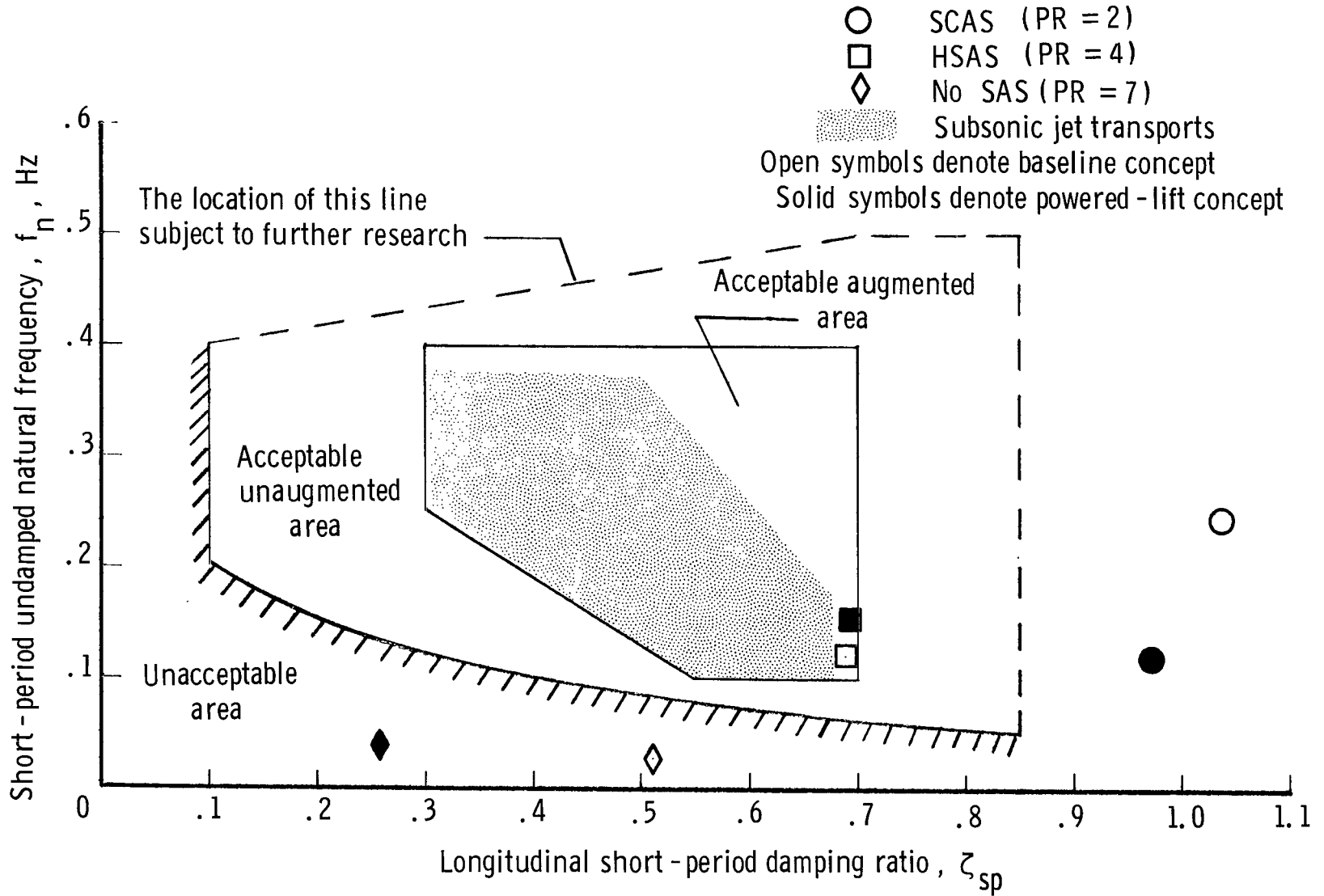


Figure 39.- Longitudinal short-period criterion for transport aircraft.
 Boundaries from reference 17.

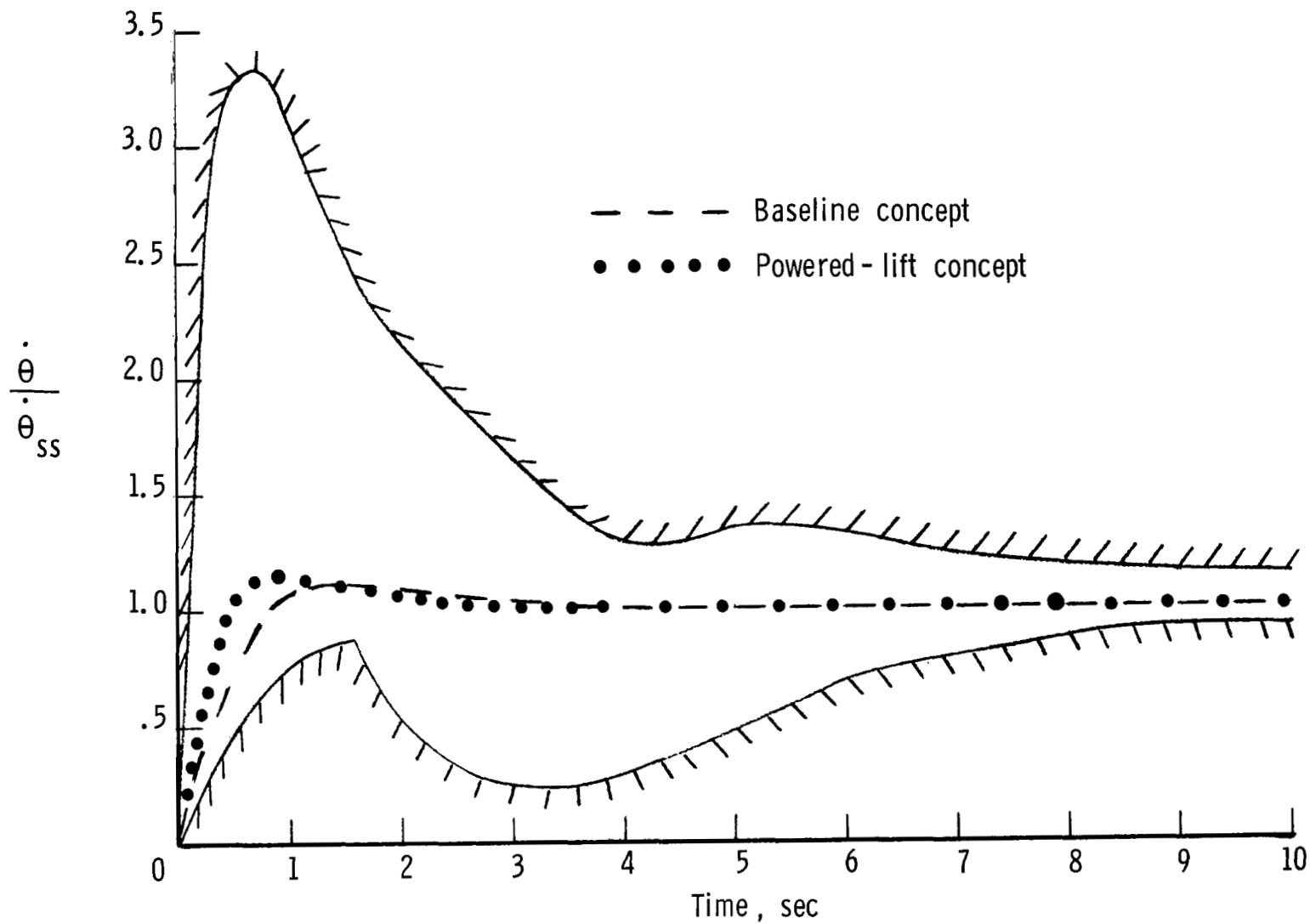


Figure 40.- Low-speed pitch rate response criterion of reference 18.
 Boundaries for normal operation ($PR \leq 3.5$).

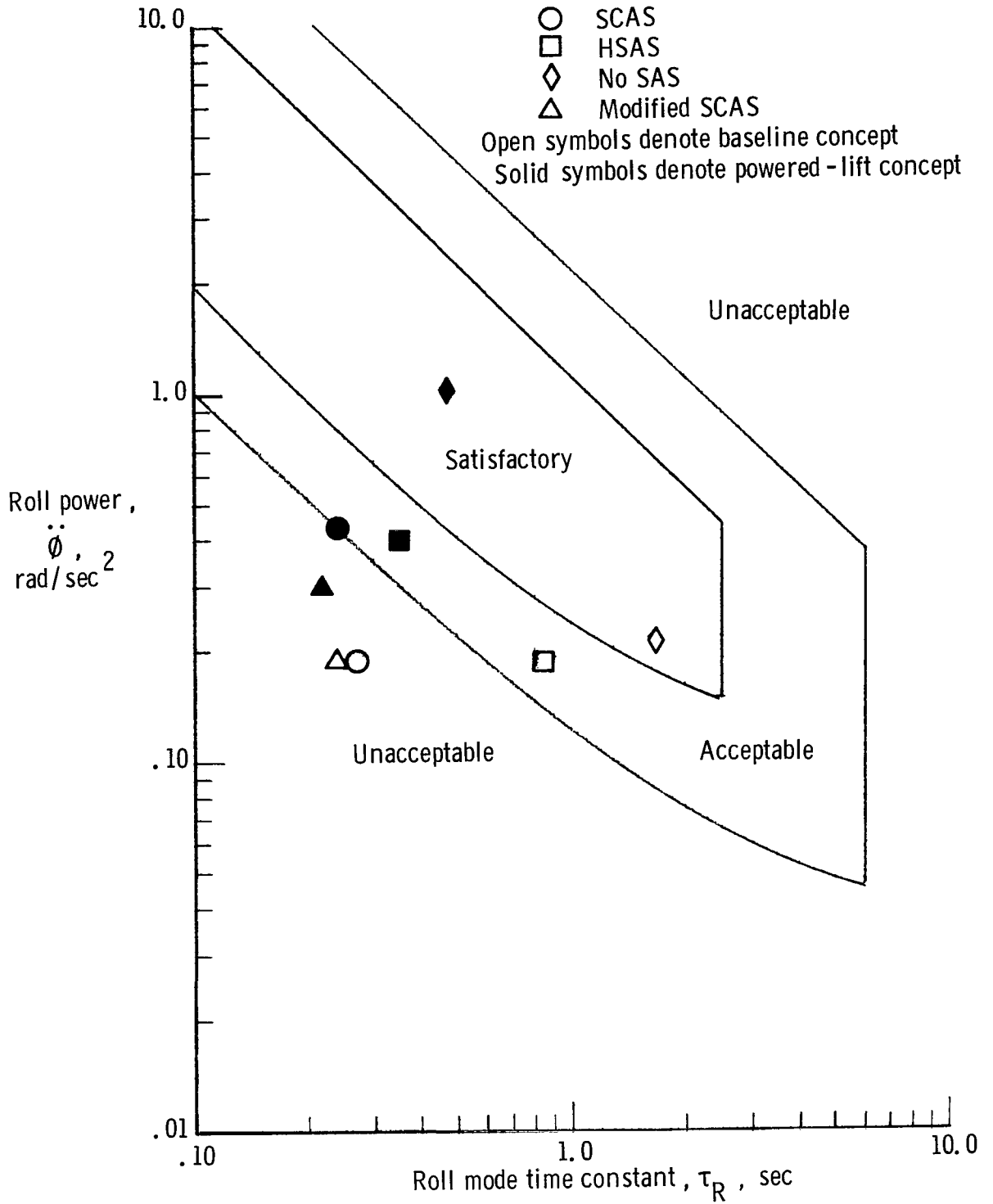


Figure 41.- Roll acceleration response boundaries for large aircraft. Boundaries from reference 12.

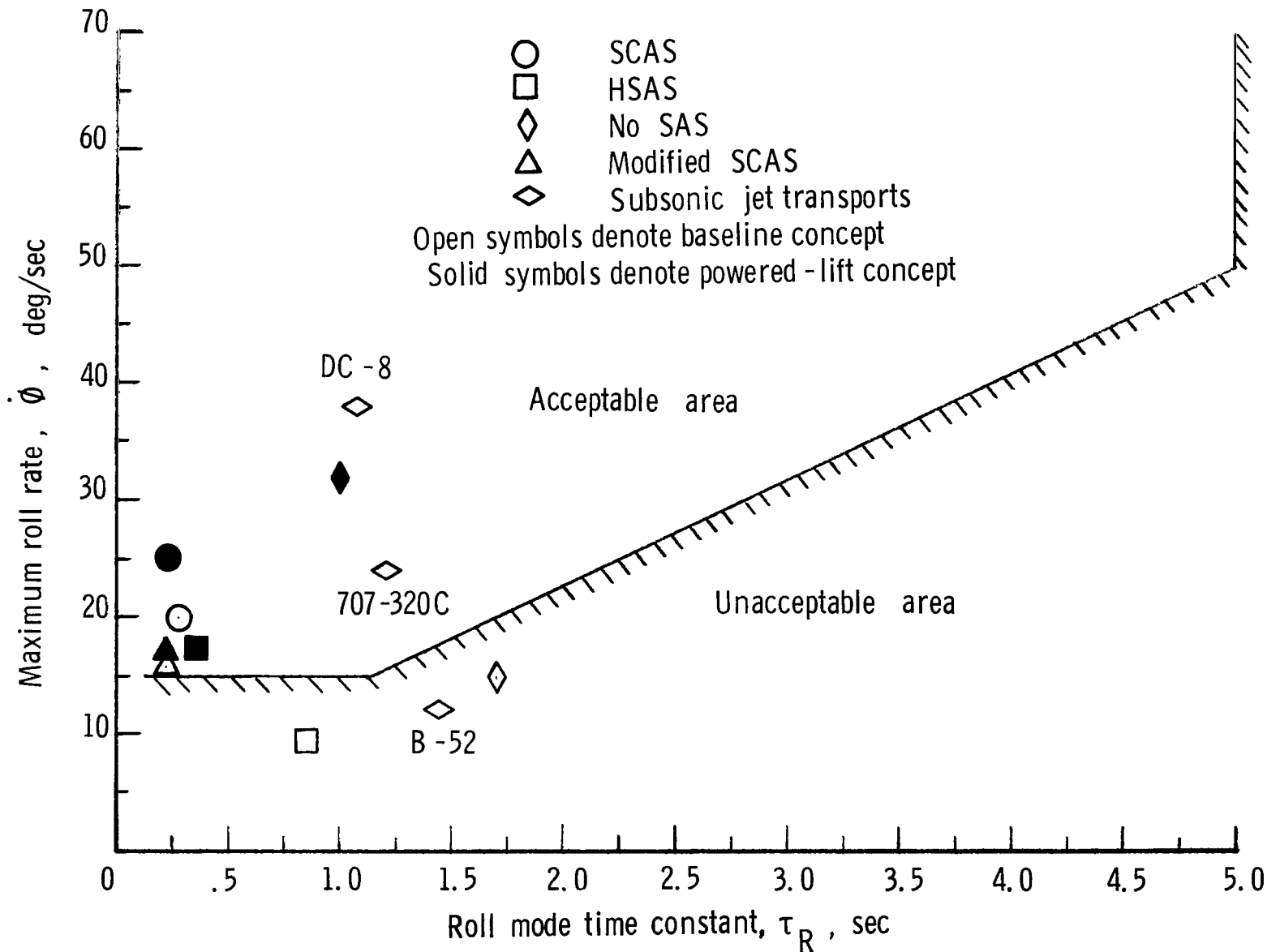


Figure 42.- Roll-rate capability criterion for transport aircraft. Boundaries from reference 17.

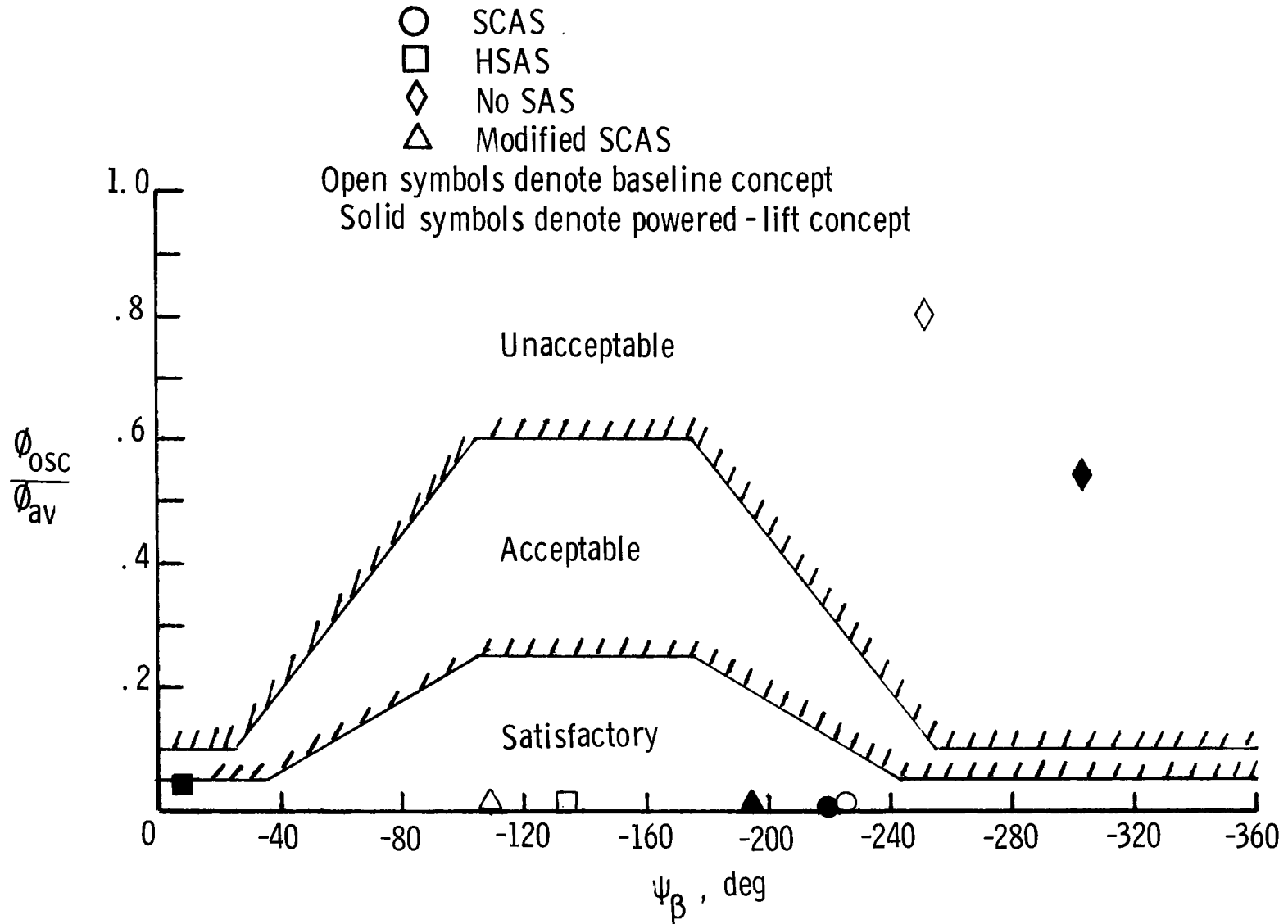


Figure 43.- Bank angle oscillation limitations of reference 12.

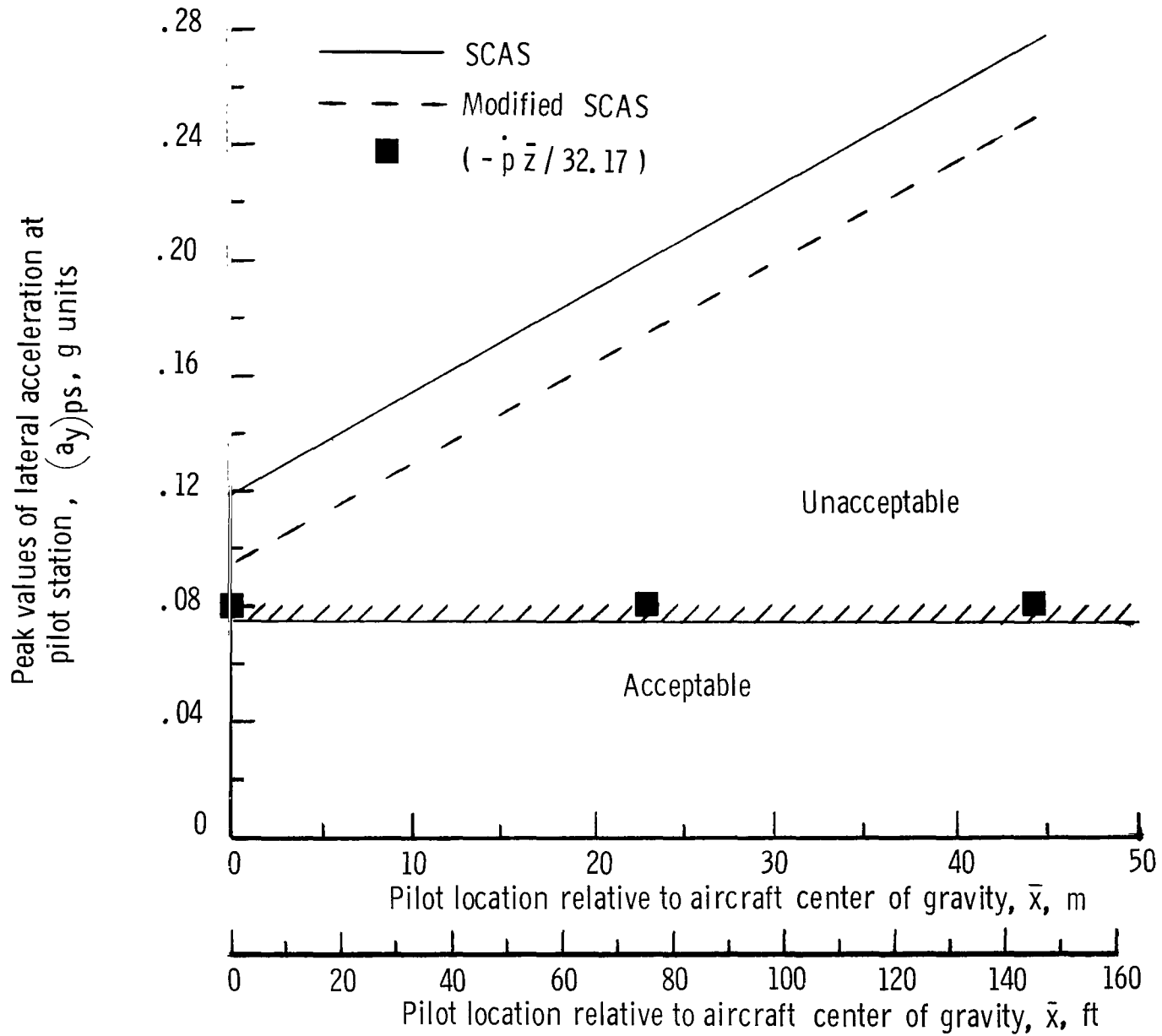


Figure 44.- Peak values of $(a_y)_{ps}$ compared with criterion of reference 11.

1. Report No. NASA TP-1240	2. Government Accession No.	3. Recipient's Catalog No.	
4. Title and Subtitle GROUND-BASED AND IN-FLIGHT SIMULATOR STUDIES OF LOW-SPEED HANDLING CHARACTERISTICS OF TWO SUPERSONIC CRUISE TRANSPORT CONCEPTS		5. Report Date July 1978	6. Performing Organization Code
7. Author(s) William D. Grantham, Luat T. Nguyen, Perry L. Deal, M. J. Neubauer, Jr., Paul M. Smith, and Major Frederick D. Gregory		8. Performing Organization Report No. L-12165	
9. Performing Organization Name and Address NASA Langley Research Center Hampton, VA 23665		10. Work Unit No. 743-04-13-01	
12. Sponsoring Agency Name and Address National Aeronautics and Space Administration Washington, DC 20546		11. Contract or Grant No.	
15. Supplementary Notes William D. Grantham, Luat T. Nguyen, Perry L. Deal, and M. J. Neubauer, Jr.: Langley Research Center, Hampton, Virginia. Paul M. Smith: Vought Corporation Hampton Technical Center, Hampton, Virginia. Major Frederick D. Gregory: Headquarters Air Force Systems Command, assigned to Langley Research Center.		13. Type of Report and Period Covered Technical Paper	
16. Abstract Fixed ground-based and in-flight simulator studies have been conducted to determine the low-speed flight characteristics of two advanced supersonic cruise transport concepts - conventional and powered lift. The primary piloting tasks were approach and landing. The results of the studies indicated that the transport concepts had unacceptable low-speed handling qualities with no augmentation, and that in order to achieve satisfactory handling qualities, considerable augmentation was required. The available roll-control power was found to be inadequate to meet existing crosswind-landing requirements for the conventional concept; but roll control was acceptable for the powered-lift concept. The results also indicated that additional research is required to obtain satisfactory ride qualities while maintaining satisfactory handling qualities for either of the simulated supersonic cruise transport concepts at low speeds.		14. Sponsoring Agency Code	
17. Key Words (Suggested by Author(s)) Supersonic transport Powered lift Handling qualities Ride qualities Simulation Approach and landing		18. Distribution Statement Unclassified - Unlimited Subject Category 05	
19. Security Classif. (of this report) Unclassified	20. Security Classif. (of this page) Unclassified	21. No. of Pages 99	22. Price* \$6.00

National Aeronautics and
Space Administration

THIRD-CLASS BULK RATE

Postage and Fees Paid
National Aeronautics and
Space Administration
NASA-451



Washington, D.C.
20546

Official Business
Penalty for Private Use, \$300

1 1 1U,A, 060978 S00903DS
DEPT OF THE AIR FORCE
AF WEAPONS LABORATORY
ATTN: TECHNICAL LIBRARY (SUL)
KIRTLAND AFB NM 87117

NASA

POSTMASTER: If Undeliverable (Section 15:
Postal Manual) Do Not Return